MOLECULAR AND FUNCTIONAL CHARACTERISATION OF LINEAR UBIQUITINATION IN THE LIVER

A THESIS

SUBMITTED TO

UNIVERSITY COLLEGE LONDON (UCL)

IN FULFILMENT OF THE REQUIREMENTS

FOR THE DEGREE OF

DOCTOR OF PHILOSOPHY

Yutaka Shimizu

July 2016

Declaration

I, Yutaka Shimizu, hereby confirm that the research work presented in this thesis is original and my own. Where information has been derived from other sources, I confirm that this has been indicated in the thesis.

July 2016

Yutaka Shimizu

Abstract

Linear ubiquitination is one of the key post-translational modifications that regulate immune signalling pathways and cell death. The only known enzyme complex capable of forming linear ubiquitin chains *de novo* is the linear ubiquitin chain assembly complex (LUBAC), and its catalytic core component is HOIP. To understand the underlying mechanisms of liver inflammation and associated carcinogenesis, the physiological role of LUBAC in the liver parenchyma was investigated. Here I report that HOIP deficiency in liver parenchymal cells triggered spontaneous cell death and inflammation in murine livers at early stages and tumourigenesis later in life. HOIP-deficient livers displayed increased cell death, including apoptosis, regeneration and immune cell infiltration. TNF-induced NF-κB activation was attenuated in HOIP-deficient primary hepatocytes and they were more susceptible to TNF-induced cell death independently of their impaired gene-activatory capacity. Unexpectedly, however, liver damage observed in HOIP-deficient livers was TNFR1-independent as co-deletion of TNFR1 did not ameliorate cell death in HOIP-deficient livers whilst mitigating their inflammation. In accordance with increased cell death, HOIP-deficient hepatocytes displayed enhanced formation of a death-inducing signalling complex containing FADD, RIPK1, caspase-8 and c-FLIP. This elevated signalling complex formation in HOIP-deficient hepatocytes was independent of lowered gene-activatory capacity and the presence of TNFR1. Moreover, combined ablation of systemic caspase-8 and MLKL completely prevented liver damage due to loss of HOIP, whereas MLKL deficiency did not have a beneficial effect. This demonstrates a crucial role for aberrant cell death in HOIP-deficient livers. Collectively, these results identify LUBAC as a previously unrecognised tumour suppressor, which acts by restraining TNFR1-independent FADD-RIPK1-caspase-8 complex formation and caspase-8-dependent apoptosis, regardless of its gene-regulatory function, in hepatocytes to prevent liver damage and inflammation.

Table of contents

Table of Figures

Abbreviations

A	Alanine
aa	Amino acid
ABIN	A20 binding inhibitor of NF-κB
ALT	alanine aminotransferase
AMP	adenosin-monophosphate
AP-1	activator protein 1
Apaf-1	apoptotic protease activating factor 1
APC	antigen presenting cell
ATP	adenosin-triphosphate
BAFF	B-cell-activating factor
Bak	BCL2 antagonist/killer
Bax	BCL2 associated X protein
BCA	bicinchoninic acid
Bcl-X_L	B-cell lymphoma extra large
BCR	B cell receptor
C	cysteine
CAD	Caspase-activated DNase
CARD	caspase activation and recruitment domain
CD	cluster of differentiation
CD40L	CD40 ligand
CD-HFD	choline-deficient high-fat diet
c-FLIP	cellular FLICE-inhibitory protein
cIAP	cellular inhibitor of apoptosis protein

CYLD	cylindromatosis
DAI	DNA-dependent activator of IFN-regulatory factors
DAMP	danger-associated molecular pattern
DC	dendritic cell
DD	death domain
DED	death effector domain
DEN	diethylnitrosamine
DISC	death-inducing signalling complex
DMEM	Dulbecco's modified Eagle's medium
ER	endoplasmic reticulum
FACS	fluorescence-activated cell sorter
FADD	Fas-associated protein with death domain
Fc	fragment crystallizable
FoxP3	forkhead box P3
G	glycine
GalN	D-galactosamine
HECT	homologous to the E6AP carboxyl terminus
HEK	human embryonic kidney
HET	heterozygosity
HFD	high-fat diet
HOIL-1	heme-oxidized IRP2 ubiquitin ligase-1
HOIP	HOIL-1L interacting protein
HRP	horse radish peroxidase
ICAD	inhibitor of CAD
IFN	interferon
IκB	inhibitory κB

IL	interleukin
IRAK	interleukin-1 receptor-associated kinase
JNK	Jun N-terminal kinase
KO	knockout
LIGHT	homologous to lymphotoxin, exhibits inducible expression and competes with HSV glycoprotein D for binding to herpesvirus entry mediator, a receptor expressed on T lymphocytes
LPC	liver parenchymal cell
LPS	lipopolysaccharide
LT	lymphotoxin
LUBAC	linear ubiquitin chain assembly complex
Lys	lysine
MAPK	mitogen-activated protein kinase
MEF	mouse embyonic fibroblast
Met	methionine
MHC	major histocompatibility complex
MnSOD	manganese superoxide dismutase
mRNA	messenger ribonucleic acid
NAFLD	non-alcoholic fatty liver disease
NEMO	NF-κB essential modulator
NF-κB	nuclear factor-κB
NK	natural killer
NOD	nucleotide-binding oligomerization domain-containing protein
NZF	Npl4 zinc finger
PAMP	Pathogen-associated molecular pattern
PARP	poly ADP ribose polymerase

PI3K	phosphoinositide 3-kinase
PIM	PUB-interacting motif
PUB	putative protein-protein interaction domain
RBR	RING-between-RING
RHIM	RIP homotypic interaction motif
RIPK	receptor-interacting protein kinase
ROS	reactive oxygen species
RT-qPCR	reverse transcription-quantitative polymerase chain reaction
SM	Smac mimetic
SOD	superoxide dismutase
SPATA2	spermatogenesis-associated protein 2
TAB	transforming growth factor β-activated kinase 1 binding protein
TAK1	transforming growth factor β-activated kinase 1
TGFβ	transforming growth factor β
T_H	T helper
TLR	Toll-like receptor
TNF	tumour necrosis factor
TNF-RSC	tumour necrosis factor-receptor signalling complex
TRADD	TNFR1-associated death domain
TRAF	TNF-receptor associated factor
Treg	regulatory T cell
TRIF	TIR-domain-containing adapter-inducing interferon-β
TrCP	transducin repeat-containing protein
UBA	ubiquitin-associated
UBAN	ubiquitin binding in ABIN and NEMO

UBL	ubiquitin-like
vICA	viral inhibitor of caspase-8-induced apoptosis
WT	wild-type
XIAP	X-linked inhibitor of apoptosis
ZF	zinc-finger

Chapter 1

1 Introduction

1.1 Inflammation and liver cancer

1.1.1 Inflammation

Inflammation is a physiological response to pathogen infection and tissue damage. Inflammation has been classically characterised by five features: heat, pain, redness, swelling and loss of function originating from the description in Latin: *calor, dolor, rubor, tumor* and *functio laesa* (Karin and Clevers, 2016). The inflamed site is characterised by vasodilation is mediated by histamine and nitric oxide, which increase blood flow and trigger heat sensation and redness. Additionally, an adhesive capacity of the blood vessels and vascular permeability are altered, allowing leukocyte migration to the infected area, which causes tissue swelling and oedema, frequently also imparing local tissue functionality. Lastly, pain can occur due to stimulation of nerve endings with inflammatory mediators.

The innate immune system detects pathogens as the first line of defence (Alberts, 2002). It recognises pathogens by means of surface-expressed pattern recognition receptors, which bind to highly conserved pathogenic structures, pathogen-associated molecular patterns (PAMPs). When innate immune cells are activated by pathogen recognition, they secrete inflammatory mediators, such as cytokines and chemokines, which alter the behaviour of other cells to trigger inflammatory responses to pathogens. Chemokines can attract other immune cells (chemoattraction), and activate them to reinforce the immune response (Janeway and Medzhitov, 2002). Cytokines do not facilitate chemotaxis unlike chemokines, but they promote transcription of genes which facilitate the inflammatory response.

An initial step to eliminate incoming pathogens is their engulfment by phagocytes. The majority of myeloid cells, including monocytes, macrophages, neutrophils, dendritic cells and mast cells are capable of phagocytosing pathogens and attacking them with ROS (Aderem and Underhill, 1998). Furthermore, the complement system can be activated by immunoglobulin bound to the surface of pathogens or lectin

molecules on pathogens themselves to be phagocytosed or lysed (Medzhitov and Janeway, 1999). Upon activiation, the complement system creates a pore-forming complex on recognized pathogens to eliminate them.

NK cells are another innate immune cell type capable of recognising pathogen-infected cells. NK cells kill target cells by releasing perforin and granzymes upon activation, which in turn create a pore in the plasma membrane of infected cells and activate caspases thereof, respectively (Vivier et al., 2008).

Additionally, phagocytes are crucial for relaying signals from the innate immune system to the adaptive immune system via antigen presentation. Phagocytosed or pinocytosed pathogens are digested in these cells. Pathogen-derived peptides are presented to naïve T cells by MHC molecules to activate adaptive immunity response. Both antigen presentation and co-stimulation are central for T cell activation to enable naïve T cells to proliferate and differentiate into effector, helper and regulatory T cells (Janeway et al., 2001). Peripheral naïve T cells mainly consist of CD4 and CD8 positive cell subsets. $CD4^+$ T cells activated by MHC class II-peptide complexes differentiate largely into helper T cells such as T_H1, T_H2, or T_H17 and inducible Treg cell subsets. The differentiation of naïve T cells is orchestrated by an array of cytokines, chemokines and growth factors produced by APCs and surrounding cells. $CD8^+$ T cells, by contrast, are activated by MHC class I-peptide complexes on APCs. The naïve $CD8^+$ T cells then differentiate into cytotoxic T cells that can recognise the foreign antigen peptides presented on MHC class I molecules in infected cells. The killing mechanisms of cytotoxic T cells upon target recognition are similar to NK cells, again involving granzymes and perforin.

B cells are triggered upon encountering their antigens from infected cells or APCs which bind to their receptor (BCR). B cells can digest antigens intracellularly and present them to T cells with corresponding T cell receptors (TCRs) via MHC class II molecules. Subsequently activated T cells secrete cytokines that activate B cells to elicit antibody production against their antigens. Secreted antibodies bind to antigens, allowing recognition and subsequent elimination by cells expressing Fc receptors, such as phagocytes and NK cells, to recognise and eliminate those (Janeway et al., 2001).

While activated innate immune cells and T cells produce pro-inflammatory cytokines, they also secrete anti-inflammatory mediators, including IL-10 and TGF-β to regulate inflammation. In addition, T cells are regulated by co-inhibitory receptors such as CTLA-4 and PD-1. Among T cells, Tregs play a crucial role in suppression of inflammation. Mutation in the *FoxP3* gene, which is a transcription factor required for regulatory T cell induction, is causative for immunodysregulation polyendocrinopathy enteropathy X-linked syndrome (IPEX), which is an autoimmune disease (van der Vliet and Nieuwenhuis, 2007). This evidence indicates that suppressive immune signalling is essential to control inflammation.

1.1.2 Inflammation and cancer

It has been argued that inflammation is strongly associated with cancer. Research showed that infections are linked to 15-20% of all cancer-related deaths (Balkwill and Mantovani, 2001). For instance, *Helicobacter pylori* infection is a major cause of stomach cancers. Also, patients with chronic inflammation carry a higher risk of tumour malignancy (Balkwill and Mantovani, 2001). Accordingly, recent large epidemiological studies implicate that non-steroidal anti-inflammatory drugs (NSAIDs) could help to circumvent tumour development (Rothwell et al., 2012; Chan and Ladabaum, 2015).

In late 19th century, Rudolf Virchow observed that leukocytes are present in neoplastic tissues and suggested a connection between inflammation and cancer (Balkwill and Mantovani, 2001). The tumour microenvironment includes leukocytes in the tumour-supporting stroma as well as intra-tumour areas. Inflammatory cells and mediators participate in tumour growth, progression, metastasis, and immunosuppression. The majority of tumour-associated leukocytes are tumour-associated macrophages (TAM), dendritic cells, and lymphocytes (Mantovani et al., 2002). Pro-inflammatory cytokines from tumour-infiltrating immune cells and tumour cells themselves contribute to tumour progression by causing DNA damage, stimulating growth, subverting antitumour immunity, and enhancing invasion (Hanahan and Weinberg, 2011).

On the other hand, the immune system is capable of detecting tumour cells and specifically killing them by the action of cytotoxic T cells and NK cells. Interestingly,

tumour cells originating from immunodeficient mice are incapable of colonising and growing in syngeneic immunocompetent mice, whilst cancer cells from immunocompetent mice are capable of doing so in both hosts. This evidence suggested that, in immunocompetent mice, immunogenic cells presenting non-self antigens are removed by the immune system so that only less immunogenic cells can thereafter survive (Kim et al., 2007). By contrast, since immunodeficient mice fail to reject immunogenic pre-cancerous cells, these cells cannot survive immunocompetent environment after transplantation (Teng et al., 2008). The concept of constant removal of tumourigenic cells is termed cancer immunosurveillance, or immunoediting (Dunn et al., 2004; Hanahan and Weinberg, 2011).

Thus, developed cancers often evade the destruction by immune cells by being less immunogenic or protected from the recognition by cytotoxic T cells (Hanahan and Weinberg, 2011). The recent success of clinical immune checkpoint blockade, which targets co-inhibitory molecules such as CTLA-4 and PD-1, proves that T cell functions in human cancers are indeed impaired by these co-inhibitory molecules (Sharma and Allison, 2015). Ligands of PD-1 can be expressed by stromal cells as well as tumour cells to dampen T cell activation. Moreover, the presence of Tregs, T_H2 and T_H17 cells in tumours is suggested to promote subversion of the immune system to block antitumour immunity, for example, by skewing TAM to M2 macrophages, which produce immunosuppressive cytokines IL-10 and TGFβ (Mantovani and Allavena, 2015).

In addition to the response to invading pathogen and regulation on tumour development, inflammation also plays a central role in wound healing and tissue regeneration (Karin and Clevers, 2016). Upon tissue injury or infection, damaged cells release PAMPs and danger-associated molecular patterns (DAMPs), as well as ROS. Thus tissue damage activates multiple signalling pathways in the surrounding cells via recognition of PAMPs and DAMPs, leading to the production of inflammatory mediators. Inflammatory cytokines, in turn, stimulate the growth of stem cells and facilitate turn-over of blood vessels and fibroblasts. Also, they can induce dedifferentiation of tissue cells, which results in the expansion of regenerative precursor cells.

1.1.3 Liver cancer

The major types of human primary liver tumour are hepatocellular carcinoma (HCC) and cholangiocarcinoma (CCA), where HCC is the most common type of liver cancer. HCC is the fifth most common cancer in men and seventh most common in women (Marquardt et al., 2015). The leading cause for HCC is hepatotropic virus infection in sub-Saharan Africa and Asia, as well as alcohol abuse worldwide. In addition, in Western countries, diabetes and obesity are increasingly associated with HCC without a history of cirrhosis. HCC is considered to be derived from mature hepatocytes, or liver progenitor cells (Marquardt et al., 2015).

Infection with hepatotropic viruses, notably HBV or HCV, is found in the large majority of patients with HCC (El-Serag, 2011). This viral infection causes chronic inflammation and subsequent cirrhosis. Some viral proteins are also capable of transforming hepatocytes to be pre-tumourigenic by blocking p53 protein, which is a tumour suppressor gene crucial for maintaining genomic stability (Wang et al., 1994; Ueda et al., 1995).

The most common frequently mutated oncogene in HCC is *CTNNB1* encoding β-catenin, whilst the most commonly mutated tumour suppressor gene is *TP53* which encodes p53 protein (Kan et al., 2013). In addition, genetic alterations leading to HCC are related to oncogenic networks, including canonical Wnt signalling (eg amplifications in *FZD6* and *RSPO2*, mutations in *CTNNB1*, *AXIN1*, *APC*), the JAK-STAT pathway (eg amplification in *IL6R*, *JAK1* mutation), chromatin modification (eg *SWI/SNF* mutation), apoptotic pathways (eg deletions in *TNFRSF10A/B*, *CASP3*) and the PI3K-AKT-mTOR pathways (eg *PTEN*, *RPS6KA3* mutations) (Kan et al., 2013; Marquardt et al., 2015).

1.1.4 Mouse models of autochthonous hepatocellular carcinoma

In order to understand the nature of liver cancer development, researchers generated several mouse models that can mimic human HCC. The models can be classified according to the trigger of tumourigenesis: 1) viral gene transgenics, 2) chemicals and 3) gene editing (Heindryckx et al., 2009; Weber et al., 2011).

1.1.4.1 Viral protein transgenics

The most common cause of HCC is viral hepatitis-induced carcinogenesis. In the case of HBV infection, the replication of HBV inside human hepatocytes can cause transformation of hepatocytes and cell death.

The replication of HBV requires the function of the HBX, which a viral protein is essential for HBV infection. HBX alters cell signalling in multiple aspects to transform hepatocytes into pre-tumourigenic cells (Murakami et al., 2001). First, HBX can serve as a coactivator of transcription by binding to transcriptional activators, CREB and NF-κB (Su et al., 1996). HBX also activates oncogenic signalling such as Src and Ras pathways (Doria et al., 1995; Bouchard et al., 2001). Furthermore, HBX inhibits the function of p53 protein by direct interaction (Wang et al., 1994; Ueda et al., 1995). Ectopic expression of the HBX gene in mice triggers an alteration of hepatocytes, resulting in HCC formation at 13 months of age (Kim et al., 1991). When combined with the overexpression of the proto-oncogene *c-myc*, liver carcinogenesis by HBX is accelerated by promoting transformation of hepatocytes (Teradillos et al., 1997).

In addition, a transgene of the HBV envelope protein induces hepatocyte cell death in mice due to the accumulation of viral surface protein HBsAg in the ER (Chisari et al., 1989). Mice transgenic for the HBV envelope protein develop inflammation and regenerative hyperplasia, which eventually leads to carcinogenesis at 15 months of age (Chisari et al., 1989).

1.1.4.2 Chemically-induced and diet-induced liver carcinogenesis

DEN is the most commonly used carcinogen to induce liver cancer in rodents. DEN is oxidised and activated in hepatocytes by cytochrome P450 to function as a DNA-alkylating agent, and it also causes ROS production (Heindryckx et al., 2009). Previous research demonstrated that DEN-induced tumours have close gene expression signatures to those of HCC patients with poor survival (Lee et al., 2004). A single injection of DEN into male mice at 2 weeks of age is sufficient to trigger tumourigenesis. Of note, as mice ages, they are more resistant to DEN-induced carcinogenesis (Lee et al., 1998). Male mice are more prone to bear DEN-induced

tumours as compared to females due to higher MyD88-dependent IL-6 production (Naugler et al., 2007).

Dietary change can be also a model of liver tumourigenesis. For instance, choline-deficient diet induces severe steatosis in murine livers. Dietary choline deficiency combined with a high level of fat intake (CD-HFD) induces steatosis, oxidative stress, hepatocyte ballooning and HCC in C57BL/6 mice, whilst HFD alone does not induce carcinogenesis (Wolf et al., 2014). CD-HFD-induced steatohepatitis and HCC is promoted by $CD8^+$ T cells and NKT cells (Wolf et al., 2014). Moreover, HFD treatment combined with DEN injection is another model of steatohepatitis-associated hepatocarcinogenesis (Park et al., 2010).

1.1.4.3 Gene deletion and editing

Mdr2 knockout mice are often employed to mimic inflammation-associated HCC formation. Mdr2 belongs to the ABC transporter family and is involved in the transport of phospholipids and cholesterol into bile. Mdr2 knockout mice develop cholestasis and severe biliary fibrosis prior to carcinogenesis (Popov et al., 2005). Defective bile secretion leads to cholangitis and fibrosis, which results in tumourigenesis.

Tyler Jacks and colleagues reported that concomitant deletion of PTEN and p53 in hepatocytes, using hydrodynamic injection and CRISPR/Cas9 system, results in rapid tumour development (Xue et al., 2014). They also succeeded in introducing oncogenic PTEN and β-catenin mutations in the liver with the same method. As CRISPR/Cas9 allows multiplexed gene deletion and editing, it is a feasible tool to mimic mutagenesis of multiple genes, thereby enabling better modeling of HCC found in human patients (Weber et al., 2015). Therefore, in parallel to classical methods of tumour initiation and promotion with chemicals, emerging genome editing technology will most likely be abundantly employed in liver cancer studies.

1.2 NF-κB and cell death signalling in liver disease

1.2.1 NF-κB signalling

NF-κB is a family of transcription factors that are activated by various immune stimulations and induce expression of pro-survival genes, pro-inflammatory cytokines and immunoregulatory proteins (Sen and Baltimore, 1986; Oeckinghaus and Ghosh, 2009). The NF-κB family consists of five proteins, RelA/p65, RelB, c-Rel, NF-κB1/p105 and NF-κB2/p100. These proteins are divided into two classes. Class 1 NF-κB proteins are p105 and p100, which are initially produced as precursor proteins and processed into p50 and p52, respectively, by the ubiquitin-proteasome system (Liang et al., 2006). Processing of p105 occurs constitutively whereas that of p50 is tightly regulated by phosphorylation. Although p50 and p52 have DNA-binding and dimerisation domains, they depend on additional factors for activation of gene transcription (Ghosh et al., 1998). These class 2 NF-κB proteins, RelA, RelB and c-Rel harbour transactivation domains in their C-termini and DNA-binding and dimerisation domains in their N-termini. RelA, RelB and c-Rel activate target gene transcription by forming homodimers or heterodimers with p50 or p52 (Ghosh et al., 1998).

NF-κB activity is tightly regulated and normally suppressed by IκB family proteins. IκB proteins contain ankyrin repeats which bind to the DNA-binding and dimerisation domain of NF-κB proteins to prevent their activity. The best characterised IκB is IκBα, which constitutively binds to the NF-κB-activating heterodimeric RelA-p50 complex (Ghosh and Baltimore, 1990). Upon NF-κB-activating stimulation, IκBα is subjected to degradation by the ubiquitin-proteasome system, which in turn releases RelA-p50 to activate gene transcription (Yaron et al., 1998; Fuchs et al., 1999). Also, precursor forms of p105 and p100 are considered to be inhibitory as their C-terminal ankyrin repeats can serve as a function of IκB proteins. These inhibitory domains of p105 and p100 are cleaved off and degraded during processing (Sun, 2011).

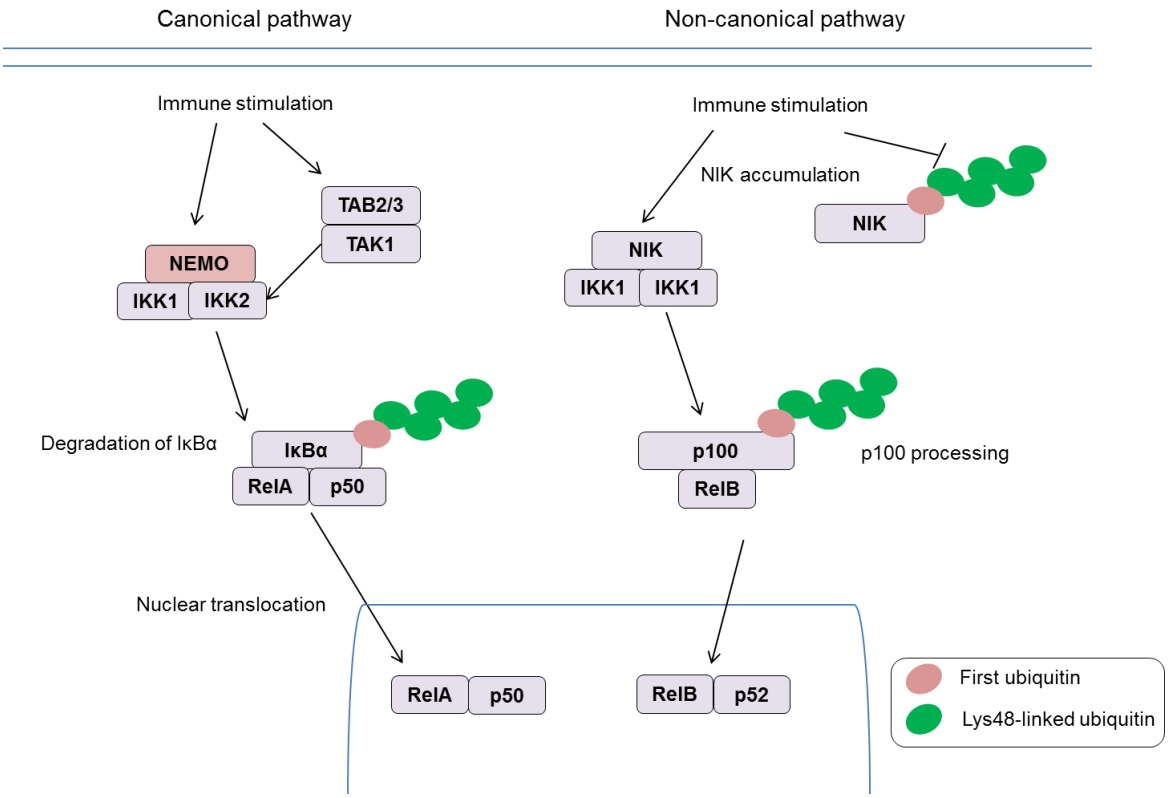

Figure 1.1 Simplified scheme of canonical and non-canonical NF-κB pathways

The IκB kinase (IKK) complex plays a critical role in activation of NF-κB (Häcker and Karin, 2006). The IKK complex initially activates NF-κB signalling by phosphorylating IκB proteins. In canonical NF-κB signalling, the IKK complex is comprised of two kinases IKK1/IKKα and IKK2/IKKβ and a scaffold protein NEMO/IKKγ (Mercurio et al., 1997; Rothwarf et al., 1998; Yamaoka et al., 1998). IKK1 and IKK2 have kinase domains in their N-terminus and bind to NEMO via C-terminal NEMO-binding domains. In canonical NF-κB signalling, which is activated by stimuli such as TNF, IL-1 or LPS, the IKK complex is activated by the recruitment to the corresponding receptor complexes. IKK2 is sufficient and essential for the IKK complex to phosphorylate IκBα in a NEMO-dependent manner and triggers its proteasomal degradation (Oeckinghaus and Ghosh, 2009) (Figure 1.1, left panel).

In non-canonical NF-κB signalling, which is activated by subsets of TNF superfamily receptors including CD40, lymphotoxin beta receptor and BAFFR, NF-κB-inducing kinase (NIK) plays a central role in activating NF-κB. Upon receptor oligomerisation, NIK is stabilised and phosphorylates IKK1 (Senftleben et al., 2001; Liao et al., 2004).

IKK1 homodimer subsequently phosphorylates p100, which results in degradation of their inhibitory C-terminal ankyrin repeats by $SCF^{\beta TrCP}$ ubiquitin ligase complex and processing into p52 (Coope et al., 2002; Liang et al., 2006). p52 forms heterodimers with RelB to activate target gene transcription (Bonizzi and Karin., 2004) (Figure 1.1, right panel). Whilst canonical NF-κB activation is rapid and transient, non-canonical NF-κB activation is slower and persistent and exerts specific functions depending on cell types and activating receptors (Sun, 2011).

1.2.2 NF-κB activating modules

NF-κB is activated upon diverse immune stimulation, such as cytokines (eg TNF and IL-1), PAMPs (eg LPS and viral DNA/RNA) and immunomodulatory receptors (eg CD40, TCR and BCR). As explained in the previous section, NF-κB activation depends on whether IKK is activated. Here I describe how IKK and NF-κB are activated by coordinated signalling cascades from representative immune receptors.

1.2.2.1 TNFR1 signalling

TNF is a well-studied potent activator of NF-κB signalling. Ligation of TNF to its receptor TNFR1 triggers trimerisation of TNFR1. Upon oligomerisation of TNFR1, the first proteins recruited to the TNFR1 are TRADD and RIPK1 via homotypic death domain (DD) interaction (Hsu et al., 1995; Zheng et al., 2006; Ermolaeva et al., 2008; Pobezinskaya et al., 2008). TRADD, in turn, recruits TRAF2/5 via TRAF binding domain, which subsequently associates with the E3 ubiquitin ligase cIAP1/2 (Hsu et al., 1996; Tsao et al., 2000). cIAP1/2 then ubiquitinate themselves, RIPK1 and other components within the TNFR1-associated signalling complex (TNF-RSC) (Ea et al., 2006; Bertrand et al., 2008; Varfolomeev et al., 2008). Ubiquitination of cIAP1/2 and RIPK1 then triggers the recruitment of another E3 ubiquitin ligase complex linear ubiquitin chain assembly complex (LUBAC), the TAK1-TAB2-TAB3 complex to ubiquitin chains formed in the TNF-RSC (Kanayama et al., 2004; Ea et al., 2006; Haas et al., 2009; Vince et al., 2009). LUBAC further ubiquitinates RIPK1, NEMO, TRADD and TNFR1 (Gerlach et al., 2011; Draber et al., 2015), thereby stabilising the TNF-RSC and allowing recruitment of the IKK complex. TAK1 is a kinase which on one hand, phosphorylates IKK1/2, leading to activation of NF-κB signalling, and, on the other hand promotes activation of MAPK signalling (Wang et al., 2001) (Figure 1.2).

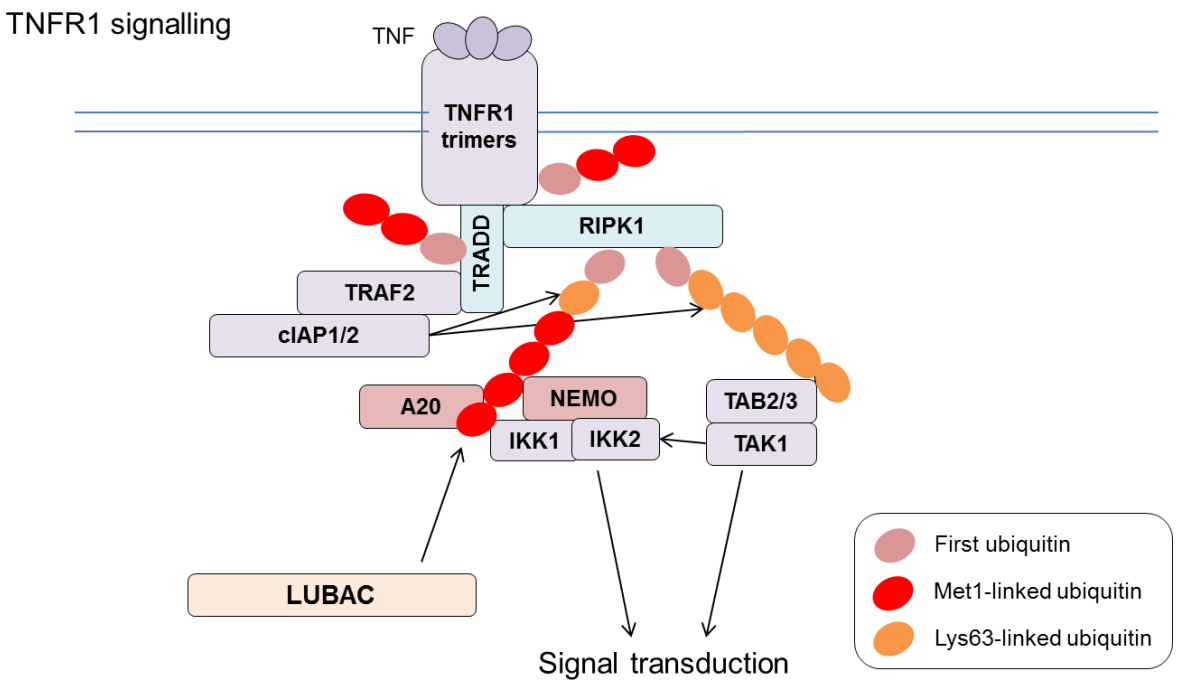

Figure 1.2 Schematic representation of TNFR1 signalling

1.2.2.2 IL-1/TLR signalling

IL-1R and TLRs activate downstream signalling in a similar manner, as they share homology in intracellular Toll/IL-1R (TIR) domains for the recruitment of respective signalling complexes. Upon binding of the respective ligand, the receptors undergo dimerisation and conformational change that allows recruitment of downstream signalling components (Akira and Takeda, 2004). MyD88 is one of the first adaptors recruited to IL-1R/TLR via TIR domain interaction. MyD88 is universally engaged in IL-1R and all TLR signalling except for TLR3 signalling (Kawai and Akira 2010). The N-terminal DD of MyD88 serves as an association platform for kinase IRAK1/2/4 through a homotypic interaction between their DDs. IRAK4 is considered to be the most important proximal kinase (O'Neill et al., 2003). IRAK4-mediated IRAK1 activation leads to interaction with the E3 ligase TRAF6, which in turn ubiquitinates itself and IRAK1, allowing the recruitment and activation of the TAK1-TAB2-TAB3

complex mediated by the ubiquitin-binding capability of TAB2/3 (Ninomiya-Tsuji et al., 1999; Ishitani et al, 2003; Kanayama et al., 2004).

1.2.2.3 NOD2 and RLR signalling

Other PAMP receptors including NOD2 and RIG-I/MDA5 can also activate canonical NF-κB signalling. NOD2 receptors bind to peptidoglycan dipeptide, muramyl dipeptide (MDP), (Girardin et al, 2003; Inohara et al, 2003). The NOD2 receptor recruits RIPK2, XIAP and cIAP1/2 upon activation and ubiquitination of RIPK2 by IAPs leads to the subsequent recruitment of the TAK1-TAB2/3 complex and the IKK complex to trigger NF-κB signalling (Inohara et al., 2000; Strober et al., 2006; Bertrand et al., 2009). In addition, LUBAC is also engaged in ubiquitination of RIPK2 to facilitate NF-κB signalling (Damgaard et al., 2012).

RIG-I and MDA5 are receptors for foreign DNA derived from infectious viruses. Upon recognition of cytosolic DNA, they bind to the adaptor protein MAVS on the outer mitochondrial membrane, thereby triggering oligomerisation of MAVS (Takeuchi and Akira, 2008). Activated MAVS recruits TRAF proteins, which in turn become a platform for recruitment of the TAK1-TAB2/3 complex and the IKK complex.

1.2.2.4 TCR/BCR signalling

In addition to innate immune signalling pathways, adaptive immune receptors are also activators of NF-κB signalling. Upon activation both TCR and BCR recruit the CBM complex consisting of CARD11/CARMA1, BCL10 and MALT1 upon engagement of receptor-proximal adaptors and kinases (Thorne et al., 2004; Beyeart, 2014). In the CBM complex, BCL10 is ubiquitinated in Lys63-linked and Met1-linked manners by a concerted action of the E3 ligases, cIAP1/2 and LUBAC, respectively (Dubois et al., 2014; Yang et al., 2014; Yang et al., 2016). Ubiquitination of BCL10 is critical for the recruitment of NEMO by its binding capacity to polyubiquitin, which in turn activates the IKK complex in T-cell and B-cell receptor signalling (Wu et al., 2008).

1.2.2.5 Non-canonical NF-κB activators

Non-canonical NF-κB activators are members of TNF superfamily receptors, including lymphotoxin beta receptor (LTβR), CD40, BAFFR (Häcker and Karin, 2006). LTβR is mainly expressed on lymphoid cells and epithelial cells. There are two ligands for LTβR: lymphotoxins and LIGHT, cytokines mainly produced by T cells. Membrane-anchored LTβ forms heterotrimers with soluble LTα ($LT\alpha_1\beta_2$ and $LT\alpha_2\beta_1$). LTβR activates non-canonical NF-κB signalling as well as canonical NF-κB signalling (Coope et al, 2002). LTβR signalling is central for lymphoid organogenesis (Sun et al., 2012). CD40 is expressed on APCs and activated B cells, and its ligand CD40L is predominantly expressed on activated T cells (Elgueta et al., 2009). CD40 is a vital co-stimulatory molecule in the immune synapse formation upon antigen presentation. CD40 signalling modulates B-cell functions, such as germinal centre formation and isotype class switching (Ma and Clark, 2009). CD40L-CD40 also elicits activation of both canonical and non-canonical NF-κB pathways (Coope et al, 2002). BAFFR is exclusively expressed on B cells and is involved in maturation of peripheral B cells (Mackay and Schneider, 2009). Unlike CD40, BAFFR specifically activates non-canonical NF-κB and is hardly capable of activating canonical NF-κB signalling (Claudio et al, 2002). BAFFR-mediated activation of non-canonical NF-κB promotes B-cell survival via induction of Bcl-2 and Bcl-X_L (Mackay and Schneider, 2009). These recepetors contain TRAF-binding motif to recruit TRAF3, which leads to the subsequent degradation of TRAF2 and TRAF3, which is mediated by cIAP1/2 (Vallabhapurapu et al, 2008; Zarnegar et al, 2008). Degradation of TRAF2/3 thereby leads to stabilisation of NIK (Sun, 2011).

It is suggested that the non-canonical pathway activation requires *de novo* synthesis of NIK as well as degradation of TRAF2 or TRAF3 (Sun, 2011). Normally, the level of NIK protein is maintained at an extremely low level due to its constant degradation by the ubiquitin-proteasome system (Liao et al., 2004). This degradation of NIK is orchestrated by TRAF3, TRAF2 and cIAP1/2, with TRAF3 being central to the inhibition of NIK (Liao et al., 2004; Vallabhapurapu et al, 2008; Zarnegar et al, 2008). TRAF3 is bound to the N-terminus of NIK and targets NIK for constant ubiquitination in a Lys48-linked manner by the E3 ubiquitin ligase cIAP1/2. Loss of TRAF2 or TRAF3, or degradation of cIAP1/2 by Smac mimetic compounds causes

accumulation of NIK and aberrant p100 processing, leading to non-canonical NF-κB activation (Vallabhapurapu et al, 2008; Zarnegar et al, 2008).

1.2.3 Cell death pathways

1.2.3.1 Apoptosis

The best characterised programmed cell death is apoptosis, executed by a cascade of activated caspases, resulting in DNA fragmentation and cell blebbing. Apoptotic pathways were initially investigated in *C. elegans* employing forward genetic methods. Thereby mutants that do not undergo cell death increase cell numbers in their bodies (Ellis et al., 1991). Apoptosis is crucial in morphogenesis as well as tissue homeostasis. In apoptotic cell death, executioner caspases cleave multiple cytoskeletal proteins including actin and nuclear lamins, which leads to the loss of cellular structure and blebbing. In addition, they cleave inhibitor of caspase-activated DNase (ICAD) to release and activate DNase CAD, resulting in fragmentation of nuclear DNA (Fischer et al., 2003).

There are two classical routes of interconnected apoptotic pathways: the intrinsic and the extrinsic pathway (Scaffidi et al., 1998; Jost et al., 2009). The intrinsic pathway is mediated by the mitochondria, whereas the extrinsic pathway is triggered by receptors for apoptosis-inducing ligands. Intrinsic death pathway is activated by cellular stresses such as DNA damage and oxidative stress. Under such stresses, activation of pro-apoptotic Bcl-2 family member proteins, Bax and Bak, leads to their oligomerisation and insertion to mitochondrial outer membranes, leading to mitochondrial outer membrane permeabilisation (MOMP) (Tait and Green, 2013). MOMP triggers the release of mitochondrial contents into the cytosol. A key mitochondrial protein initiating apoptosis is cytochrome *c*, which is a component of the electron transport chain in the mitochondria. Released cytochrome *c* binds to Apaf-1 and provokes its conformational change, which leads to the formation of a heptameric complex of Apaf-1-cytochrome *c*, referred to as apoptosome (Li et al., 1997). The apoptosome also contains procaspase-9 which is recruited to Apaf-1 by CARD domain interaction between these proteins (Riedl et al., 2007). Dimerisation of pro-caspase-9 at the apoptosome results in cleavage and activation of caspase-9. Activated caspase-9 subsequently cleaves and activates the executioner caspase-3

and -7 (Tait and Green, 2013). In addition to cytochrome *c*, the mitochondrial proteins Smac/Diablo and HtrA2/Omi promote apoptosis execution by inhibiting anti-apoptotic IAPs, which normally bind to executioner caspases and suppress their activation (Jost et al., 2009).

The extrinsic apoptosis pathway is activated by TNF superfamily receptors, referred to as death receptors (DRs), such as TNF-R1, DR3/TRAMP, TRAIL-R1/DR4, TRAIL-R2/DR5 (in *H. sapiens*; *M. musculus* has only one TRAIL-R), CD95/Fas, and DR6 (Walczak, 2013). In the cases of TRAIL-Rs and CD95, upon ligation by their respective ligands, these receptors trimerise (oligomerise) and their intracellular DDs recruit FADD as an adaptor protein. In turn, FADD recruits caspase-8 via DED interaction and subsequently activates caspase-8 by forming the DISC (Kischkel et al., 1995; Boldin et al., 1996; Muzio et al., 1996; Bodmer et al., 2000; Kischkel et al., 2000; Sprick et al., 2000). Caspase-8 activated at DRs cleaves executioner caspases, leading to apoptosis of stimulated cells. Caspase-8 activity is controlled by a negative regulator c-FLIP, which harbours DED domains on its N-terminus and a caspase-like domain on its C-terminus which does not have proteolytic activity. c-FLIP forms heterodimers with caspase-8 and hence restricts its apoptotic function (Irmler et al., 1997; Oberst et al., 2011; Dillon et al., 2012) (Figure 1.3).

The extrinsic cell death pathway is connected to the mitochondrial apoptosis pathway. The pro-apoptotic BH3-only family protein Bid is cleaved by caspase-8 to initiate the mitochondrial pathway. Truncated Bid (tBid) translocates to the mitochondria, where it activated Bax and/or Bak to induce MOMP (Wei et al., 2000).

Whilst the primary function of TNF is to promote gene activation, in certain contexts TNF can induce cell death. When the TNF-RSC is not properly assembled or gene activation is not optimally executed, a part of the TNF-RSC is released into the cytosol, including TRADD and RIPK1, and nucleates a secondary cytosolic complex, termed complex II, together with FADD and pro-caspase-8, which results in activation of the initiator caspase-8 and subsequent apoptosis (Micheau and Tschopp, 2003, Conrad et al., 2016).

1.2.3.2 Necroptosis

When the TNF-RSC formation is compromised or caspase-8 is inhibited or lacking in cells, TNF executes another type of cell death, termed programmed necrosis or necroptosis. This emerging type of cell death was shown to be non-apoptotic and caspase-independent (Wang et al., 2005). Despite this interesting finding, a physiological role of necroptosis was unclear and questioned for several years. Recent studies clarified that viral proteins such as vICA protein of CMV blocks caspase-8 when the virus infect cells in order to avoid apoptosis of host cells. However, infected cells can still undergo necroptosis (Mocarski, 2015). This suggests that cells can execute necroptosis as an alternative cell death mechanism when caspases are inhibited. In addition, human biopsies of patients with ischemia-reperfusion injury and DILI display a sign of necroptosis in biopsies (Linkermann et al., 2013, Wang et al., 2014). Thus viral infections and tissue injury may involve necroptosis in some cases.

Mechanistically, necroptosis is orchestrated by the RIP kinases, RIPK1 and RIPK3, and the pseudo-kinase MLKL (Sun et al., 2012). When RIPK3 is activated by the RHIM domain interaction with RIPK1 and the kinase activity of RIPK1, RIPK3 autophosphorylates itself and phosphorylates MLKL. Phosphorylation of MLKL, in turn, results in a conformational change and translocation of MLKL to the plasma membrane (Dondelinger et al., 2014; Cai et al., 2014). Pore-forming MLKL interacts with phospholipids in the plasma membrane, leading to perforation and death of the cells.

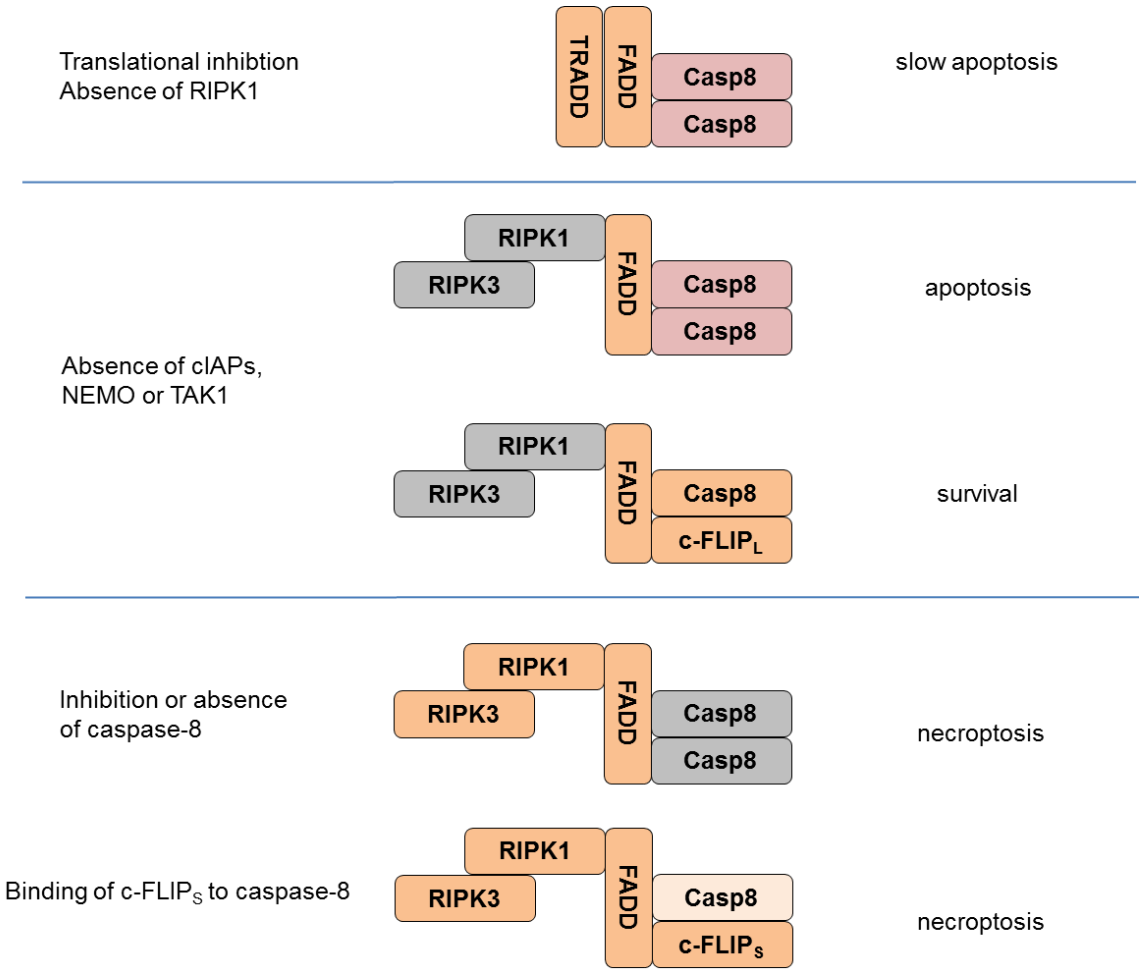

Figure 1.3 TNF-induced formation of cell death-inducing complexes. TNF stimulation can trigger cell death under certain circumstances. When translation is inhibited or RIPK1 is absent, TNF stimulation leads to formation of the TRADD-FADD-caspase-8 complex and activation of caspase-8. Absence of cIAPs, NEMO or TAK1 results in RIPK1-FADD-caspase-8 complex formation. c-FLIP$_L$ restricts activation of caspase-8 and also prevents necroptosis by cleaving RIPK1/3. Formation of caspase-8 homodimers causes apoptosis. In the absence or inactivation of caspase-8 or recruitment of c-FLIP$_S$, TNF signalling leads to RIPK1-RIPK3-MLKL-mediated necroptosis (Figure modified from Conrad et al., 2016).

When caspase-8 is functional, activated caspase-8 dimers inactivate RIPK1 and RIPK3 by cleaving them (Figure 1.3). Therefore, the apoptotic pathway prevents the activation of necroptosis. (Kaiser et al., 2011; Oberst et al., 2011; Zhang et al., 2011). Accordingly, FADD is required for activation of caspase-8 to prevent necroptosis. Indeed, FADD deficiency in mice causes RIPK3-dependent necroptosis (Welz et al., 2011; Bonnet et al., 2011). Moreover, the longer isoform of c-FLIP (c-FLIP$_L$) is a suppressor of caspase-8-mediated apoptosis but c-FLIP$_L$ allows a partial activation of caspase-8 by forming heterodimers with caspase-8, which are able to cleave

RIPK1 and RIPK3 to prevent cells from necroptotic death (Oberst et al., 2011) (Figure 1.3). By contrast, the shorter isoform of c-FLIP (c-FLIP$_S$) rather promotes formation of the death-inducing complex and subsequent necroptosis (Feoktistova et al., 2011). In addition, RIPK3 activity is also negatively controlled by the phosphatase Ppm1b through dephosphorylation (Chen et al., 2015).

An additional RHIM-containing protein, TRIF is also capable of activating RIPK3, independently of RIPK1 (Mocarski et al., 2012; Dillon et al., 2014). TRIF is an adaptor protein of TLR3 and TLR4 signalling, and has been shown to mediate cell death upon TLR3 and TLR4 activation. Another RHIM-containing protein DAI is a cytosolic double-stranded DNA sensor, which is able to interact with RIPK1 and RIPK3 via RHIM domain upon viral infection (Upton et al., 2012).

1.2.4 Crosstalk between NF-κB signalling and cell death pathways

The transcpritional activity of NF-κB induces the expression of target genes including a wide range of pro-survival proteins which antagonise the action of cell death pathway (Kucharczak et al., 2003). This includes, for instance, cIAP1/2 and XIAP, c-FLIP and Bcl-2 family member proteins, such as Bcl-2, Bcl-X$_L$ and A1. Also, it upregulates anti-oxidative protein and SODs, which quench ROS to prevent cell death mediated by oxidative stress in the liver (Kondylis et al., 2015).

Additionally, recent studies demonstrated that NF-κB pathway components suppress cell death independently of NF-κB's transcriptional activation. Indeed, IKK1/2 and NEMO have an additional role in inhibiting RIPK1-dependent cell death in addition to their role in activating NF-κB (Dondelinger et al., 2015; Kondylis et al., 2015; Vlantis et al., 2016). Mechanistically, the IKK complex appears to phosphorylate RIPK1 which prevents it from forming a death-inducing complex (Dondelinger et al., 2015). Also, RelA/p65 is capable of suppressing RIPK1-dependent apoptosis of intestinal Paneth cells and death of mouse embryos (Vlantis et al., 2016). Yet, it is still not entirely clear how RelA inhibits RIPK1-dependent cell death.

1.2.5 Implication of NF-κB and cell death pathways in mouse models of liver diseases

Cell death is one of the central players in inflammation. Previous studies highlighted the significance of protection against cell death in order to maintain tissue homeostasis. For instance, genetic deletions of anti-apoptotic proteins Mcl-1 and Bcl-X_L in liver parenchymal cells results in hepatocyte apoptosis and subsequent HCC formation (Weber et al. 2009, Hikita et al. 2012). These reports underpin the importance of apoptosis regulation to prevent liver inflammation and subsequent tumourigenesis.

The fact that NF-κB is a pivotal player of inflammatory signalling has led scientists to investigate the role of NF-κB signalling in liver cancer. The first study of NF-κB signalling in liver carcinogenesis employed Mdr2 knockout mice (Pikarsky et al, 2004). In this model, suppression of canonical NF-κB signalling by hepatocyte-specific expression of IκB super-repressor inhibits the progression to a malignant tumour via downregulation of anti-apoptotic factors (Pikarsky et al, 2004). In Mdr2 knockout mice, NF-κB activation was mediated by TNF produced by adjacent endothelial cells and immune cells. Consequently anti-TNF therapy also inhibits tumour progression (Pikarsky et al, 2004). Therefore, at least in Mdr2 knockout mice, NF-κB signalling is a tumour-promoting factor. Furthermore, truncation of a tumour suppressor and negative regulator of NF-κB signalling CYLD in hepatocytes also leads to periportal hepatocyte apoptosis, hepatitis, hepatomegaly, fibrosis and cancer (Nikolaou et al, 2012), whereas systemic CYLD deletion apparently does not recapitulate this phenotype (Massoumi et al., 2006; Reiley et al., 2006; Zhang et al., 2006).

Lymphotoxins and their receptor LTβR are upregulated in patients suffering from viral hepatitis or HCC. Ectopic expression of LTα and LTβ specifically in hepatocytes (AlbLTαβ mice) leads to chronic hepatitis from 6 months of age and HCC at 12 months (Haybaeck et al., 2009). Hepatitis and cancer development in AlbLTαβ mice were ameliorated by ablation of mature T and B cells by crossing to *Rag1*^{KO} mice. This indicates that lymphocytes play a major role in promoting hepatitis triggered by lymphotoxins. More importantly, the pathology is also prevented by deletion of IKK2 in hepatocytes. This evidence suggests that canonical NF-κB signalling in

hepatocytes, activated by lymphotoxins, is crucial for creating an inflammatory environment by producing chemokines including CCL2 and CXCL1 (Haybaeck et al., 2009, Wolf et al, 2010).

On the contrary to the studies demonstrating the pro-tumourigenic role of NF-κB, genetic models have illustrated the protective role of NF-κB against liver carcinogenesis. First, mice devoid of IKK2 specifically in hepatocytes are more susceptible to DEN-induced liver tumourigenesis (Maeda et al., 2005). IKK2 in hepatocytes suppresses DNA damage by a reduction in hepatic ROS via NF-κB activation (Maeda et al., 2005). Moreover, liver parenchymal deletion of NEMO triggers spontaneous hepatocyte apoptosis, fibrosis, steatohepatitis leading to eventual HCC formation (Luedde et al., 2007). This phenotype in NEMO-deficient livers is reversed by constitutive activation of IKK2 in hepatocytes (Kondylis et al., 2015). Furthermore, TAK1 deletion in hepatocytes results in early tumourigenesis and death of the animals (Betterman et al., 2010). Thus, these results demonstrate that NF-κB signalling is required for protection against liver carcinogenesis. It appears that optimal control of NF-κB activation is crucial for maintaining liver homeostasis as the abrogation of both activator and inhibitor of NF-κB can be a cause of liver inflammation and cancer.

Of note, deletion of NF-κB signalling components not only impairs NF-κB activation but also activates cell death pathways. Pasparakis and colleagues demonstrated that concomitant ablation of all the three NF-κB transcription factors, RelA, RelB and c-Rel, in mouse livers does not recapitulate the tumourigenic phenotype seen in NEMO-deficient livers, although it causes mild liver damage (Kondylis et al., 2015). RIPK1-dependent apoptosis plays a central role in initiating the inflammation and promotes carcinogenesis as co-ablation of RIPK1 and TRADD or inactivation of RIPK1 kinase activity prevents hepatocyte apoptosis and HCC in NEMO-deficient livers (Kondylis et al., 2015). Furthermore, caspase-8 deletion in hepatocytes also suppressed TAK1 deletion-mediated hepatocyte death and carcinogenesis (Vucur et al, 2013). This evidence suggests that apoptosis is a major driver of hepatitis-driven oncogenesis in the liver devoid of NEMO or TAK1.

1.3 Linear ubiquitination

1.3.1 Ubiquitination

Ubiquitination is one of the post-translational protein modifications where one or more ubiquitin molecules are attached to a target protein. Ubiquitin is an evolutionarily conserved small protein, consisting of 76 amino acids (8.6 KDa) (Hershko and Ciechanover, 1998). There are four genes encoding ubiquitin in mammals. Ubiquitin proteins are generated as polyubiquitin, where ubiquitin moieties are fused in a head-to-tail configuration, or expressed as fusion proteins Ub_{L40} and Ub_{S27}, a ubiquitin molecule conjugated to a ribosomal protein L40 and S27, respectively. These polyubiquitin precursors are cleaved by deubiquitinases to create a pool of free ubiquitin molecules (Kimura and Tanaka, 2010).

Ubiquitination is coordinated by sequential actions of three classes of enzymes: ubiquitin-activating enzymes (E1), ubiquitin-conjugating enzymes (E2) and ubiquitin ligating enzymes (E3) (Hershko and Ciechanover, 1998). First, E1 activates ubiquitin in an ATP-dependent fashion to form an intermediate ubiquitin adenylate, followed by generation of a thioester bond between the C-terminal glycine residue of a ubiquitin and a catalytic cysteine residue of an E1 enzyme. The activated ubiquitin is subsequently transferred to a cysteine residue in the active site of E2, which is a ubiquitin-carrier protein. In the last step, an E3 ligase catalyses the attachment of ubiquitin to target proteins. *H. sapiens* bears only two E1 enzymes, approximately 40 E2 enzymes and over 600 E3 ligases (Glickman and Ciechanover, 2002).

Ubiquitin can be conjugated together to form polyubiquitin, which adds a layer of complexity to this protein modification. Ubiquitin has seven lysine residues (Lys6, Lys11, Lys27, Lys29, Lys33, Lys48, and Lys63), and all of the lysines can be ubiquitinated. This type of ubiquitination results in the formation of an isopeptide bond between the carboxyl group of the C-terminal glycine of a ubiquitin and the ε-amino group of a lysine residue of another ubiquitin moiety (Kulathu and Komander, 2012). Additionally, an unconventional linkage was discovered and reported in 2006. The N-terminal methionine (Met1) of a ubiquitin moiety was found to be capable of mediating the di-ubiquitin linkage (Kirisako et al., 2006), where this peptide bond

generates the same polyubiquitins translated as ubiquitin precursors. Thus, depending on the lysine or methionine residue engaged in an inter-ubiquitin bond, two ubiquitin moieties can be tied with eight different possible di-ubiquitin linkages.

Each type of di-ubiquitin linkages confers distinct conformation of polyubiquitin. Lys6-, Lys11- and Lys48-linked di-ubiquitins take packed structures due to intramolecular interactions, whereas Lys63- and Met1-linked di-ubiquitins display rather stretched structures (Kulathu and Komander, 2012). The divergent topologies of each linkage mediate individual biological outcomes as they determine which ubiquitin receptors are bound to which linkage type and to which signalling complex (Shimizu et al., 2015). For instance, Lys48-linked polyubiquitin mediates the degradation of substrates, whereas Lys63- and Met1- linked polyubiquitin modulates intracellular signalling pathways (Kulathu and Komander, 2012).

More recently, ubiquitin modifications are perceived to be far more complex. A substrate protein is not necessarily ubiquitinated with a single type of linkages. It can be a mixture of multiple linkage types; for instance, Lys63- and Met1-linked polyubiquitin coexists on the same signalling molecule in TLR signalling, hence creating hybrid ubiquitin chains (Emmerich et al., 2013; Emmerich et al., 2016). Furthermore, ubiquitin can be phosphorylated or acetylated. Proteomics studies identified several potential phosphorylation sites and acetylation sites in ubiquitin (Swatek et al., 2016). Whilst the role of ubiquitin acetylation still remains elusive, scientists have started to understand the role of ubiquitin phosphorylation. Ubiquitin is phosphorylated at Ser65 by PINK1 on depolarised mitochondria, and subsequently phosphorylated ubiquitin activates ubiquitin E3 ligase Parkin (Koyano et al., 2014; Kane et al., 2014).

1.3.2 Linear ubiquitin and LUBAC

Among the eight ubiquitin linkage types, Met1-linked, or linear ubiquitination is an emerging type of non-proteolytic ubiquitin modification (Kulathu et al., 2012). Linear ubiquitination was first identified to be engaged in IL-1 and TNF signalling where it regulates NF-κB and MAPK signalling (Tokunaga et al., 2009; Haas et al., 2009). Linear ubiquitin is present in diverse innate and adaptive immune signalling

pathways and regulates their outputs, which is covered in more detail in the review I wrote during the PhD programme (Shimizu et al., 2015).

LUBAC is the only enzyme complex identified to date that generates the linear di-ubiquitin linkage *de novo*. LUBAC consists of HOIP, HOIL-1 and SHARPIN, where HOIP is the catalytic core component of LUBAC. HOIP and HOIL-1 are RBR E3 ubiquitin ligases, but HOIL-1 does not appear to have an E3 activity within LUBAC in cells, as the expression of the catalytically inactive mutant of HOIL-1 does not affect linear ubiquitin synthesis (Kirisako et al., 2006). Yet, HOIP alone is not sufficient to produce linear ubiquitin and it requires at least one of the other LUBAC components, HOIL-1 or SHARPIN, to do so efficiently (Gerlach et al., 2011, Ikeda et al., 2011, Tokunaga et al., 2011). This means that HOIP has a self-inhibitory regulation which is neutralised by binding to HOIL-1 or SHARPIN. HOIP interacts with the UBL domain of HOIL-1 and SHARPIN via its UBA domain (Kirisako et al., 2006; Tokunaga et al., 2011).

The C-terminal RBR domain and linear ubiquitin chain determining domain (LDD) of HOIP are the minimal catalytic core capable of forming Met1-linked di-ubiquitin linkage (Smit et al., 2012, Stieglitz et al., 2013). HOIP acts as a RING/HECT hybrid E3 ligase, similar to other members of the RBR E3 proteins including Parkin (Stieglitz et al., 2012). As a first step, HOIP binds to ubiquitin-loaded E2 via its RING1 domain so that E2 and E3 catalytic centres are aligned for ubiquitin transfer (Lechtenberg et al., 2016). Ubiquitin is subsequently transferred from E2 to HOIP RING2 domain. Next, in the proximity of the catalytic cysteine, a histidine residue in RING2 acts as a basic residue to activate the ε-amino group of Met1. Activated Met1 creates the thioester bond with the C-terminus of the proximal ubiquitin which is attached to catalytic cysteine (Stieglitz et al., 2013).

Interestingly, a most recent study reported an allosteric regulation on HOIP by an additional ubiquitin molecule, which interacts with the third ubiquitin binding region (UBR3) of HOIP within its RBR domain (Lechtenberg et al., 2016). This allosteric regulation promotes a conformational change in HOIP's RBR domain to accommodate an activated ubiquitin, and thereby enables linear di-ubiquitin linkage formation. In accordance, the regulation via UBR3 is required for activation of HOIP E3 activity and NF-κB activating capacity.

In TNF signalling, where LUBAC was first identified in a signalling complex, LUBAC is recruited to the TNF-RSC depending on the E3 activity of cIAP1/2 and ubiquitinates RIPK1, NEMO, TRADD and TNFR1 (Haas et al., 2009; Gerlach et al., 2011; Draber et al., 2015) (also see Figure 1.2). LUBAC not only regulates NF-κB and MAPK signalling but also, more importantly, prevents TNF-induced cell death (Haas et al., 2009; Gerlach et al., 2011; Ikeda et al., 2011; Peltzer et al., 2014).

1.3.3 *In-vivo* function of linear ubiquitination

The role of linear ubiquitin in animal models has been extensively examined using chronic proliferative dermatitis mice (C57BL/KaLawRij, referred to as *cpdm* mice). *Cpdm* mice harbour a single-base pair deletion in the first exon in the *Sharpin* gene leading to complete loss of the SHARPIN protein (Seymour et al, 2007). *Cpdm* mice develop chronic proliferative dermatitis and multi-organ inflammation, such as in the liver, intestine and joint, at 3-4 weeks of age (HogenEsch et al., 1992). In addition, *cpdm* mice display immune aberrations such as loss of Peyer's patches and disorganisation of lymphoid architecture (HogenEsch et al., 1999). The loss of SHARPIN is causative for both inflammatory and lymphoid phenotypes (Seymour et al, 2007).

Researchers investigated the role of inflammatory mediators in *cpdm* mice to understand how *cpdm* mice develop spontaneous inflammation. However, lymphocyte or eosinophil depletion is unable to ameliorate inflammation. By contrast, *cpdm* skin transplantation to nude mice transferred the donor's skin pathology to the recipient (Gijbels et al., 1995), which suggested that the aetiology of the dermatitis is intrinsic in the *cpdm* skin.

Strikingly, genetic ablation of TNF or TNFR1 rescues the inflammatory phenotype in *cpdm* mice; however, their lymphoid aberration is unaltered by TNF or TNFR1 deletion (Gerlach et al., 2011; Kumari et al., 2014). TNF-induced cell death is causative for *cpdm* phenotype, as genetically demonstrated by the following studies; co-deletion of RIPK3 and heterozygosity of caspase-8 (Rickard et al., 2014), epidermal ablation of FADD with systemic deletion of RIPK3 (Kumari et al., 2014), and RIPK1 kinase inactivation (Berger et al., 2014) corrected the *cpdm* phenotypes, including lymphoid distortion. These studies together illustrated that the inflammatory

and immune phenotype is mediated by cell death triggered by SHARPIN deficiency, which firmly support the notion that cell death is a leading cause of inflammation.

In contrast to *cpdm* mice, deletion of the catalytic component of LUBAC, HOIP, leads to embryonic lethality at mid-gestation due to aberrant endothelial cell death (Peltzer et al., 2014). This cell death is rescued by TNFR1 deletion, suggesting that TNFR1-mediated cell death is responsible for mid-gestational death of the animals, although it does not rescue their death at late gestation. Mutant mice expressing catalytically inactive HOIP also suffer from embryonic lethality at a similar stage to HOIP-deficient embryos (Emmerich et al., 2013). Our group also found that HOIL-1 knockout mice manifest an equivalent phenotype to HOIP knockout animals (Peltzer et al., manuscript in preparation), whilst HOIL-1 knockout mice were previously reported to be viable by another group (Tokunaga et al., 2009). HOIL-1-deficient mice made by Tokunaga *et al.* exhibit amylopectin-like deposits in the myocardium but show minimal signs of hyper-inflammation (MacDuff et al., 2015). Moreover, loss-of-function mutations of *HOIL-1* and *HOIP* genes in human are causative for autoinflammation, immunodeficiency, amylopectinosis, and lymphangiectasia (Boisson et al., 2012; Boisson et al., 2015).

1.3.4 LUBAC substrates and regulation of signalling

Recent studies identified several targets of linear ubiquitination in multiple immune signalling pathways. Among them, TNFR1 and NOD2 signalling pathways are best characterised. In TNFR1 signalling, RIPK1 and NEMO are identified to be linearly ubiquitinated upon stimulation by mass-spec analysis (Gerlach et al., 2011). Furthermore, affinity purification assay for linear ubiquitin unravelled that TNFR1 and TRADD are additional substrates of LUBAC (Draber et al., 2015).

In NOD2 signalling, RIPK2 is the only protein that is linearly ubiquitinated and predominantly ubiquitinated upon MDP stimulation, as defined by mass-spec analysis using stable isotope labelling with amino acids in cell culture (SILAC) approach (Fiil et al., 2013). Functionally, linear ubiquitination of RIPK2 is required for optimal NF-κB and MAPK signalling outputs by recruiting IKK complex.

1.3.5 Deubiquitinases for linear ubiquitin chains

Deubiquitinases (DUBs) remove ubiquitin from substrates and process ubiquitin precursors after translation of initial polyubiquitin (Komander, 2009). Functions of DUBs are characterised by which ubiquitin chain they hydrolyse. Biological roles of DUBs on non-degradative ubiquitin modifications, including on Met1-mediated linkages, is at present not entirely clear. Interestingly, two DUBs, OTULIN and CYLD are capable of cleaving Met1-linked ubiquitin, and they have recently been shown to be a part of a complex with LUBAC (Figure 1.4) (Takiuchi et al., 2014). Of note, LUBAC-OTULIN and LUBAC-CYLD complexes exist in a mutually exclusive fashion (Draber et al., 2015).

1.3.5.1 OTULIN

OTULIN, or FAM105B, is a member of the OTU family of DUBs (Keusekotten et al., 2013). While the other 14 annotated OTU DUBs do not cleave Met1-linked diubiquitin, OTULIN is highly specific for cleaving linear ubiquitin linkage as compared to Lys63-linked di-ubiquitin (more than 100-fold) and it retains its specificity even at a very high concentration (Keusekotten et al., 2013; Rivkin et al., 2013; Hospenthal et al., 2015). OTULIN interacts with the PUB domain of HOIP via its PIM motif, which is regulated by phosphorylation of Tyr56 in OTULIN. This phosphorylation prevents the binding of OTULIN to HOIP (Schaeffer et al., 2014, Elliot et al., 2014). However, it is unknown which kinase and phosphatase control phosphorylation state of the tyrosine residue of OTULIN.

In line with a role for OTULIN in counteracting linear ubiquitination, OTULIN deficiency in cells greatly enhances the amount of linear ubiquitin in the cytosol (Draber et al., 2015). The role of OTULIN in TNF and NOD2 signalling has been controversial. Whilst a study identified OTULIN as a component of the TNF-RSC by mass spectrometry analysis (Wagner et al., 2016), our laboratory reported that OTULIN is not recruited to TNF- and NOD2- signalling complexes and does not drastically affect linear ubiquitination in these complexes (Draber et al., 2015). Furthermore, other groups claimed that OTULIN overexpression delays LUBAC-mediated NF-κB and JNK activation upon TNF, whereas the inducible knockdown of OTULIN increases these signalling outputs (Keusekotten et al., 2013; Fiil et al.,

2013). It appears that the interaction of OTULIN within those complexes is transient and unstable and therefore in some cases OTULIN does not drastically affect the signalling outcome of those signalling when expressed at physiological levels.

Loss-of-function mutations of *Otulin/Fam105b* gene in mice are causative for the *gumby* phenotype, which manifests reduced craniofacial vasculature and embryonic lethality at mid-gestation (Rivkin et al., 2013). *Gumby* mice exhibit abnormal vessel branching in the head and trunk, whereas the major vessels develop normally. OTULIN is shown to bind to dishevelled 2(DVL2), a Wnt signalling adaptor, suggesting that linear ubiquitination could be involved in canonical Wnt signalling and mediates angiogenesis during development (Rivkin et al., 2013). Yet, the mechanism as to how LUBAC and OTULIN would regulate Wnt signalling remains enigmatic.

1.3.5.2 CYLD

Cylindromatosis (CYLD) is a tumour suppressor belonging to the USP family of DUBs. CYLD preferentially cleaves Lys63- and Met1- ubiquitin linkages. Mutations in *Cyld* gene are responsible for familial cylindromatosis (Bignell et al., 2000), where the majority of mutations are clustered around the catalytic USP domain. Loss of CYLD leads to aberrantly increased activation of NF-κB (Sun, 2010). Loss of CYLD function in mice is associated with the formation of inflammation-associated cancers including colorectal, skin and liver cancer (Massoumi et al., 2006; Zhang et al., 2006; Nikolaou et al., 2012). Furthermore, CYLD is downregulated in multiple cancers such as colon and liver cancer in human (Pannem et al., 2014). CYLD plays a role in various immune signalling pathways and hydrolyses ubiquitin chains on several signalling components and thereby shut off signal transduction.

CYLD is also important for cell death induction via TNFR1 as it has been shown to be required for the induction of necroptosis by facilitating the formation of complex II of TNFR1 signalling. Activated caspase-8 can cleave CYLD which results in its degradation and prevention of CYLD-dependent necroptosis (O'Donnell et al., 2011).

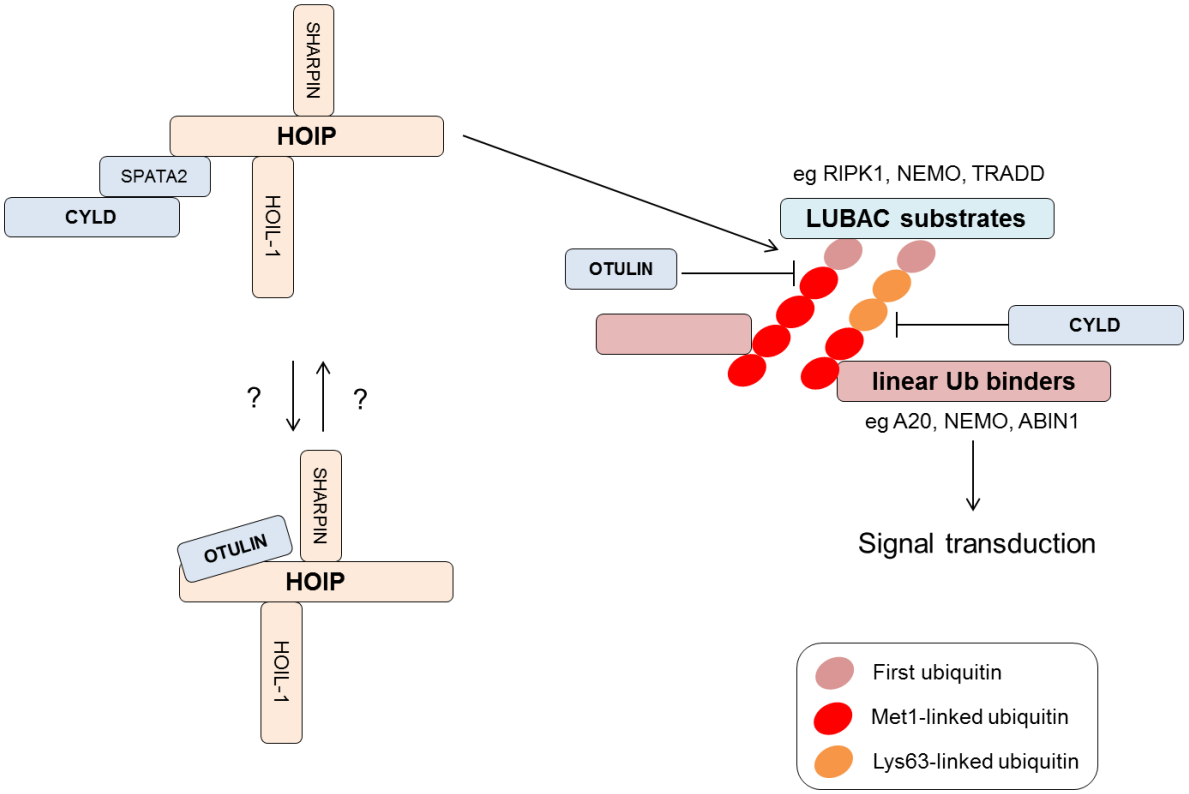

Figure 1.4 LUBAC-mediated signalling. LUBAC-CYLD complex appears to be predominantly recruited to the receptor signalling whereas LUBAC-OTULIN complex stays in the cytosol. Recruited LUBAC ubiquitinates substrates to facilitate signalling, which is counteracted by CYLD and, possibly, OTULIN to regulate signalling. In addition to ubiquitination and deubiquitination, linear ubiquitin binders are bound on linear polyubiquitin, and further potentiate or regulate its signalling outputs.

CYLD is constitutively associated with LUBAC (Takiuchi et al., 2014). However, the association is indirect; SPATA2 has been identified as a bridging factor between CYLD and LUBAC, and is essential for CYLD to be recruited to the TNF-RSC (Wagner et al., 2016; Kupka et al., 2016). SPATA2 is bound to the PUB domain of HOIP and the USP domain of CYLD. Also, the recruitment of CYLD to the TNF-RSC is dependent on the scaffolding function of HOIP, but not on its catalytic activity (Draber et al., 2015). It appears that LUBAC, SPATA2 and CYLD are together recruited to the TNF-RSC and CYLD inhibits LUBAC-mediated NF-κB activation in the complex by cleaving Lys63-linked and linear ubiquitin therein (Figure 1.4).

1.3.6 Linear ubiquitin-binding proteins

LUBAC regulates the function of its substrates by ubiquitination, but ubiquitins must be recognised by other proteins to fully exert its function to signal to the downstream. Figure 1.4 indicates how LUBAC can mediate the signalling by ubiquitination, and ubiquitin is 'read' by ubiquitin receptors, or binders. Within ubiquitin receptors, most of the ubiquitin binding domains interact specifically with particular types of ubiquitin linkages. Therefore these binders are recruited to specific ubiquitin linkages on particular targets in signalling complexes (Shimizu et al., 2015).

Studies have shown that the ubiquitin binding domains in NEMO, ABIN-1 and A20 bind preferentially to linear ubiquitin for Met1-linked polyubiquitin. It is crucial for understanding the biological role of linear ubiquitination by reviewing the nature of these proteins.

1.3.6.1 NEMO

The adaptor protein NEMO/IKKγ is engaged in the IKK complex with the kinase heterodimer IKKα/β, which phosphorylates IκBα and activates canonical NF-κB signalling. NEMO harbours a C-terminal ubiquitin recognition motif, the UBAN motif. The UBAN motif specifically recognises linear ubiquitin over Lys48- and Lys63-linked polyubiquitin (Rahighi et al., 2009). NEMO mutations are causative for incontinentia pigmenti and anhidrotic ectodermal dysplasia with immunodeficiency (EDA-ID) (Aradhya et al., 2001; Döffinger et al., 2001). Noteworthy, mutations in the UBAN domain of NEMO are linked to EDA-ID (Döffinger et al., 2001; Hubeau et al., 2011). A point mutation in its UBAN motif hampers the binding to polyubiquitins, particularly linear chains, and thereby dampens IKK activation and increases susceptibility to TNF-induced cell death, despite an unaltered folding of NEMO protein (Wu et al., 2008; Rahighi et al., 2009; Hubeau et al., 2011; O'Donnell et al., 2012).

Loss of NEMO in different tissues results in severe inflammation. NEMO deletion in skin epithelium leads to perinatal lethality preceded by dermatitis, which is reminiscent of incontinentia pigmenti phenotype in humans (Nenci et al., 2006). Also, the intestinal ablation of NEMO results in severe spontaneous colitis (Nenci et al., 2007). In both cases, TNF drives the inflammation and, at least in the latter,

inflammation due to NEMO deficiency was driven by RIPK1-dependent cell death (Vlantis et al., 2016). By contrast, LPC-specific deletion of NEMO leads to TNF-independent steatohepatitis and liver carcinogenesis (Luedde et al., 2007; Ehlken et al., 2014). NEMO together with IKKα/β suppresses activation of RIPK1 to undergo cell death (Dondelinger et al., 2015). Thus, the recognition of linear ubiquitin is essential for NEMO to optimally activate NF-κB signalling and prevent aberrant cell death.

1.3.6.2 ABIN-1

ABIN-1 harbours a C-terminal UBAN motif, similar to NEMO, which preferentially binds to linear ubiquitin as compared to Lys63-linked chains (Nanda et al., 2011). ABIN-1 suppresses NF-κB activation in TNFR1 and TLR signalling by binding to NEMO (Mauro et al., 2006). ABIN-1 restricts TNF-induced cell death by binding to ubiquitin chains (Oshima et al., 2009).

Deletion of ABIN-1 in mice causes lethality late during embryonic development. Its lethality is rescued by concomitant TNF ablation, and TNF-induced cell death appears to be accountable for the cause of death of ABIN-1-deficient embryos (Oshima et al., 2009). A missense mutation in its UBAN domain leads to loss of binding capacity to Met1- and Lys63-linked ubiquitins and cells expressing this mutant fail to protect against TNF-induced cell death (Oshima et al., 2009; Nanda et al., 2011). The knock-in mice of UBAN mutant of ABIN-1 spontaneously develop immune defects including lymphadenopathy and autoimmunity. Interestingly, these immune abnormalities are corrected by MyD88 deficiency (Nanda et al., 2011). Yet, the UBAN mutant mice did not phenocopy the embryonic lethality of ABIN-1-deficient mice, suggesting that ABIN-1 has other regulatory domains to modulate immune signalling.

1.3.6.3 A20

A20 (also known as TNFAIP3) has an OTU domain at the N-terminus and seven ZF domains at the C-terminus (Ma et al., 2012). The function of A20's DUB activity has been controversial. A20 was initially thought to act as a suppressor of NF-κB by cleaving Lys63-linked ubiquitin linkages (Wertz et al., 2004, Wertz et al., 2015).

However, other studies indicated that A20 is incapable of hydrolysing Lys63-linked ubiquitin linkages (Lin et al., 2008; Mevissen et al., 2013; Ritorto et al., 2014). Following studies showed that A20 binds to linear ubiquitin and stabilises it and that, on the other hand, the presence of linear ubiquitin prevents the DUB activity of A20 (Draber et al., 2015; Wertz et al., 2015).

A20 inhibits activation of NF-κB in various immune signalling including TNFR1, CD40, IL-1R/TLR (Wertz et al., 2004; Turer et al., 2008; Hitotsumatsu et al., 2008, Chu et al., 2011). A20-deficient mice develop multi-organ inflammation in a MyD88-dependent manner, and suffer from lethality within two weeks of birth (Lee et al., 2000; Turer et al., 2008). A20-deficient cells show TNF-induced NF-κB hyperactivation and also increased cell death. However, inactivation of A20's DUB activity in the OTU domain does not elicit spontaneous inflammation in mice, and neither is it required for prevention of TNF-induced cell death (De et al., 2014; Draber et al., 2015). The inactive mutant only marginally impacts NF-κB activation in macrophages and dendritic cells (De et al., 2014). The OTU domain appears to regulate ubiquitination of TNFR1 and contribute to the inhibition of inflammation, but the precise mechanism is unclear (Wertz et al., 2015).

A20 has two ubiquitin binding sites in its C-terminus, the ZF4 and ZF7 domains. The ZF4 motif is the preferential binding site to Lys63-linked, as compared to Lys11-, Lys48- or Met1-linked polyubiquitin (Bosanac et al., 2010). Mutation of ZF4 in mice does not affect their development (Lu et al., 2013), although ubiquitin binding of ZF4 is required for attenuation of TNFR1 signalling (Bosanac et al., 2010; Lu et al., 2013; Wertz et al., 2015). In contrast to ZF4, the ZF7 domain specifically binds to linear ubiquitin and is essential for recruitment of A20 to the TNF-RSC, depending on the presence of linear polyubiquitin (Tokunaga et al., 2013; Draber et al., 2015). The ZF7 motif directly inhibits TAK1-dependent activation of NF-κB signalling by binding to polyubiquitin chains (Skaug et al., 2013, Verhelst et al., 2013, Tokunaga et al., 2013). Also, TNF-induced cell death was suppressed by linear ubiquitin binding of ZF7 (Draber et al., 2015). It appears that concerted actions of the OTU, ZF4 and ZF7 domains are essential for the anti-inflammatory function of A20 as none of the mutants of single domains fully recapitulates the phenotype of systemic A20 deficiency.

1.4 Aims of the project

Our laboratory and others have investigated the role of LUBAC and established that linear ubiquitination regulates NF-κB signalling as well as MAPK signalling and prohibits TNF-induced cell death. Furthermore, perturbation of TNFR1 signalling is strongly associated with liver pathogenesis in mice.

The aim of this research is to elucidate the role of linear ubiquitination in the liver parenchyma by observing how linear ubiquitination or its loss impacts inflammation and cell death in the development of hepatitis, and possibly, liver cancer formation. The major research questions are:

1. Does perturbation of linear ubiquitination in hepatocytes exacerbate or prevent the induction of hepatitis and/or HCC *in vivo*? If so, what is the mechanism engaged?

2. How does perturbation of linear ubiquitination in hepatocytes alter their response to TNF and other death receptor ligands, such as TRAIL and CD95L, in terms of gene activation and cell death induction?

To answer these questions, I have utilised a mouse model relying on HOIP deficiency in liver parenchymal cells. On the basis of this model, I have investigated the role of linear ubiquitination in regulating cell death and inflammation in the liver and how this affects liver carcinogenesis with the aim to broaden our understanding of hepatic diseases.

Chapter 2

2 Material and methods

2.1 Material

2.1.1 Chemical and reagents

All the chemicals and reagents used in this thesis were purchased from the following companies unless stated otherwise: Abcam, Biovision, Merck, Invitrogen, Pierce, R&D systems, Roche, Roth and Sigma-Aldrich. All chemicals were purchased in pA quality unless indicated otherwise.

2.1.2 Inhibitors

inhibitor name	manufacturer
Complete Protease Inhibitor Cocktail	Roche
PhosSTOP	Roche
Sodium fluoride (NaF)	Sigma-Aldrich
Sodium Orthovanadate (Na_3VO_4)	Sigma-Aldrich
Necrostatin-1	Sigma-Aldrich
Nec-1s	Biovision
QVD-fmk (QVD)	R&D systems
zVAD-fmk (zVAD)	Abcam

2.1.3 Buffers and solutions

Primary antibody diluent	2.5% (w/v) BSA in PBS-T
Blocking Buffer	2.5% (w/v) skimmed milk in PBS-T
Citrate Buffer	10 mM sodium citrate, pH 6.0
Freezing medium (for cells)	90 % FCS (v/v) 10 % DMSO (v/v)

IP-lysis Buffer	30 mM Tris-Base, 120 mM NaCl, 2 mM EDTA, 2 mM KCl, 10 % Glycerol (v/v), 1 % Triton X-100 (v/v)
PBS	137 mM NaCl, 8.1 mM Na_2HPO_4, 2.7 mM KCl, 1.5 mM KH_2PO_4
PBS-T	PBS, 0.05% (v/v) Tween-20
Liver perfusion buffer	NaCl 8 g/L, KCl 0.2 g/L, Na_2HPO_4 33 mg/L, HEPES 2.38 g/L, pH 7.65
RIPA buffer:	50 mM Tris HCl pH 8.0, 150 mM NaCl, 1% NP-40, 0.5% sodium deoxycholate, 0.1% SDS
Stripping buffer	50 mM glycine, pH 2.3
TBS:	150 mM NaCl, 20 mM Tris, pH7.6
TEX buffer:	10 mM Tris, 1 mM EDTA, 0.1% Triton X-100 pH 8.0
Transfer buffer:	25 mM bicine, 25 mM Tris, 1 mM EDTA, 10% Methanol (v/v), pH 7.2
Tris-EDTA buffer:	10 mM Tris, 1 mM EDTA, pH 8.0

2.1.4 Biological agents

agent	source
His-TNF	previously produced in *E.coli* and purified in our laboratory (kindly provided by Dr Peter Draber)
iz-TRAIL (mouse)	produced in *E.coli* and purified
CD95L-Fc	previously produced in HEK293T cells (kindly provided by Mr Torsten Hartwig)

2.1.5 Antibodies

Unconjugated primary antibody for western blot

antibody	manufacturer	catalogue number	host/isotype
Bax	Santa Cruz	sc-7480	mouse IgG2b
Bcl-2	Santa Cruz	sc-7382	mouse IgG1
Bcl-xL	Cell signaling	2764	rabbit
Bid	R&D systems	AF860	goat
caspase-8	Enzo Life Sciences	ALX-804-447	rat
c-FLIP	Adipogen	AG-20B-0005	rat
cIAP1/2	R&D systems	315301	mouse IgG2a
cleaved caspase-3	Cell Signaling	9661	rabbit
cleaved caspase-8	Cell Signaling	9429	rabbit
ERK1/2	Cell Signaling	9102	rabbit
FADD	Assay Design	AAM-121	mouse IgG1
GAPDH	Abcam	ab8245	mouse IgG1
HOIL-1	in-house	-	mouse IgG2a
HOIP	in-house	-	rabbit
IκBα	Cell Signaling	9242	rabbit
JNK	Cell Signaling	9258	rabbit
Mcl-1	Cell signaling	94296	rabbit
phospho-ERK	Cell Signaling	9101	rabbit
phospho-IκBαα	Cell Signaling	9246	mouse IgG1
phospho-JNK	Cell Signaling	4671	rabbit
RIPK1	BD Biosciences	610459	mouse IgG2a
RIPK3	Enzo Life Sciences	ADI-905-242	rabbit
SHARPIN	Proteintech	14626-1-AP	rabbit
XIAP	Cell Signaling	2042	rabbit

Unconjugated primary antibody for immunoprecipitation

antibody	manufacturer	catalogue number	isotype
FADD	Santa Cruz	sc-6036	goat

Unconjugated primary antibody for immunofluorescence

antibody	manufacturer	catalogue number	isotype
F4/80	AbD serotec	MCA497G	rat
γH2AX	Cell Signaling	9718	rabbit
HNF4	Abcam	ab41898	mouse IgG2a
Ki-67	Abcam	ab16667	rabbit
Ly6G	Biolegend	4767	rat
p21	BD Biosciences	556430	mouse IgG1

Conjugated primary antibody for flow cytometry

antibody	manufacturer	catalogue number	fluorophore
B220	Biolegend	103243	Brilliant Violet 650
CD3	Biolegend	100326	PerCP
CD4	eBioscience	25-0041-82	PE-Cy7
CD45	Biolegend	103128	Alexa Fluor 700
CD8	Biolegend	100714	APC-Cy7
F4/80	Biolegend	123110	PE
Ly6G	Biolegend	127606	FITC
NK1.1	Biolegend	108731	Brilliant Violet 421

2.1.6 Cell culture media and supplements

Antibiotic-Antimycotic (100x)	Gibco
BSA fraction V (7.5%)	Gibco
DMEM	Gibco
PenStrep (100x)	Gibco
Trypsin/EDTA	Gibco
William's E medium, Glutamax supplement	Gibco

2.1.7 Ready-to-use kits and solutions

BCA Protein assay	Pierce
ECL Plus	PerkinElmer
RevertAid cDNA synthesis kit	Thermo Scientific
RNeasy mini kit	Qiagen
TUNEL	Millipore
TSA Ampflification kit	PerkinElmer

2.1.8 Consumables

Cell Culture Petri dishes	TPP
Cell Culture Plates (6-, 12-, 24-well)	TPP
Cell strainer (40 µm, 70 µm)	BD Biosciences
Conical tubes (15 ml and 50 ml)	TPP
Cryogenic vials	Nunc
Dialysis membrane	KMF
LDS-Sample buffer	Invitrogen
NuPAGE® 4-12% Bis-Tris Gels	Invitrogen
PCR Tubes	StarLab
Pipette tips (0.1-10, 1-200, 101-1000 µl)	StarLab
Plastic pipettes (5 ml, 10 ml and 15 ml)	StarLab
Polypropylene round bottom tube (5 ml)	BD Biosciences
Round and flat bottom 96-well test plates	TPP
Safe-Lock Reaction Tubes (1,5ml, 2 ml)	Eppendorf
SeeBlue Plus2 Pre-Stained Standards	Invitrogen
Single-Use Syringe (1ml, 5 ml, 50 ml)	Terumo
Single-Use Scalpel	Feather
Single-Use Needles	BD Biosciences
SmartLadder DNA Standards	Eurogentec
Sterile filter (0.22 µm)	Millipore

Tissue Culture flasks (75, 150 cm^2)	TPP
Whatman paper	Schleicher&Schuell
X-Ray film	VWR

2.1.9 Instruments

Accuri C6	BD Biosciences
Blotting equipment	Invitrogen
Digital Camera	Olympus
Evos FL	Life Technologies
Fortessa LSR II	BD Biosciences
Freezer -20°C	Liebherr
Freezer -80°C	Forma Scientific
Gene Amplification PCR system 9700	Applied Bioscience
Light Microscope	Zeiss
LaboStar™ TWF Water Purification	Evoqua
Microwave	AEG
Mithras	Berthold
Multiskan Ascent	Thermo Labsystems
NanoDrop Spectrophotometer ND-1000	NanoDrop Technologies
pH Meter	Mettler
Pipetboy	Integra Bioscience and StarLab
Pipettes (10 µl, 100 µl, 200 µl, 1 ml)	Gilson and Eppendorf
Power Supply for agarose gels	BioRad
Table Centrifuge Biofuge	Heraeus
Thermomixer compact	Eppendorf
Vortex	Heidolph
X-Ray film Developer	KONICA

2.1.10 Software

Adobe Photoshop CS6	Adobe
Adobe Illustrator CS6	Adobe
ApE	Wayne Davis (University of Utah)
Ascent Software Version 2.6	Thermo Labsystems
EndNote	Thomson Reuters
FACSDiva	BD Biosciences
FlowJo 7.6.5	TriStar
GraphPad Prism 6	GraphPad Software
ImageJ	NIH
Microsoft Excel 2010	Microsoft
Microsoft Powerpoint 2010	Microsoft
Microsoft Word 2010	Microsoft
ND1000 V3.3.0	NanoDrop Technology

2.2 Cell biological methods

2.2.1 Isolation and culture of mouse primary hepatocytes

Primary hepatocytes were isolated from 7-12 week-old mice. First, mice were anaesthetised with ketamine and xylazine. Mice were cannulated via the inferior vena cava and subsequently the portal vein was incised. Mouse livers were perfused with warm perfusion buffer supplemented with 0.5 mM EDTA for 7 minutes. The Second perfusion with warm perfusion buffer plus 0.5 mg/ml collagenase (Sigma, C5138) and 10 mM $CaCl_2$ was subsequently performed for 3 minutes. Digested livers were isolated in warm hepatocyte culture medium (William's E medium Glutamax supplement with 1x Antibiotic-antimycotic, 0.1 % (w/v) BSA fraction V and 25 nM dexamethasone (Sigma)) with 10% FCS. Liver lobules were opened with forceps and scissors and vigorously shaken in the medium to release cells. Cells were passed through 70 um nylon mesh and spun at 29×g for 2 minutes at room temperature. Cell pellets were washed twice with hepatocyte culture medium with

FCS. Live cell numbers were counted by means of trypan blue exclusion. Isolated hepatocytes were plated on plates coated with collagen type I (Sigma, C3867) in hepatocyte culture medium with 10% FCS at 37ºC in humidified 5% CO_2 chamber. The culture media were replaced 3-4 hours after plating with hepatocyte culture medium without FCS.

2.2.2 Cell viability assay

Culture media were removed and primary hepatocytes were lysed in diluted Cell Titer Glo solution (1:6 in PBS) (Promega). Cell lysates were incubated on a shaker for 10 minutes, and lysates were transferred to opaque 96-well plates for measurement. Luminescence reflecting the ATP level in cells was quantified with Mithras (Berthold).

2.3 Biochemical methods

2.3.1 iz-TRAIL production from *E.coli*

Endotoxin-free isoleucine zipper-tagged murine TRAIL (izTRAIL) was purified from Rosetta strain of *E.coli* transformed with plasmid encoding izTRAIL as described by Ganten *et al*. (Ganten et al., 2005). *E.coli* lysate were subjected to a sequential purification employing AKTA micro system with hydroxyapatite column and Ni-NTA column to obtain concentrated fraction. Purified fractions were evaluated by means of UV absorbance, Bradford protein assay and SDS-PAGE. Level of contaminating LPS was examined by LAL assay.

2.3.2 Preparation of cell lysates from primary cells for western blot

Cells were lysed with ice-cold IP lysis buffer supplemented with Complete protease inhibitor cocktail (the solution prepared by dissolving a tablet in water, and added to lysis buffer in 1:50), 10 mM NaF and 1mM Na_3VO_4. Lysates were spun at 13300 rpm at 4°C for 15 minutes to remove insoluble fraction. Supernatants were mixed with 4x LDS sample buffer with 50 mM DTT (3:1) and boiled at 92°C for 5 minutes for PAGE.

2.3.3 Liver lysate preparation for western blot

Livers were dissected from 4 week-old mice, snap-frozen in liquid nitrogen and stored at -80ºC until the following manipulation. Frozen livers were processed with a mortar and a pestle pre-chilled with liquid nitrogen until tissues became a fine powder. Processed livers were incubated in ice-cold RIPA buffer with Complete protease inhibitor cocktail solution (1:50) and PhosSTOP soliution (1:50) at 4ºC. Lysates were vortexed briefly and sonicated for 20 seconds four times, with one-minute intervals on ice between each sonication. Lysates were incubated with continuous inversion for another 10 minutes. Samples were spun at 15000 *g* at 4ºC for 15 minutes to remove insoluble fraction.

2.3.4 Determination of protein concentration

Protein concentrations of liver lysates were determined by BCA protein assay (Pierce) with BSA as a protein standard. RIPA buffer was added to each sample to adjust protein concentration.

2.3.5 Immunoprecipitation

For immunoprecipitation for FADD-associated complex, cell lysates were diluted in IP lysis buffer. Lysates were pre-cleared with Sepharose CL-4B (Sigma) for 2 hours. Protein G-coupled sepharose (GE) was blocked with 1% BSA in IP lysis buffer for 1 hour and washed extensively with IP lysis buffer prior to incubation. Pre-cleared lysates were incubated overnight with blocked Protein G-coupled sepharose and anti-FADD (M-19) antibody or isotype control, normal goat IgG (Santa Cruz), at 4ºC. Beads were washed 5 times with ice-cold IP lysis buffer and vortexed and proteins were eluted in 1x LDS buffer at 92ºC.

2.3.6 Polyacrylamide gel electrophoresis

Denatured lysates were separated on 4-12% Bis-Tris NuPAGE gel (Invitrogen) with MOPS buffer at 80 V for 15 min and at 180 V for 50 min.

2.3.7 Western blotting

Proteins separated on polyacrylamide gels were transferred to nitrocellulose-based membranes by wet or semi-dry transfer using 1x transfer buffer. Membranes were blocked with blocking buffer for 1 hour and they were washed briefly with PBS-T and were incubated overnight with primary antibodies diluted in 2.5% (w/v) BSA (VWR) in PBS-T plus 0.1% (w/v) sodium azide. Membranes were washed briefly with PBS-T and were incubated with HRP-conjugated secondary antibodies for 1-2 hours. Membranes were washed extensively with PBS-T (at least 3 times) and developed with ECL plus substrate (Pierce) using X-ray films (VWR).

2.3.8 Stripping of Western blot membranes

Protein-transferred membranes were incubated with acidic stripping buffer (pH 2.3) to remove antibodies prior to the incubation with another primary antibody of the same host/isotype as previously used.

2.3.9 Tissue RNA extraction and RT-qPCR

Snap-frozen liver pieces were broken into fine powder with a mortar and a pestle and RNA was extracted from livers using RNeasy Mini kit (Qiagen). Purified RNA was subsequently employed for cDNA synthesis using RevertAid First Strand cDNA Synthesis Kit and poly A primer (Thermo Scientific). Synthesised cDNA was used for RT-PCR, with ROX polymerase mix, Universal Probe system (Roche) and specific primers:

IL-6 forward	GCTACCAAACTGGATATAATCAGGA
IL-6 reverse	CCAGGTAGCTATGGTACTCCAGAA
TNF forward	CTGTAGCCCACGTCGTAGC
TNF reverse	TTGAGATCCATGCCGTTG
Hprt forward	TGATAGATCCATTCCTATGACTGTAGA
Hprt reverse	AAGACATTCTTTCCAGTTAAAGTTGAG
Light forward	CTGCCAGATGGAGGCAAA
Light reverse	GGTCCACCAATACCTATCAAGC
LTb forward	GGGGAACCAGAAACTGACCT
LTb reverse	CCTTGCCCACTCATCCAA
CCL3 forward	TGCCCTTGCTGTTCTTCTCT
CCL3 reverse	GTGGAATCTTCCGGCTGTAG

CXCL1 forward	GACTCCAGCCACACTCCAAC
CXCL1 reverse	TGACAGCGCAGCTCATTG

2.4 Animal studies

All the animal studies stated are conducted according to the appropriate licence under Animals (Scientific Procedures) Act 1986.

2.4.1 Liver-specific HOIP knockout mice

HOIP-floxed mice were generated at the Walter and Eliza Hall (Melbourne, Australia) (Peltzer et al., 2014). HOIP-floxed mice were subsequently crossed to *Alb-Cre* mice (purchased from Jackson laboratories) for analysis. Both strains had and were maintained in C57BL/6 background. Mice were maintained in Charles River (Margate, UK) or UCL Biological Service Unit (London, UK) under the specific pathogen-free condition and 12-hour dark/light cycle, and fed *ad libitum* with standard chow.

2.4.2 Crossings

TNFR1 knockout mice (Pfeffer et al., 1993) were obtained from Jackson laboratories. They were derived from mixed 129S2/Sv and C57BL/6 background but were maintained in C57BL/6 background. Caspase-8 knockout mice were kindly provided by Dr William Kaiser, which were maintained in C57BL/6 background. MLKL knockout mice were generated in C57BL/6 background in our laboratory using transcription activator-like effector nuclease (TALEN) designed by Mr Sebastian Kupka. Liver-specific HOIP knockout mice were crossed to these mice for analysis.

2.4.3 Genotyping

Mice were sampled at 2-3 weeks of age for genotyping. Ear or tail samples were lysed in genotyping lysis buffer at 95°C for 30 min, and neutralised with an equal amount of genotyping neutralising buffer. Samples were preserved at 4°C until use.

PCR mix was prepared with 5 Prime master mix or Dream Taq (Thermo Fisher Scientific) and appropriate sets of primers:

HOIP forward	CTCATTTGAATTCTATGATGC
HOIP reverse	GAAACAGGGACCAGGAGT
Cre forward	TTGCCCCTGTTTCACTATCCAG
Cre reverse	TGCTGTTTCACTGGTTATGCGG
TNFR1 WT	TGTGAAAAGGGCACCTTTACGGC
TNFR1 common	GGCTGCAGTCCACGCACTGG
TNFR1 mutant	ATTCGCCAATGACAAGACGCTGG
Casp8 WT forward	GTAGAAATGGAGAAGAGGACCATG
Casp8 KO forward	TTGAGAACAAGACCTGGGGACTG
Casp8 reverse	GGATGTCCAGGAAAAGATTTGTGTC
MLKL common forward	CAAGGAAAGAAGAACCTGCCCGA
MLKL WT reverse	GGATGCTGGCTGGCTGACA
MLKL KO reverse	CCTGCTGCCATCTGAAACGG

2.4.4 Dissection and fixation of tissues for histology

Mice were euthanised and whole livers were resected with forceps and scissors. Tissues were cut into no more than 2 cm pieces, and pieces of livers were fixed in 10% neutral-buffered formalin (Sigma). The rest of the tissues were snap-frozen in liquid nitrogen for further analysis. Formalin was replaced with 70% ethanol to avoid over-fixation before embedding.

2.4.5 Histological sections

Formalin-fixed tissues were embedded in paraffin blocks by sequential incubation with ethanol, histoclear and paraffin and sliced into thin sections in 4 μm thickness. Hematoxylin and eosin (H&E) staining was performed to observe tissue structure. Tissue embedding and sectioning were performed by Ms Lorraine Lawrence (NHLI, Imperial College London).

2.4.6 Immunohistochemistry

Paraffin sections were dewaxed by sequential treatment with histoclear, 100% industrial methylated spirit (IMS), 90% IMS, 75% IMS, 50 % IMS and distilled water. For antigen retrieval, heat-induced epitope retrieval with citrate buffer was used for Ki-67 and cleaved caspase-3 or Tris-EDTA buffer for Ly6G and γH2AX staining. Proteinase K (Promega) 10 µg/mL diluted in TEX buffer was used for demasking F4/80 antigen. Tyramide signal amplification (TSA) system (Perkin Elmer) was utilised to enhance signals. To detect cell death, terminal deoxynucleotidyl transferase dUTP nick end labelling (TUNEL) was performed using ApopTag In situ detection kit (Millipore).

2.4.7 Flow cytometric analysis of liver immune cells

Livers were processed in PBS with syringe plungers and the cell suspension was filtered with 70-µm cell strainer (BD). Cells were washed with PBS and red blood cells were removed using RBC lysis buffer (R&D). Cells were incubated with anti-mouse CD16/CD32 and Fixable Viability Dye eFluor 660 (eBioscience) for 30 min prior to incubation with antibodies. Cells were subsequently stained with fluorophore-coupled antibodies for 1 hour. Cells were fixed with fixation/permeablization concentrate (eBioscience) diluted 1:4 in fixation/permeablization diluent (eBioscience) until the day of measurement and were washed with PBS shortly before measurement. For absolute quantification, 10 µL of 123count eBeads (eBioscience) were added to each cell suspension, and cells were measured on Fortessa LSR II (BD), followed by analysis using FlowJo 7.6.5 (Tristar).

2.4.8 Serum analysis

Blood was withdrawn from the submandibular vein using a lancet and collected into Microtainer tube with separation gels (BD). Sampled blood was kept on ice and spun to isolate serum. Isolated sera were diluted in 0.9 % (v/w) sodium chloride and 30 µL of diluted sera were placed on Reflotron ALT test strip (Roche), which subsequently measured on Reflovet (Roche).

Chapter 3

3 Results

3.1 Characterisation of liver-specific HOIP-deficient mice

3.1.1 Generation of liver-specific HOIP-deficient mice

Systemic deficiency in the catalytic component of LUBAC, HOIP, in mice causes embryonic lethality at mid-gestation (Peltzer et al., 2014). At this stage, the developing livers accommodate the precursor of mature hepatocytes and bile duct cells, hepatoblasts (Zorn, 2008). Due to the death of the animals and immaturity of liver tissue at this embryonic stage, it is not possible to understand the role of linear ubiquitination in the mature liver cells from the study of HOIP-deficient embryos.

To overcome this issue and specifically investigate the role of linear ubiquitination in mature hepatocytes, our laboratory generated mice with liver parenchyma-specific deletion of HOIP by crossing *Hoip*^{flox} mice with transgenic mice expressing Cre recombinase under the regulation of the serum albumin promoter (*Alb-Cre* mice) (Postic et al., 1999). Mice deficient for HOIP in the liver, which we named *Hoip*$^{\Delta hep}$ mice, showed a reduction in HOIP expression levels in whole liver cell lysates to approximately half of the control mice (Figure 3.1A). This partial penetrance of Cre-mediated deletion can be explained by the expression of HOIP protein in non-parenchymal cells. Thus, to specifically analyse the level of HOIP expression in hepatocytes, primary hepatocytes were isolated by means of two-step perfusion. In contrast to whole liver lysates, hepatocytes isolated from *Hoip*$^{\Delta hep}$ animals displayed a drastic reduction in the level of HOIP protein (Figure 3.1B). HOIP-deficient hepatocytes also displayed a slight decline in the levels of the other LUBAC components HOIL-1 and SHARPIN, which is in agreement with previous studies showing that loss of HOIP destabilises HOIL-1 and SHARPIN in MEFs, keratinocytes and cancer cell lines (Peltzer et al., 2014; Draber et al., 2015; Taraborrelli et al., submitted).

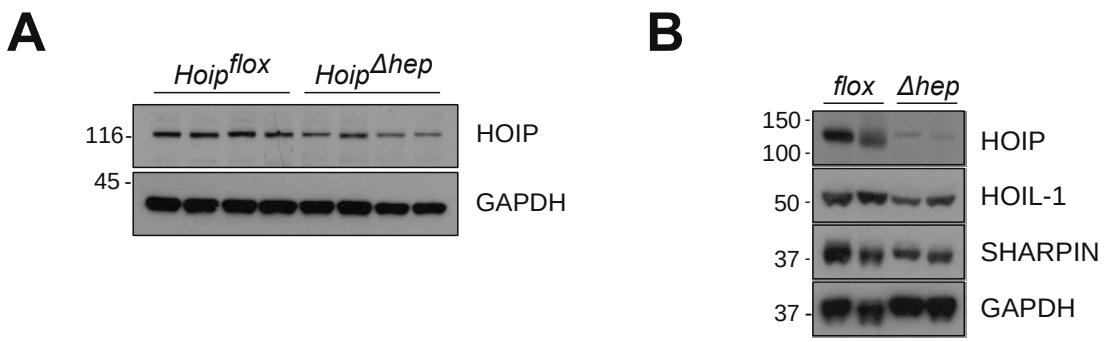

Figure 3.1 HOIP liver-specific deletion reduces the protein levels of LUBAC components in hepatocytes. (A) Whole liver lysates from *Hoip*^{flox} and *Hoip*$^{\Delta hep}$ mice at 4 weeks of age were immunoblotted for HOIP. (B) Isolated primary hepatocytes from *Hoip*^{flox} and *Hoip*$^{\Delta hep}$ mice at 8 weeks of age were lysed and immunoblotted for the LUBAC components. These results are representative of two independent experiments.

The expression level of HOIP in the murine liver was also examined by immunohistochemistry. The staining was performed in collaboration with Professor Teresa Marafioti and her team (UCL Cancer Institute). As an internal control, spleen sections were stained together with liver sections. The anti-HOIP antibody was previously validated for immunohistochemistry in our laboratory (Taraborrelli et al., submitted). Whereas HOIP was strongly positive in splenic lymphocytes, hepatocytes displayed a faint staining for HOIP. In the liver, HOIP was positive in the sinusoids and Kupffer cells (Figure 3.2). Due to the weak staining in hepatocytes, there was no obvious difference in staining intensity between *Hoip*^{flox} and *Hoip*$^{\Delta hep}$ hepatocytes. Together with the results from western blot analysis, these data indicated that HOIP is expressed at a lower level in hepatocytes than in leukocytes and sinusoidal cells.

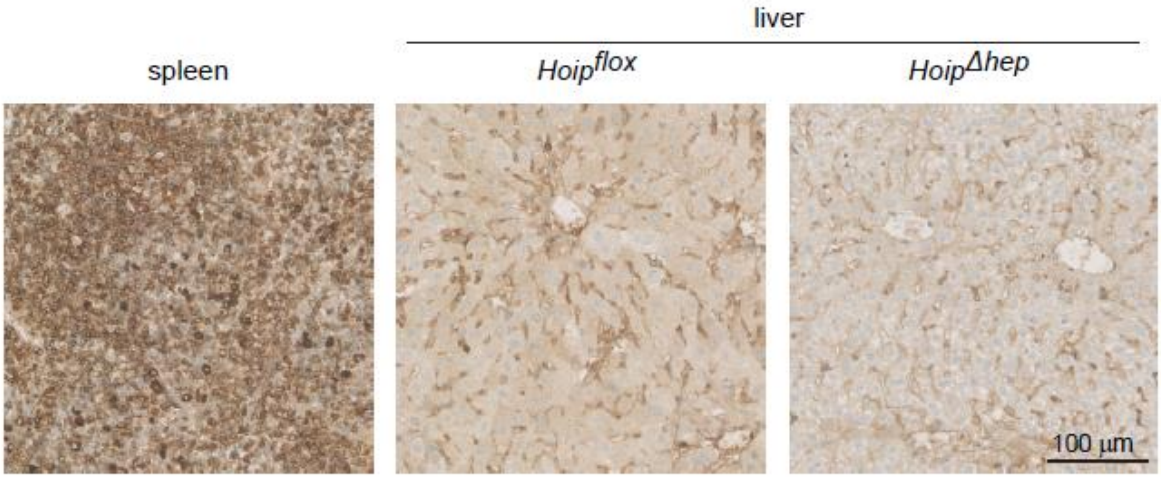

Figure 3.2 Expression of HOIP in mouse spleen and liver. HOIP immunostaining (brown) was performed using anti-murine HOIP antibody and Ventana system (Roche) by Prof Teresa Marafioti's laboratory (UCL Cancer Institute). Sections of the spleen from *Hoip*$^{\Delta hep}$ mice and livers from *Hoip*^{flox} and *Hoip*$^{\Delta hep}$ mice at 4 weeks of age were employed in the staining. The data is collected from a single experiment.

Furthermore, the survival rate of *Hoip*$^{\Delta hep}$ mice was monitored from their birth to 18 months of age. *Hoip*$^{\Delta hep}$ mice were as viable as littermate controls up to 18 month-old (Figure 3.3). This result suggests that HOIP ablation in the liver does not affect the viability of mice, despite an efficient deletion of HOIP in hepatocytes.

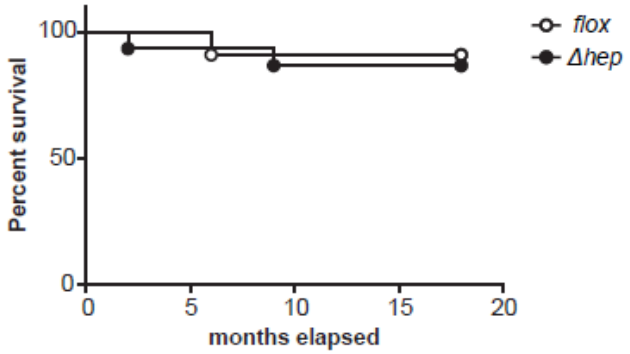

Figure 3.3 Survival curves of *Hoip*^{flox} and *Hoip*$^{\Delta hep}$ mice. Kaplan-Meier plot of *Hoip*^{flox} and *Hoip*$^{\Delta hep}$ male mice up to 18 months (*Hoip*^{flox} n=13 and *Hoip*$^{\Delta hep}$ n=15).

Hepatic abrogation of the anti-apoptotic protein c-FLIP using *Alfp-Cre* leads to perinatal lethality whilst its deletion by *Alb-Cre* does not (Piao et al, 2012). Given that *Alfp-Cre* contains an additional enhancer of the *Afp* gene in its regulatory sequence and that deletion by Alfp-Cre occurs earlier than by Alb-Cre, *Alfp-Cre* could cause a more severe phenotype than *Alb-Cre* (Postic et al., 1999; Kellendonk et al., 2000). Consequently, HOIP deletion in hepatocytes using *Alfp-Cre* could results in premature lethality. To test this, HOIP was deleted in LPCs using *Alfp-Cre*. For this purpose, *Hoip*$^{flox/+}$ *Alfp-Cre* male mice were crossed to *Hoip*$^{flox/flox}$ female mice. *Hoip*$^{flox/flox}$ *Alfp-Cre* mice were born approximately at Mendelian ratio and were viable at least up to a weaning age (2-3 weeks of age) (Table 3.1). Nevertheless, it is yet to be analysed whether they would show impaired survival at a later stage in life. In sum, the two Cre driver lines demonstrated that ablation of HOIP in LPCs does not seem to affect the viability of mice.

Table 3.1 *Alfp-Cre*-mediated HOIP deletion in liver parenchyma does not cause perinatal lethality

	weaning
Hoip$^{flox/flox}$ *Alfp-Cre*	5
Hoip$^{flox/+}$ *Alfp-Cre*	3
Hoip$^{flox/flox}$	4
Hoip$^{flox/+}$	5
total	17

3.1.2 HOIP deficiency in the liver parenchyma results in spontaneous liver tumour formation

Disruption of the NF-κB signalling and cell death pathway in hepatocytes can lead to pathogenesis such as hepatitis and fibrosis as well as liver tumourigenesis at a later stage of life (Luedde et al., 2007; Betterman et al., 2010; Weber et al., 2010). However, these genetic manipulations do not lead to lethality of the animals in most of the cases, except for c-FLIP deletion, which causes perinatal death using *Alfp-Cre* (Piao et al., 2012). Although *Hoip*$^{\Delta hep}$ mice displayed an unaltered survival rate, HOIP deletion could be pathogenic at a later stage in life. Therefore, the livers from *Hoip*$^{\Delta hep}$ mice were analysed at 18 months of age.

Strikingly, the large majority of male *Hoip*$^{\Delta hep}$ mice at 18 months of age exhibited macroscopic nodules in the liver. At this stage, control mice did not show any overt aberration in the liver (Figure 3.4A). The size, number and severity of macroscopic lesions appearing in *Hoip*$^{\Delta hep}$ livers were variable. Four mice out of 13 showed mild phenotype with smaller lesions (lesion diameter < 2 mm). Another five mice developed a moderate phenotype with multiple lesions and nodules (including maximal lesion diameter = 2-5 mm). Lastly, the other three mice suffered from severe pathology with large nodules (diameter > 5 mm) together with cystic lesions (Figure 3.4A). HCC formation was observed in over a half (5 out of 8) of the *Hoip*$^{\Delta hep}$ animals displaying moderate and severe pathologies (Figure 3.4B, bar graph). The other mice that did not have HCC displayed pre-cancerous anisokaryosis or inflammatory foci (Figure 3.4B, middle pictures).

Furthermore, *Hoip*$^{\Delta hep}$ livers exhibited focal lipid accumulation, which suggests that *Hoip*$^{\Delta hep}$ mice develop steatosis (Figure 3.5). In addition, Sirius red-positive mild fibrotic lesions were present at peri-tumour areas (Figure 3.5). Taken together, HOIP deletion in liver parenchyma causes liver tumourigenesis and steatosis.

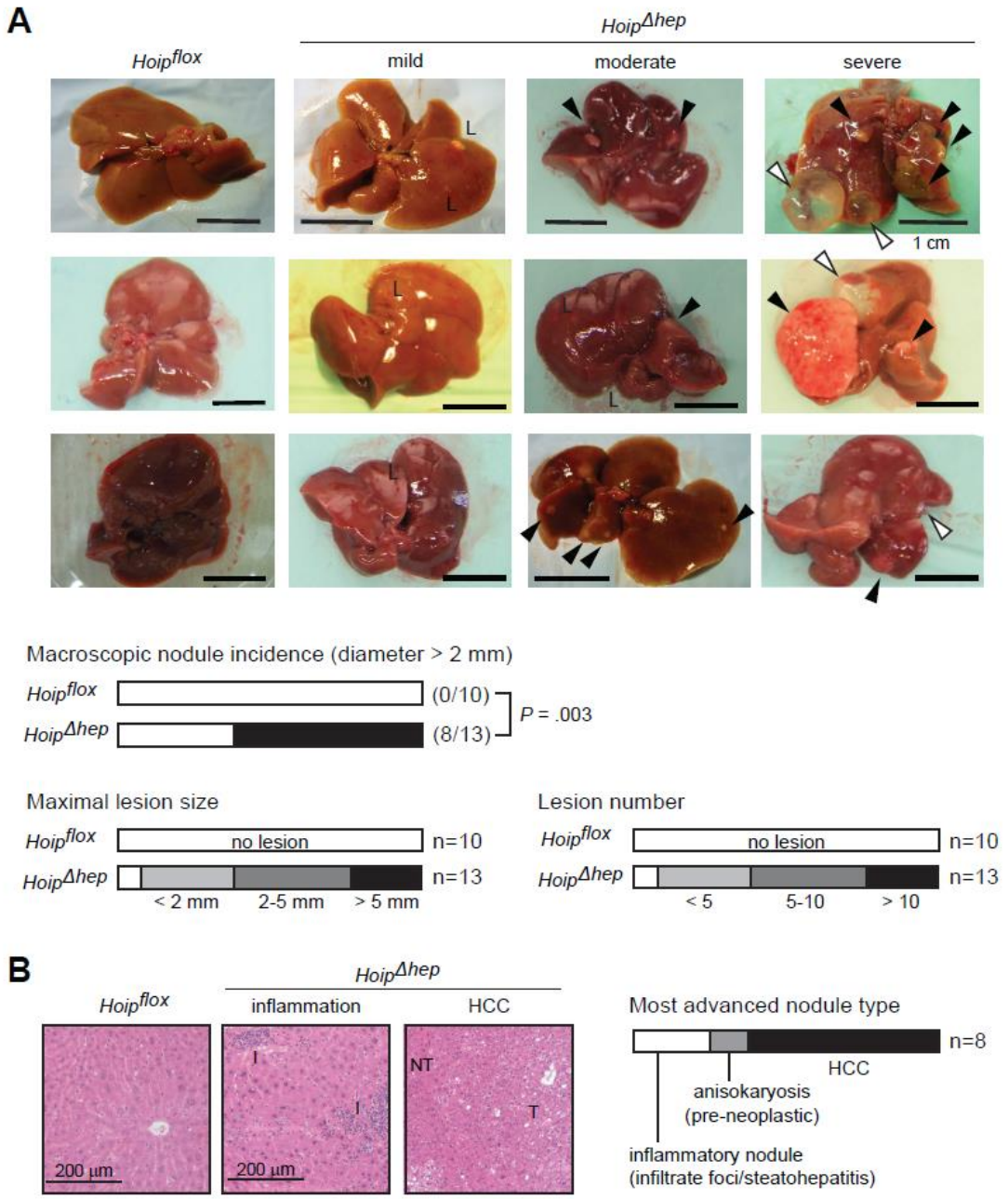

Figure 3.4 *Hoip*$^{\Delta hep}$ mice spontaneously develop liver tumours at 18 months of age. (A) Macroscopic images of livers from *Hoip*^{flox} and *Hoip*$^{\Delta hep}$ mice at 18 months of age. The severity of pathology observed in *Hoip*$^{\Delta hep}$ livers was classified into three levels: mild (5/13), moderate (5/13), and severe (3/13). Black and white arrowheads indicate nodules and cysts, respectively. L: small lesion. Fisher's exact test was employed in nodule incidence analysis. (B) H&E sections of livers from *Hoip*^{flox} and *Hoip*$^{\Delta hep}$ mice at 18 months of age (left panel). I: inflammatory foci, NT: non-tumour, T: tumour. The bar graph indicates the most advanced nodule type on the liver which showed moderate and severe phenotype (right panel).

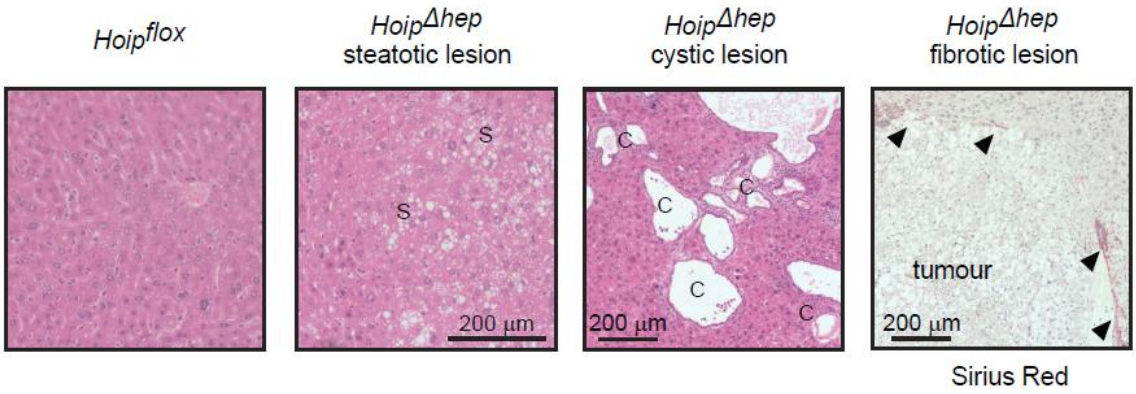

Figure 3.5 *Hoip*$^{\Delta hep}$ mice spontaneously develop steatosis, cystic lesions and fibrotic lesions at 18 months of age. Macroscopic images of livers from *Hoip*^{flox} and *Hoip*$^{\Delta hep}$ mice at 18 months of age. Left panel, S: steatotic lesion. Middle panel, C: cystic lesion. Right panel, paraffin-embedded tumour-bearing *Hoip*$^{\Delta hep}$ livers were stained with Sirius red. Arrowheads indicate Sirius-red-positive fibrotic lesion around the tumour.

3.1.3 Inflammation emerges at early stages of life in HOIP-deficient livers

The primary cause of liver cancer in human is chronic inflammation (El-serag, 2011). Inflammation in several types of cancer promotes the initiation and establishment of pro-tumourigenic environment. I hypothesised that an earlier inflammation predisposes *Hoip*$^{\Delta hep}$ mice to liver tumourigenesis. The presence of liver inflammation at an early stage of life in *Hoip*$^{\Delta hep}$ mice was therefore assessed.

Firstly, in order to detect the presence of inflammation, the number of hepatic leukocytes of *Hoip*^{flox} and *Hoip*$^{\Delta hep}$ mice from postnatal day 7 up to 8-9 weeks of age was quantified by means of flow cytometry. Leukocytes were present in the liver at equivalent levels in *Hoip*^{flox} and *Hoip*$^{\Delta hep}$ mice at postnatal day 7 and 15. However, at 4 weeks of age, *Hoip*$^{\Delta hep}$ mice accommodated a significantly higher number of leukocytes in the liver as compared to littermate controls (Figure 3.6). At 8-9 weeks of age, the leukocyte count of *Hoip*$^{\Delta hep}$ livers returned to a similar level to that of *Hoip*^{flox} livers. This result indicated that *Hoip*$^{\Delta hep}$ livers suffered from transient inflammation which peaked at 4 weeks of age.

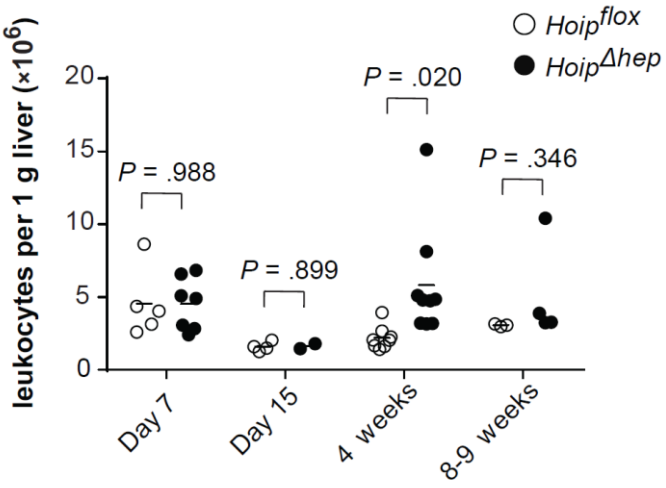

Figure 3.6 Quantification of hepatic leukocyte in *Hoip*^{flox} and *Hoip*$^{\Delta hep}$ mice at an early stage. Livers from *Hoip*^{flox} and *Hoip*$^{\Delta hep}$ mice at the indicated ages were processed and stained, and the number of CD45^{+} cells was quantified by flow cytometry. Data were collected from a single experiment for Day 7, 15 and 8-9 week time points. The results from the two independent experiments were pooled for 4 weeks' data. Statistics was performed by two-tailed *t* test.

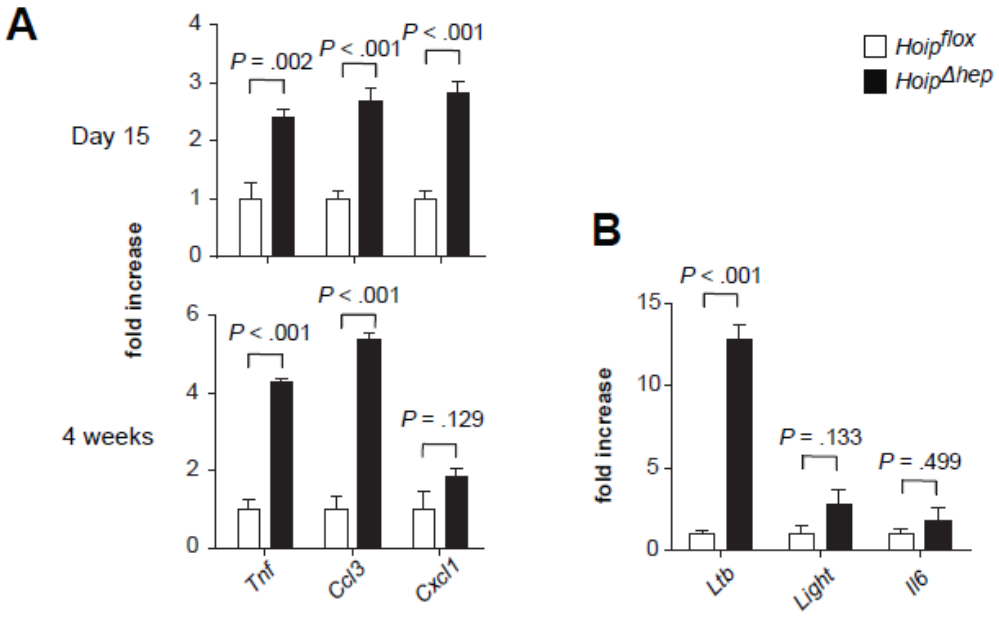

Figure 3.7 Relative quantification of hepatic cytokine/chemokine transcript levels in *Hoip*^{flox} and *Hoip*$^{\Delta hep}$ mice at an early stage. (A) (B) Livers from *Hoip*^{flox} and *Hoip*$^{\Delta hep}$ mice at the indicated ages were homogenised and mRNAs of indicated genes were relatively quantified by qRT-PCR. Gene expression levels in *Hoip*$^{\Delta hep}$ samples are depicted as fold increase of that of *Hoip*^{flox} sample. (B) Livers were from the animals at 4 weeks of age and mRNAs of indicated genes were relatively quantified by qRT-PCR. Data were collected from a single experiment for each time point. The bar graphs indicate means and standard error of means. Statistics was performed by two-tailed *t* test.

In agreement with the emergence of inflammation at 4 weeks of age, elevated levels of TNF, CCL3 and CXCL1 cytokine/chemokine were detected at this stage (Figure 3.7A). Intriguingly, the increases in these cytokine/chemokine levels were already present at 2 weeks of age, when anatomically inflammation was not yet established in *Hoip*$^{\Delta hep}$ livers.

A previous study pointed out the contribution of LTβR signalling to the NASH-related HCC formation in a CD-HFD model (Wolf et al., 2014). Levels of LTβR ligands, LTβ and LIGHT, were therefore evaluated. LTβ transcript was significantly increased, and the expression of LIGHT also showed a similar tendency (Figure 3.7B). Next, the level of pro-tumourigenic cytokine IL-6 was assessed, as this is one of the key factors to drive liver carcinogenesis (Naugler et al., 2007). However, IL-6 mRNA merely showed a marginal increase (Figure 3.7B).

Coinciding with the exacerbated leukocyte number and cytokine/chemokine levels at 4 weeks of age, myeloid cell infiltration was present in *Hoip*$^{\Delta hep}$ livers as detected by Ly6G and F4/80 immunostaining. Myeloid cells were accumulated at the site of inflammation in *Hoip*$^{\Delta hep}$ livers (Figure 3.8A). To investigate further which particular immune cell subpopulations were recruited to inflamed *Hoip*$^{\Delta hep}$ livers at 4 weeks of age, the different populations of hepatic leukocytes were quantified by flow cytometric analysis. F4/80^{+} monocytes/macrophages, Ly6G^{+} granulocytes, CD4^{+} and CD8^{+} T cells and B220^{+} B cells were accumulated in *Hoip*$^{\Delta hep}$ livers as compared to control livers (Figure 3.8B). Additionally NK and NKT cells were also increased, albeit not to a statistically significant degree, in *Hoip*$^{\Delta hep}$ livers. This result suggested that a wide range of both myeloid and lymphoid compartments appear to be indiscriminately recruited to the inflamed *Hoip*$^{\Delta hep}$ livers and participate in inflammatory responses.

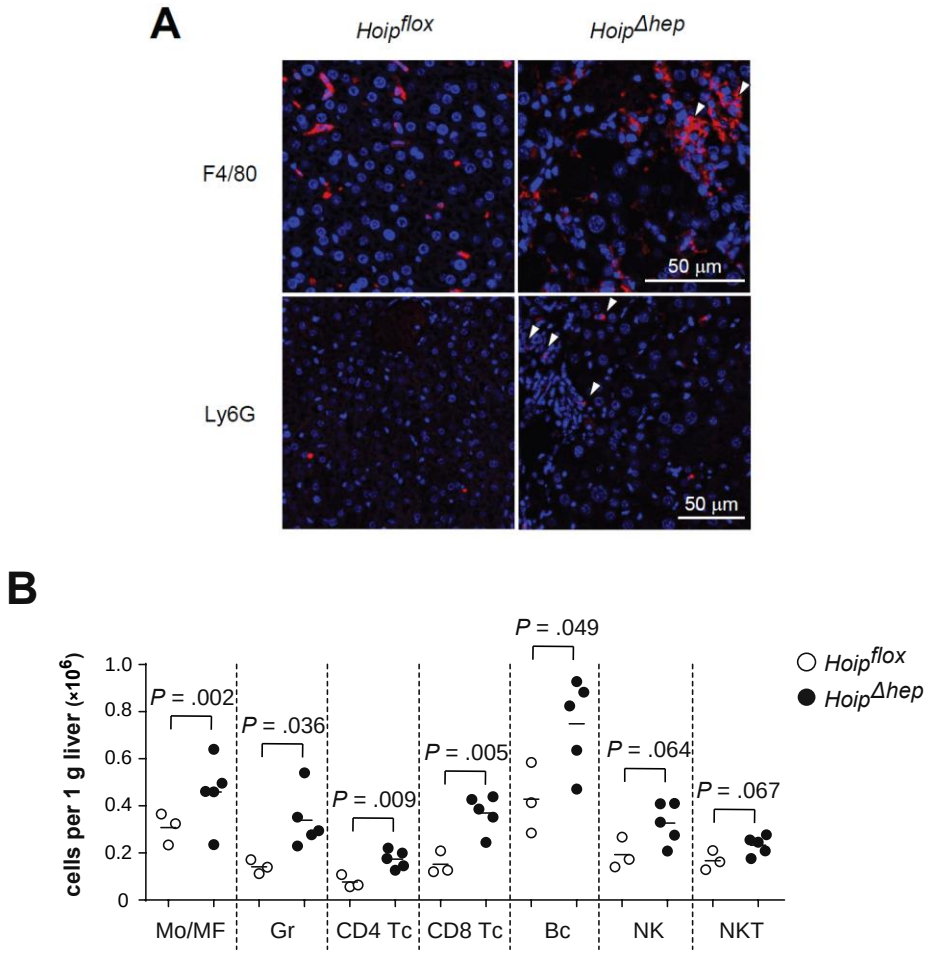

Figure 3.8 Characterisation of immune infiltrates at the peak of early inflammation in *Hoip$^{\Delta hep}$* livers. (A) Liver sections from *Hoip^{flox}* and *Hoip$^{\Delta hep}$* mice at 4 weeks of age were stained for F4/80 (upper panel) and Ly6G (lower panel), indicated in red. White arrowheads indicate an accumulation of corresponding immune cell staining. (B) Liver cells from *Hoip^{flox}* and *Hoip$^{\Delta hep}$* mice were stained and the numbers of hepatic immune subpopulations were quantified by flow cytometry. Mo/MF: F4/80$^+$ cells, Gr: Ly6G$^+$ cells, CD4 Tc: CD3$^+$ CD4$^+$ cells, CD8 Tc: CD3$^+$CD8$^+$ cells, Bc: B220$^+$ cells, NK: CD3$^-$ NK1.1$^+$ cells, NKT: CD3$^+$ NK1.1$^+$ cells. Data were collected from a single experiment. Statistics was performed by two-tailed *t* test.

It was reported that the liver undergoes compensatory growth and replenish hepatocytes and other types of liver cells by the proliferation of mature hepatocytes and liver cell progenitors in response to tissue injury (Miyajima et al., 2014). Despite the fact that inflammation underlies chronic liver diseases, it also initiates tissue repair by providing damaged tissues with cytokines and growth factors (Karin and Clevers, 2016). The proliferation of liver cells was thus investigated in HOIP-

proficient and -deficient livers. Indeed, as detected by Ki-67 expression, a higher number of proliferating liver cells was observed in *Hoip*$^{\Delta hep}$ mice at 2-4 weeks of age as compared to littermate controls. Therefore, HOIP deletion leads to the initiation of liver regeneration, consistent with the presence of inflammation (Figure 3.9).

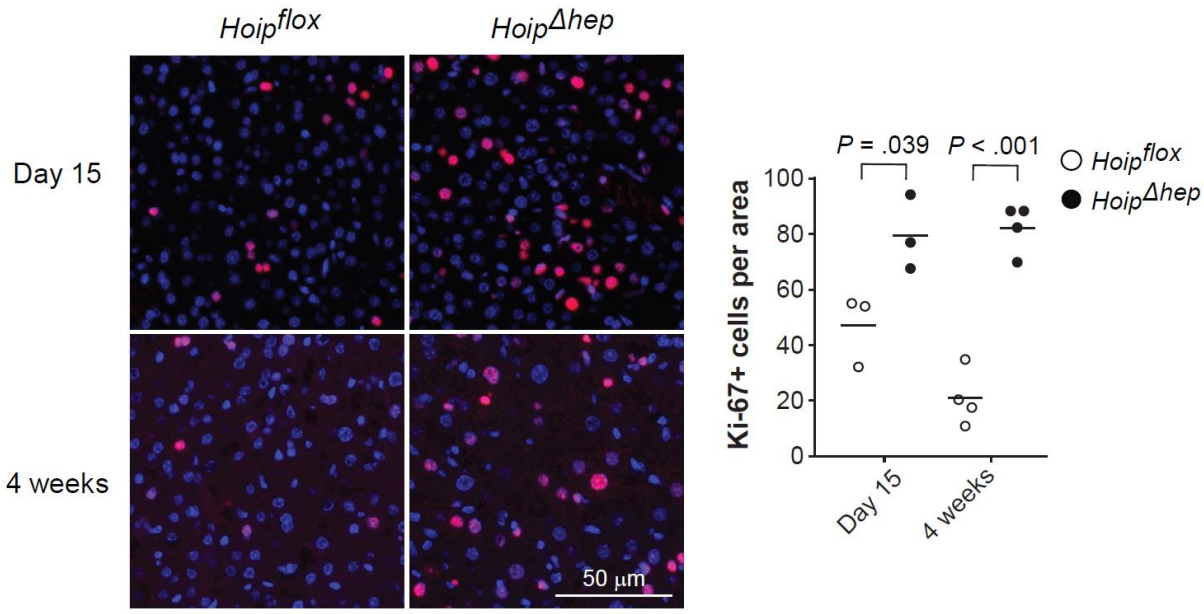

Figure 3.9 *Hoip*$^{\Delta hep}$ livers have increased proliferating cells at an early stage. Liver sections from *Hoip*^{flox} and *Hoip*$^{\Delta hep}$ mice at the indicated ages were stained for Ki-67. The right graph shows the quantification of Ki-67^{+} cells per optical area (magnification: 400x). Data were collected from a single experiment. Statistics was performed by two-tailed *t* test.

In addition, inflammation can also lead to DNA damage by producing reactive oxygen species (ROS) which is associated with inflammation-associated liver carcinogenesis (Maeda et al., 2005; Ohnishi et al., 2013). To determine whether there is underlying DNA damage response in HOIP-deficient hepatocytes, liver sections from 4 week-old *Hoip*$^{\Delta hep}$ and control mice were stained for phosphorylated histone H2AX (γH2AX), a marker for DNA damage. Intriguingly, *Hoip*$^{\Delta hep}$ livers presented increased γH2AX^{+} foci, which is suggestive of increased DNA damage in *Hoip*$^{\Delta hep}$ livers (Figure 3.10). In summary, deficiency in HOIP in liver parenchyma leads to transient inflammation at early stages of life, accompanied by proliferation of regenerative liver cells and a concurrent accumulation of DNA damage.

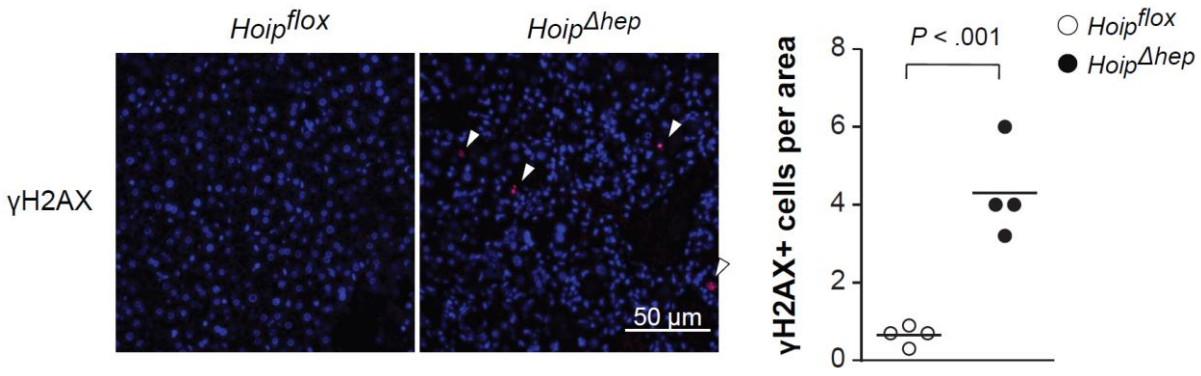

Figure 3.10 *Hoip*$^{\Delta hep}$ livers displayed elevated DNA damage at an early stage. Liver sections from *Hoip*^{flox} and *Hoip*$^{\Delta hep}$ mice at 4 weeks of age were stained for phosphorylated H2AX. The right graph shows the quantification of γH2AX^{+} cells per optical area (magnification: 200x). Data were collected from a single experiment. Statistics was performed by two-tailed *t* test.

3.1.4 HOIP deficiency renders hepatocytes more susceptible to cell death which precedes the emergence of inflammation in mice

In order to quantitatively evaluate the extent of liver damage in *Hoip*$^{\Delta hep}$ mice, serum ALT levels were measured. ALT is a hepatocyte-specific enzyme which is released into the circulation when these cells are damaged. The serum level of ALT from *Hoip*$^{\Delta hep}$ mice showed a mild but significant surge at 2 weeks of age, and it peaked at 4 weeks. Yet the value declined between 4 and 8 weeks of age (Figure 3.11). This evidence implied that ablation of HOIP in liver parenchyma causes hepatocyte death, which is initiated even before the emergence of inflammation at 4 weeks of age.

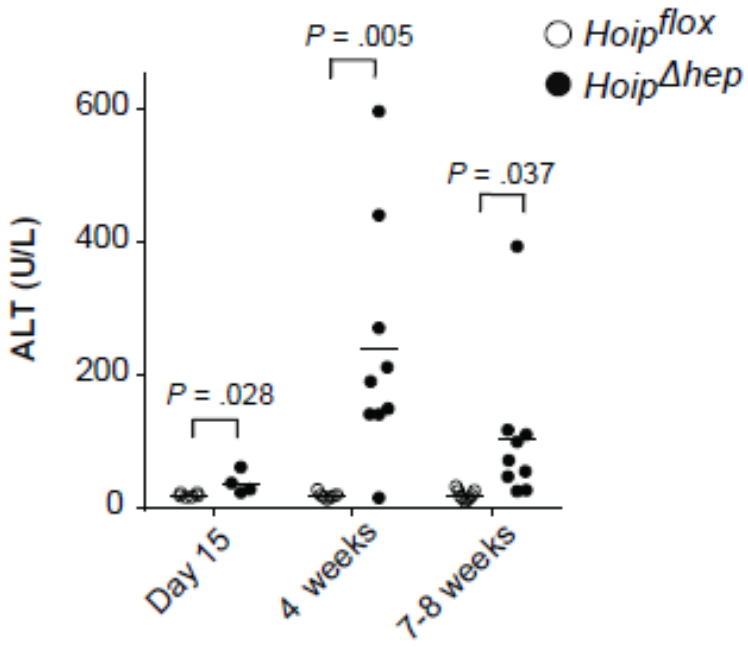

Figure 3.11 *Hoip*$^{\Delta hep}$ mice showed higher levels of serum ALT. Serum ALT levels from *Hoip*^{flox} and *Hoip*$^{\Delta hep}$ mice at the indicated ages were quantified. Data were collected from multiple independent experiments. Statistics was performed by two-tailed *t* test.

Next, to examine the event leading to the emergence of inflammation in *Hoip*$^{\Delta hep}$ livers at 4 weeks of age, pathohistological analyses of *Hoip*$^{\Delta hep}$ mice from postnatal day 1 up to 8 weeks of age were performed. Whilst no aberration in *Hoip*$^{\Delta hep}$ livers was observed at postnatal day 1, apoptotic bodies in *Hoip*$^{\Delta hep}$ livers were detected at postnatal day 7, which became more prevalent at 2 weeks of age as compared to controls (Figure 3.12). At 4 weeks of age, the peak of inflammation, we additionally observed ductular reactions, proliferation of liver progenitor cells around the veins in *Hoip*$^{\Delta hep}$ livers. Consistent with the observation that inflammation was ameliorated at 8 weeks of age, apoptotic bodies and ductular reactions were also reduced in *Hoip*$^{\Delta hep}$ livers at this stage (Figure 3.12).

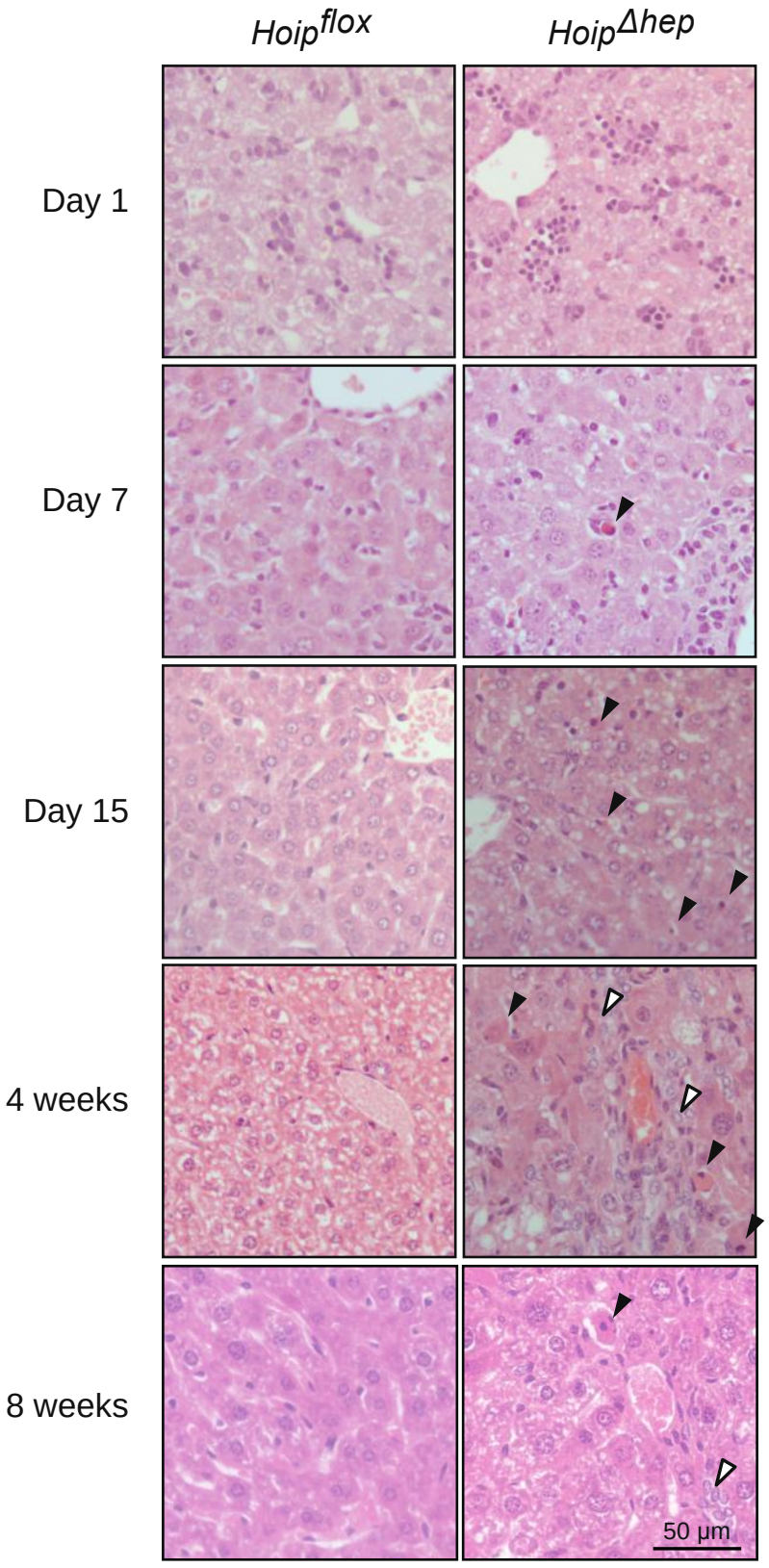

Figure 3.12 *Hoip*$^{\Delta hep}$ mice suffer from transient liver damage. Liver sections of *Hoip*^{flox} and *Hoip*$^{\Delta hep}$ mice at the indicated ages are shown. Black arrowheads indicate apoptotic bodies and white arrowheads indicate proliferating progenitor cells (ductular reactions).

Because inflammation followed the occurrence of cell death at postnatal day 7 onwards and there was no prior aberration detected in HOIP-deficient livers, cell death appeared to be the first pathological event in these livers. To better understand the cell death observed histologically in *Hoip*$^{\Delta hep}$ livers, terminal deoxynucleotidyl transferase dUTP nick end labelling (TUNEL) and immunohistochemistry against cleaved caspase-3 (CC3) were performed to visualise and quantify dead and apoptotic cells, respectively. In accordance with the histological observation, TUNEL^{+} cells per area of the liver sections significantly increased at 2 weeks, 4 weeks and 8 weeks of age in *Hoip*$^{\Delta hep}$ livers (Figure 3.13). The number of CC3^{+} apoptotic cells per area was also elevated from postnatal day 7 up to 8 weeks of age, although they were statistically significant only at 2 weeks of age. TUNEL^{+} and CC3^{+} cell numbers reached their maximal level at 2 weeks of age, which preceded the peak of liver leukocyte count at 4 weeks of age (Figure 3.6).

HOIP-deficient MEFs display increased caspase-8 and caspase-3 activation in response to TNF (Peltzer et al., 2014). To evaluate caspase-8 activation in HOIP-deleted livers, primary hepatocyte lysates and whole liver lysates were immunoblotted for cleaved caspase-8. Primary hepatocytes from *Hoip*$^{\Delta hep}$ mice at 8-10 weeks of age displayed activation of caspase-8 as well as caspase-3 cleavage in the lysates (Figure 3.14A). Caspase-8 cleavage was detected in *Hoip*$^{\Delta hep}$ livers as well (Figure 3.14B).

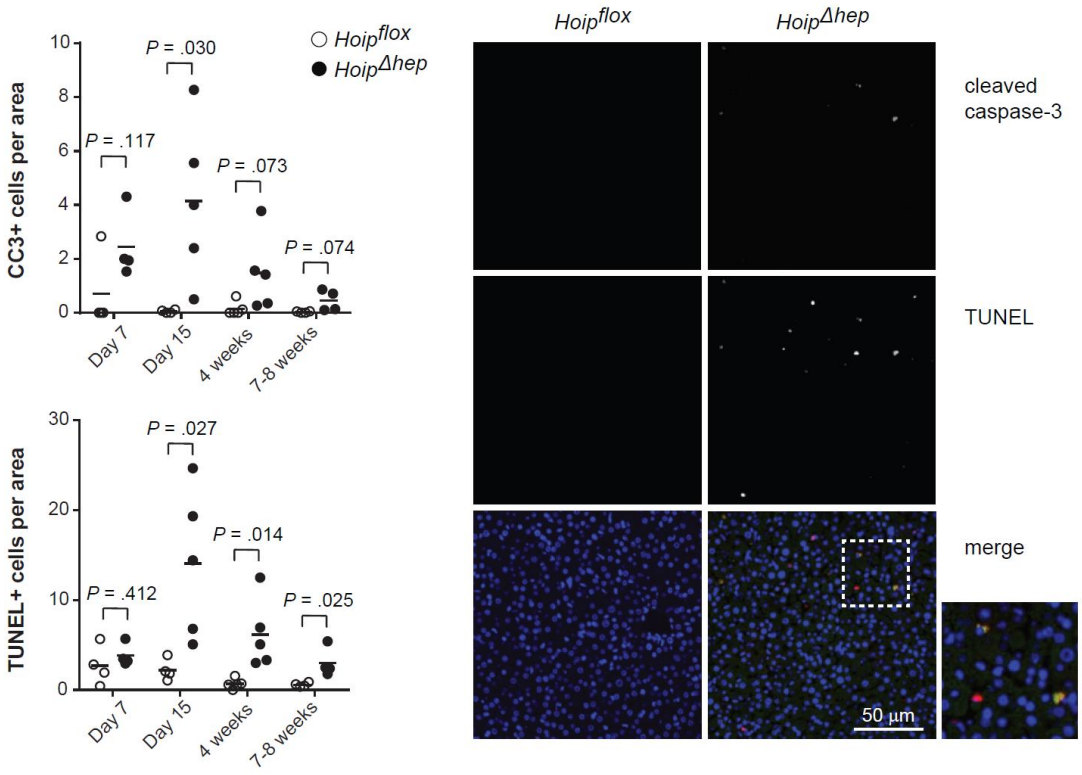

Figure 3.13 *Hoip*$^{\Delta hep}$ mice suffer from increased liver cell death. Liver sections from *Hoip*^{flox} and *Hoip*$^{\Delta hep}$ mice at the indicated ages were stained for cleaved caspase-3 (CC3) and TUNEL. Stained cells per area of the liver sections were quantified and shown in the graphs (left). Data were collected from a single experiment. Statistics was performed by two-tailed *t* test. Cleaved caspase-3 (green in the merged picture) and TUNEL staining (red) on *Hoip*^{flox} and *Hoip*$^{\Delta hep}$ liver sections at 15 days of age are shown in the pictures (right).

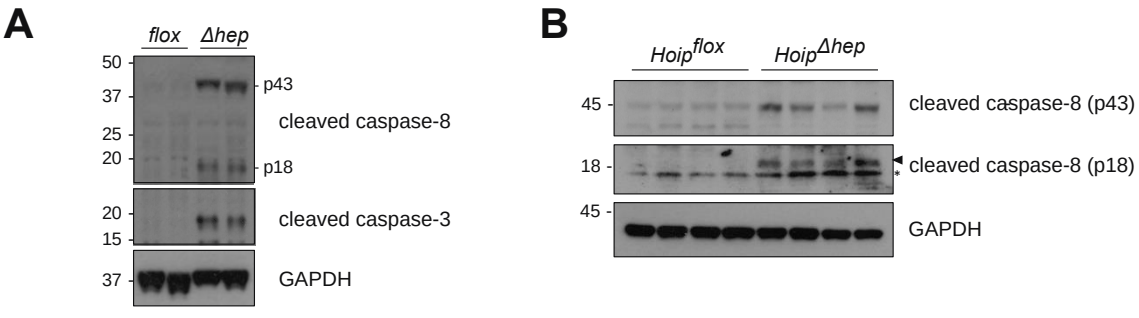

Figure 3.14 Caspase activation occurs in HOIP-deleted hepatocytes. (A) Isolated primary hepatocytes from *Hoip*^{flox} and *Hoip*$^{\Delta hep}$ mice at 8-9 weeks of age were lysed two days after plating and immunoblotted for cleaved caspase-8 and caspase-3. (B) Whole liver lysates from *Hoip*^{flox} and *Hoip*$^{\Delta hep}$ mice at 4 weeks of age were immunoblotted for cleaved caspase-8. Data are representative of those from two independent experiments.

In NEMO-deficient hepatocytes, which also show spontaneous apoptosis in the liver and primary culture, levels of anti-apoptotic proteins, cIAP1/2 and c-FLIP, are downregulated (Kondylis et al., 2015). Therefore the downregulation of anti-apoptotic proteins and/or upregulation of pro-apoptotic proteins could account for caspase activation and impaired survival of HOIP-deleted hepatocytes. However, there was no obvious difference in the levels of any of the major pro-apoptotic and anti-apoptotic proteins tested in HOIP-deficient hepatocytes (Figure 3.15). Moreover, Bid cleavage, which mediates mitochondrial apoptosis pathway, was undetected in HOIP-deficient hepatocytes.

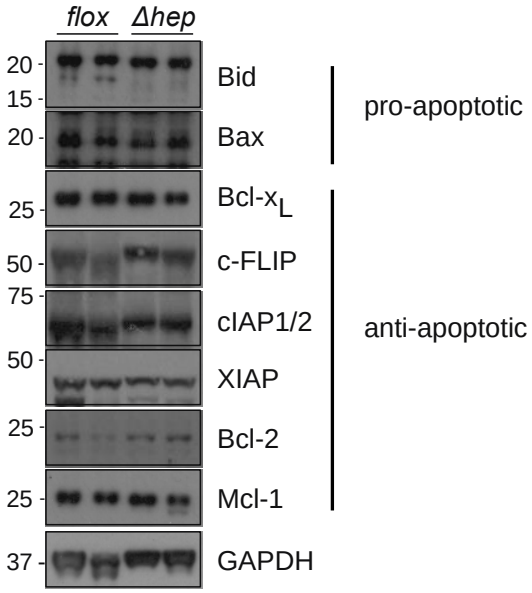

Figure 3.15 Levels of major pro-apoptotic and anti-apoptotic proteins in HOIP-deleted hepatocytes are unaltered. Isolated primary hepatocytes from *Hoip*^{flox} and *Hoip*$^{\Delta hep}$ mice were lysed and immunoblotted for the indicated pro-apoptotic and anti-apoptotic proteins.

3.1.5 Summary

The biological effect of LUBAC deficiency in the liver parenchyma was evaluated in this chapter by creating LPC-specific HOIP knockout mice, *Hoip*$^{\Delta hep}$ mice. HOIP deletion in LPCs, utilising *Alb-Cre* mice, resulted in an efficient deletion of the protein. Although there was no impairment in viability up to 18 months of age, the majority of *Hoip*$^{\Delta hep}$ mice developed macroscopic nodules and lesions in the liver, which included malignant tumour at this age. At the perinatal stage, *Hoip*$^{\Delta hep}$ mice began to suffer from hepatocyte apoptosis which is exacerbated up to 2-4 weeks of age. The cell death of hepatocytes in *Hoip*$^{\Delta hep}$ mice was followed by the emergence of inflammation. At this stage, leukocyte infiltration and the levels of inflammatory mediators were increased, where a wide range of myeloid and lymphoid cells were recruited to *Hoip*$^{\Delta hep}$ liver and engaged in their hepatitis. In line with the aggravated cell death and inflammation, liver cell proliferation occurred to compensate the damage and increased DNA damage response was detected in *Hoip*$^{\Delta hep}$ mice. HOIP-deficient primary hepatocytes underwent apoptosis characterised by the activation of caspase-8 and caspase-3. These results suggest that LUBAC deficiency in LPCs is detrimental as it provokes hepatocyte death, notably apoptosis, and inflammation. These early events associated with the late tumourigenesis in the liver.

3.2 Dissecting the role of cell death pathways in HOIP deficiency-induced liver damage

3.2.1 The role of TNFR1 signalling in HOIP-deficient livers

As described above, *Hoip*$^{\Delta hep}$ livers exhibit increased levels of cell death that precede the development of hepatitis. It has been shown that LUBAC deficiency leads to attenuated gene activation and impaired cell survival in TNFR1 signalling (Haas et al., 2009; Gerlach et al., 2011). TNFR1 deletion rescues the cell death and inflammatory phenotype in LUBAC-impaired animals (Kumari et al., 2014; Rickard et al., 2014; Peltzer et al., 2014). Therefore it is hypothesised that TNFR1 signalling is responsible for the observed hepatocyte death and subsequent hepatitis in HOIP-deleted livers. To test this hypothesis, HOIP-deficient primary hepatocytes were stimulated with TNF and downstream gene-activatory signaling was assessed. As expected, IκBα is phosphorylated and subsequently degraded upon TNF stimulation in HOIP-proficient hepatocytes whereas phosphorylation and degradation of IκBα were markedly attenuated in HOIP-deleted cells (Figure 3.16). Activation of MAP kinases, such as ERK and JNK, was unaffected, although HOIP-deficient cells displayed high basal ERK activity.

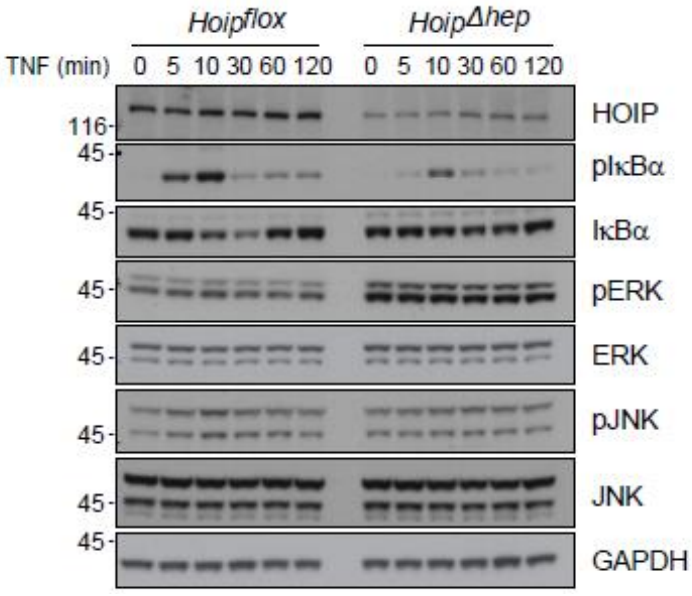

Figure 3.16 TNF-induced canonical NF-κB activation is impaired in HOIP-deficient hepatocytes. Isolated primary hepatocytes from *Hoip*^{flox} and *Hoip*$^{\Delta hep}$ mice were stimulated with 10 ng/mL TNF for the indicated times and cell lysates were immunoblotted for the indicated proteins involved in TNFR1 signalling. This result is representative of those of three independent experiments.

Next, to test whether TNF-induced cell death is affected in HOIP-deficient primary hepatocytes, the viability of these cells was assessed. Upon TNF treatment alone, cell viability of HOIP-deficient cells was reduced by approximately 30% compared to HOIP-proficient cells, indicating that HOIP-deficient hepatocytes are more sensitive to TNF-induced cell death, which is akin to the response of HOIP knockout MEFs (Figure 3.17; Peltzer et al., 2014). This effect could be due to loss of NF-κB target gene expression as HOIP-deficient hepatocytes have impaired NF-κB activation upon TNF stimulation (Figure 3.16). To test this, TNF treatment was combined with a translational inhibitor cycloheximide (CHX). Although co-treatment with CHX decreases cell viability in both cells, it does not alter the 30% decrease in viability observed between HOIP-deficient versus HOIP-proficient cells (Figure 3.17). This result suggests that HOIP can block TNF-induced cell death in hepatocytes independently of its function in activating downstream target genes.

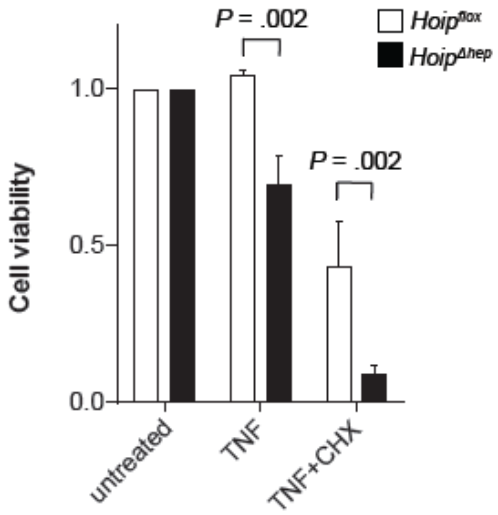

Figure 3.17 HOIP-deficient hepatocytes are sensitised to TNF-induced cell death. Isolated primary hepatocytes from *Hoip*^{flox} and *Hoip*$^{\Delta hep}$ mice were stimulated with TNF and TNF+CHX for 24 hours. Relative cell viability was evaluated and shown in the bar graph. The results were collected from three independent experiments. The bar graphs indicate means and standard error of means. Statistics was performed by two-tailed *t* test.

In order to test whether TNFR1 signalling mediates the observed hepatocyte death and the subsequent inflammation in HOIP-deficient livers, *Hoip*$^{\Delta hep}$ mice were crossed with systemic TNFR1 knockout mice (*Tnfr1*^{KO}) (Pfeffer et al., 1993). Surprisingly, TNFR1 deletion did not reduce the degree of liver damage in HOIP-deficient livers, as quantified by serum ALT values (Figure 3.18).

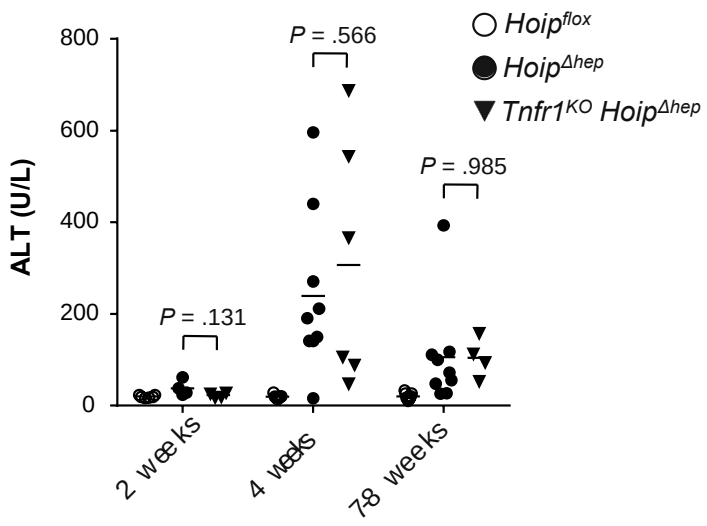

Figure 3.18 Depletion of TNFR1 does not ameliorate liver damage in *Hoip$^{\Delta hep}$* mice. Serum ALT levels from *Hoip^{flox}*, *Hoip$^{\Delta hep}$* and *Tnfr1^{KO} Hoip$^{\Delta hep}$* mice at the indicated ages were quantified. Statistics was performed by two-tailed *t* test.

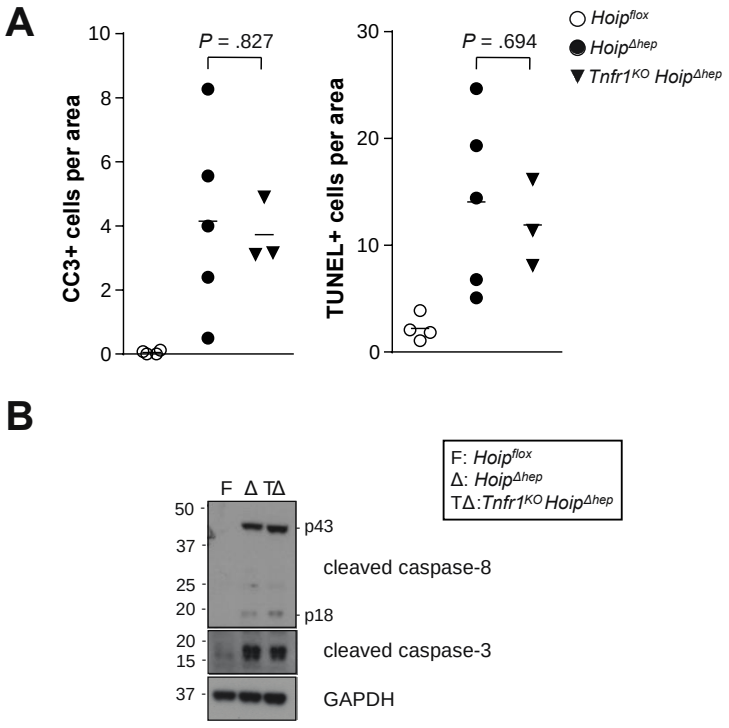

Figure 3.19 Abrogation of TNFR1 does not reduce cell death in HOIP-deficient livers. (A) Cleaved caspase-3 (CC3) and TUNEL-positive cells per optical area were quantified on the liver sections from *Hoip^{flox}*, *Hoip$^{\Delta hep}$* and *Tnfr1^{KO} Hoip$^{\Delta hep}$* mice at 2 weeks of age. The results were collected from a single experiment. Statistics was performed by two-tailed *t* test. (B) Primary hepatocytes from *Hoip^{flox}*, *Hoip$^{\Delta hep}$* and *Tnfr1^{KO} Hoip$^{\Delta hep}$* mice at 8-10 weeks of age were lysed and immunoblotted for cleaved caspase-8 and -3. This result is representative of those of two independent experiments.

In line with the extent of liver damage, the numbers of apoptotic cells and/or dead cells per area in *Hoip*$^{\Delta hep}$ livers also remain unaffected by deletion of TNFR1 (Figure 3.19A). Furthermore, isolated primary hepatocytes from *Tnfr1*^{KO} *Hoip*$^{\Delta hep}$ mice displayed similar activation of caspase-8 and caspase-3 to HOIP-deficient cells (Figure 3.19B).

Intriguingly, even though TNFR1 deletion did not rescue the death and caspase activation in HOIP-deficient hepatocytes, leukocyte recruitment to HOIP-deficient livers was markedly attenuated in *Tnfr1*^{KO} *Hoip*$^{\Delta hep}$ mice reaching similar levels to HOIP-proficient livers (Figure 3.20, left panel). Additionally, mRNA levels of TNF and CCL3 were strongly decreased in *Tnfr1*^{KO} *Hoip*$^{\Delta hep}$ livers (Figure 3.20, right panel). This suggests that TNFR1 ablation significantly alleviates the inflammatory phenotype triggered by HOIP deficiency in liver parenchyma. Since the inflammation in HOIP-deficient livers was resolved by TNFR1 deletion, it was hypothesised that the subsequent DNA damage caused by inflammation was ameliorated as well. Indeed, a significant reduction in the number of γH2AX^{+} cells in *Tnfr1*^{KO} *Hoip*$^{\Delta hep}$ livers was observed as compared to *Hoip*$^{\Delta hep}$ livers (Figure 3.21). Collectively, these results show that, regardless of the TNFR1-independent cell death of HOIP-deficient hepatocytes, TNFR1 signalling mediates the inflammation in HOIP-deficient livers.

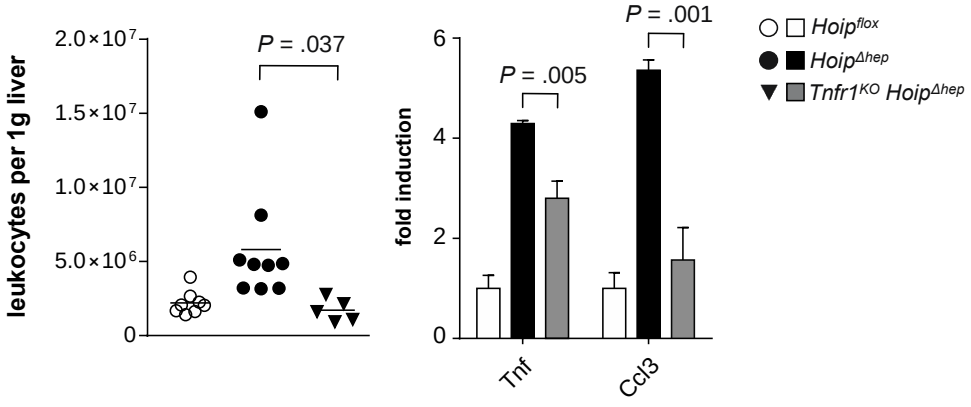

Figure 3.20 TNFR1 ablation ameliorates inflammation in HOIP-deficient livers. Leukocyte count per gramme of the liver in *Hoip*^{flox}, *Hoip*$^{\Delta hep}$ and *Tnfr1*^{KO} *Hoip*$^{\Delta hep}$ mice at 4 weeks of age were quantified (left panel). The levels of *Tnf* and *Ccl3* transcripts were quantified from *Hoip*^{flox}, *Hoip*$^{\Delta hep}$ and *Tnfr1*^{KO} *Hoip*$^{\Delta hep}$ livers by qRT-PCR (right panel). The levels were normalised to those from *Hoip*^{flox} livers. The results for leukocyte count were collected and pooled from two independent experiments. The results for cytokine were collected from a single experiment. The bar graphs indicate means and standard error of means. Statistics was performed by two-tailed *t* test.

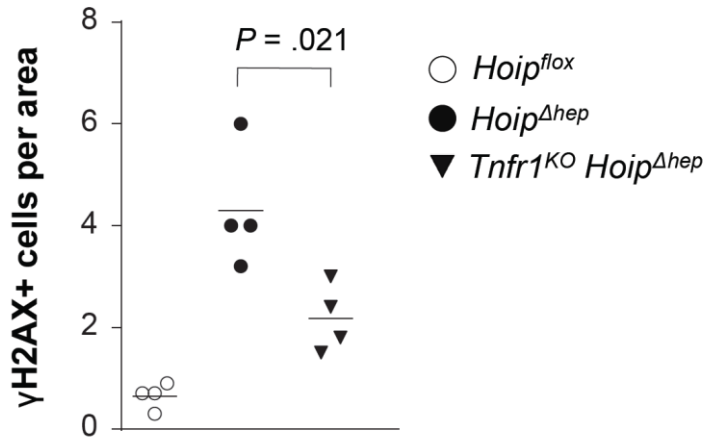

Figure 3.21 TNFR1 deletion mitigates DNA damage in HOIP-deficient livers. Liver sections from *Hoip*^{flox}, *Hoip*$^{\Delta hep}$ and *Tnfr1*^{KO} *Hoip*$^{\Delta hep}$ mice at 4 weeks of age were stained for phosphorylated H2AX. The right graph shows the quantification of γH2AX^{+} cells per optical area (magnification: 200x). The results were collected from a single experiment. Statistics was performed by two-tailed *t* test.

Because TNFR1 ablation did not rescue liver damage in HOIP-deficient livers (Figure 3.19), death-inducing extracellular ligands, other than TNFR1 ligands such as TNF and LTα, could be responsible for the cell death observed in HOIP-deficient livers. Therefore, the sensitivity of HOIP-proficient and -deficient hepatocytes to TRAIL and CD95L-induced cell death was evaluated. Treatment with soluble TRAIL failed to induce cell death in both cells, with no obvious sensitisation due to HOIP deficiency. It was already reported that soluble TRAIL fails to induce cell death in primary mouse hepatocytes in previous studies (Walczak et al., 1999; Corazza et al., 2006). In contrast to TRAIL, CD95L-induced cell death was observed in both HOIP-proficient and -deficient hepatocytes (Figure 3.22). Interestingly, HOIP-deficient hepatocytes were more sensitive to CD95L-induced cell death than HOIP-proficient cells (Figure 3.22).

In addition to death receptor signalling, TLR3 has recently been described to induce cell death via recruiting the cell death-inducing signalling platform (Feoktistova et al., 2011). In line, HOIP-deficient hepatocytes are also sensitised to cell death induced by the TLR3 ligand poly(I:C).

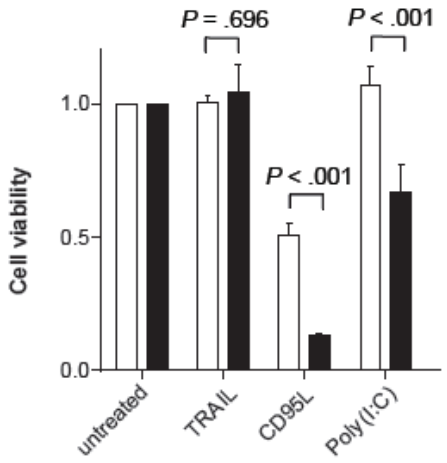

Figure 3.22 HOIP-deficient hepatocytes are more sensitive to CD95L- and Poly(I:C)-induced cell death. Primary hepatocytes from *Hoip*^{flox} and *Hoip*$^{\Delta hep}$ mice were treated with 1 µg/mL TRAIL, CD95L and poly(I:C) for 24 hours, and relative cell viability was quantified. The results were collected from three independent experiments. The bar graphs indicate means and standard error of means. Statistics was performed by two-tailed *t* test.

3.2.2 Formation of cell death-inducing signalling complex

As hepatocyte death occurs to a similar degree in *Hoip*$^{\Delta hep}$ and *Tnfr1*^{KO} *Hoip*$^{\Delta hep}$ livers, they may share the same molecular mechanism underlying hepatocyte death. Activated caspase-8 is a major player in apoptosis and its activation is mediated by a cell-death-inducing platform containing FADD, RIPK1 and caspase-8, formation of which can be triggered by various exogenous stimuli (Tenev et al., 2011; Feoktistova et al., 2011; Conrad et al., 2016). As both *Hoip*$^{\Delta hep}$ and *Tnfr1*^{KO} *Hoip*$^{\Delta hep}$ hepatocytes displayed caspase-8 activation (Figure 3.19B), the presence of a FADD-containing complex in a basal condition was analysed in primary hepatocytes from *Hoip*$^{\Delta hep}$ and *Tnfr1*^{KO} *Hoip*$^{\Delta hep}$ mice. Of note, these experiments were performed in the presence of zVAD in order to stabilize a FADD-associated signalling complex. In HOIP-deficient primary hepatocytes, regardless of the presence of TNFR1, strikingly elevated levels of caspase-8, c-FLIP and RIPK1 were found to be associated with FADD, independently of the presence of TNFR1 (Figure 3.23A). In the FADD-associated cell death-inducing complex, an increased amount of cleaved caspase-8 was detected, indicating that caspase-8 is activated therein. Consistent with caspase-8 cleavage, its modulator c-FLIP$_L$ was also found to be cleaved, presumably by associated activated caspase-8. Furthermore, ubiquitinated form of

both cleaved caspase-8 and RIPK1 are found in the complex (Figure 3.23A). Thus, HOIP deficiency results in spontaneous formation of a FADD-RIPK1-caspase-8-c-FLIP death-inducing signalling platform, independently of TNFR1 signalling, which could be responsible for activation of caspase-8 and apoptosis in HOIP-deficient hepatocytes.

Since LUBAC suppresses TNF-induced cell death independently of its gene-activatory role (Figure 3.17), it was tested whether such cell death-inducing platform is formed independently of HOIP's gene-activatory capacity as well. Therefore, primary hepatocytes were treated with CHX to abrogate protein translation and subsequently the FADD-associated complex was immunoprecipitated. Treatment with CHX did not increase the complex formation in HOIP-proficient cells to the level of HOIP-deficient cells (Figure 3.23B). This result suggests that the FADD-RIPK1-caspase-8 complex formation was not triggered by impaired gene activation.

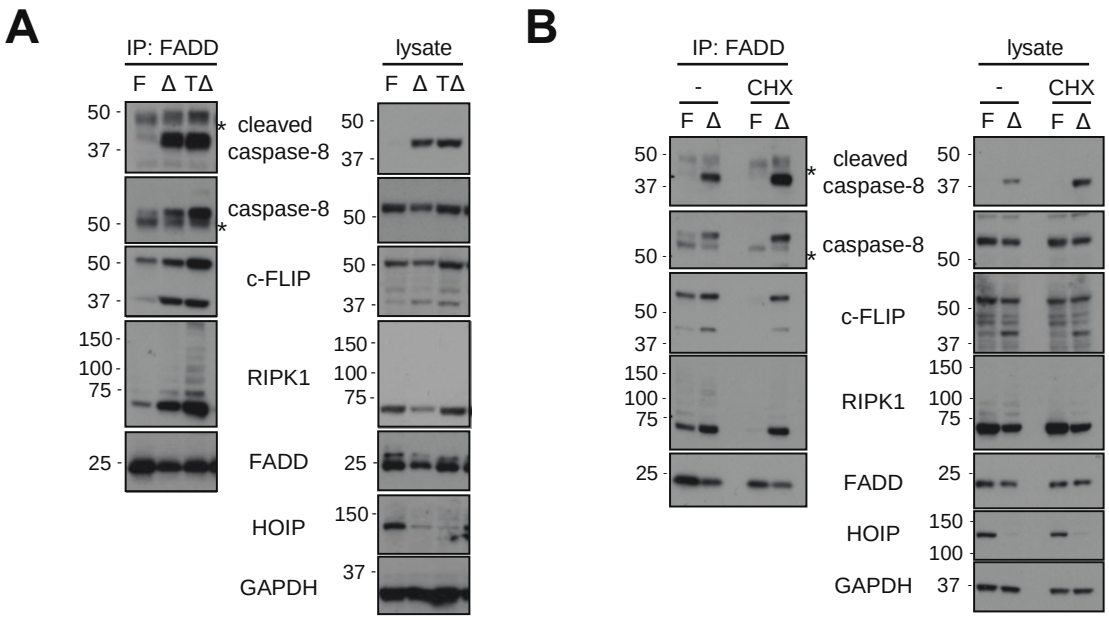

Figure 3.23 HOIP-deficient hepatocytes display increased apoptosis-inducing signalling complex formation independently of TNFR1 signalling and loss of gene activation. (A) Primary hepatocytes from *Hoip*^{flox} (F), *Hoip*$^{\Delta hep}$ (Δ) and *Tnfr1*^{KO} *Hoip*$^{\Delta hep}$ mice (TΔ) were treated with zVAD for 24 hours and subjected to immunoprecipitation using anti-FADD antibody. (B) Primary hepatocytes from *Hoip*^{flox} (F) and *Hoip*$^{\Delta hep}$ (Δ) were treated with zVAD for 24 hours in the presence or absence of CHX for 24 hours and FADD was subsequently immunoprecipitated from cell lysates. These results are representative of those of three independent experiments.

RIPK1 is the central regulator for the assembly of a FADD-RIPK1-caspase-8 death-inducing complex (Conrad et al., 2016). Previous studies have demonstrated that the kinase activity of RIPK1 is required for this complex formation and subsequent cell death (Tenev et al., 2011). Therefore, it was analysed whether the FADD-RIPK1-caspase-8-containing complex spontaneously accumulating in HOIP-deficient cells was dependent on the RIPK1 kinase activity. To do so, the FADD-RIPK1-caspase-8 complex was immunoprecipitated from RIPK1 inhibitor Nec-1s- and zVAD-treated primary hepatocytes isolated from *Hoip*^{flox} and *Hoip*$^{\Delta hep}$ mice. Although treatment with Nec-1s reduced the complex formation in HOIP-proficient hepatocytes, Nec-1s did not largely affect that of HOIP-deficient hepatocytes (Figure 3.24). This result demonstrates that the enhanced formation of the death-inducing complex in the absence of HOIP cannot be inhibited by Nec-1s, whilst its basal formation in HOIP-proficient cells can be.

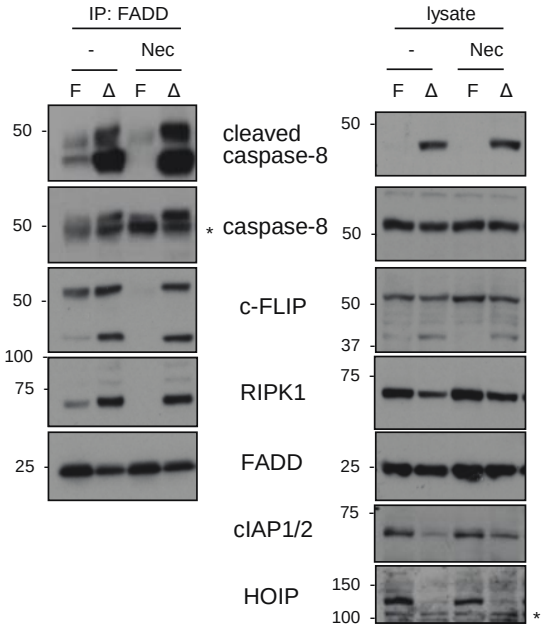

Figure 3.24 Apoptosis-inducing signalling complex in HOIP-deficient hepatocytes is uninhibited by treatment with the allosteric RIPK1 inhibitor Nec-1s. Primary hepatocytes from *Hoip*^{flox} and *Hoip*$^{\Delta hep}$ mice were treated with zVAD for 24 hours in the presence or absence of Nec-1s (Nec, added to culture 1 hour before zVAD addition) and were subjected to immunoprecipitation using anti-FADD antibody. Lysates and precipitates were immunoblotted for the indicated proteins. This result is representative of those of three independent experiments.

3.2.3 Genetic deletion of MLKL and caspase-8 affects the early pathology of the HOIP-deficient livers

Caspase-8-mediated apoptosis is attributed to carcinogenesis in TAK1-deficient livers (Vucur et al., 2013). Therefore, inhibition of apoptosis by deleting caspase-8 gene could prevent liver damage and inflammation in HOIP-deficient livers. In line, heterozygosity of caspase-8 prevents hepatocarcinogenesis in liver-specific NEMO-deficient mice (*Nemo*$^{LPC\text{-}KO}$ mice) (Liedtke et al., 2011). To investigate whether early liver damage in *Hoip*$^{\Delta hep}$ mice is mitigated by halving the gene dosage of caspase-8, *Hoip*$^{\Delta hep}$ mice were crossed to systemic caspase-8 heterozygous mice (*Casp8*$^{+/-}$, *Casp8*^{HET}) as systemic knockout of caspase-8 is embryonically lethal (Kang et al., 2004). Serum ALT values of *Casp8*^{HET} *Hoip*$^{\Delta hep}$ mice were comparable to those of *Hoip*$^{\Delta hep}$ mice (Figure 3.25), suggesting that that deletion of one allele of caspase-8 is not sufficient to alleviate the early liver damage in *Hoip*$^{\Delta hep}$ mice.

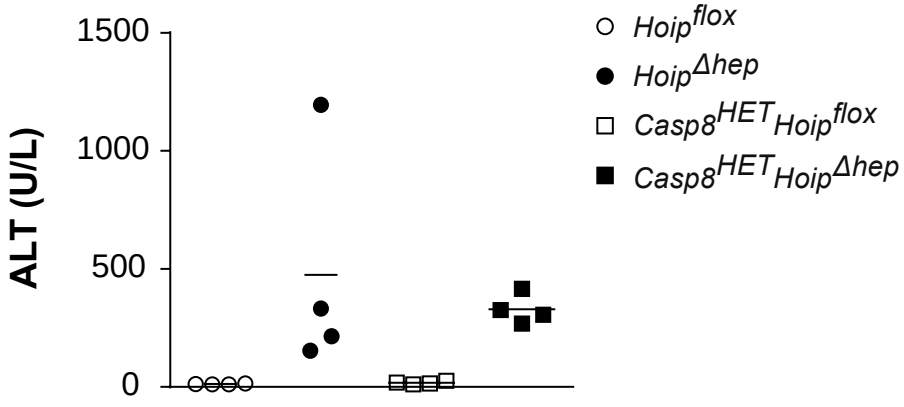

Figure 3.25 Caspase-8 heterozygosity does not alleviate liver damage of *Hoip*$^{\Delta hep}$ mice. Serum ALT values from mice at 4 weeks of age with the indicated genotypes are shown in the graph. The data is collected and pooled from two independent experiments.

Although caspase-8 heterozygosity did not decrease ALT values, a reduction in the numbers of CC3^{+} and TUNEL^{+} cells per area was observed (Figure 3.26). This result suggests that the remaining apoptosis is sufficient to trigger liver damage and that an additional apoptosis-independent process is responsible for the liver damage in *Casp8*^{HET} *Hoip*$^{\Delta hep}$ mice.

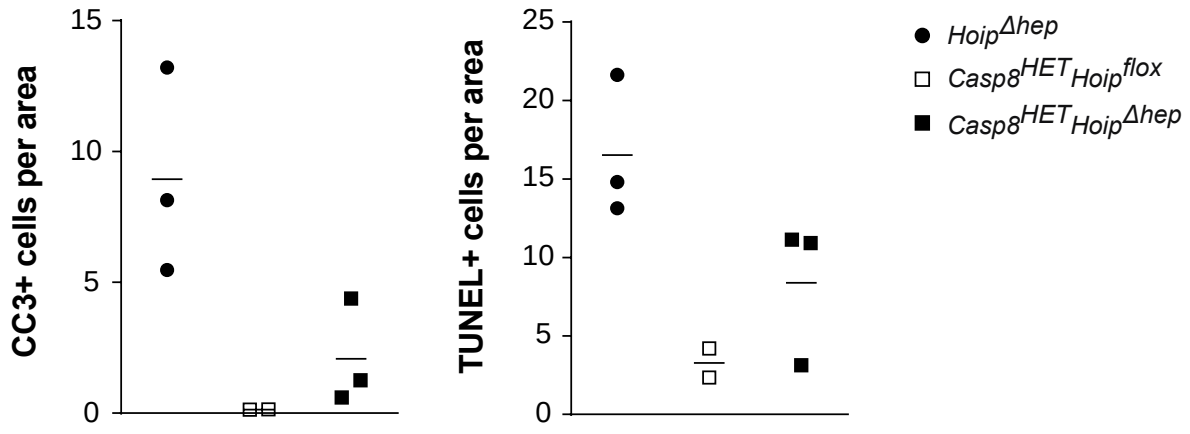

Figure 3.26 Caspase-8 heterozygosity reduces apoptosis in *Hoip$^{\Delta hep}$* livers. The numbers of CC3^{+} cells and TUNEL^{+} cells per area in livers from *Hoip$^{\Delta hep}$*, *Casp8^{HET} Hoip^{flox}* and *Casp8^{HET} Hoip$^{\Delta hep}$* mice at 2 weeks of age are shown in the graphs. The data is collected from a single experiment.

Despite the decrease in apoptotic cells in the liver, the percentage of hepatic leukocytes in *Casp8^{HET} Hoip$^{\Delta hep}$* mice was elevated to an equivalent extent as *Hoip$^{\Delta hep}$* mice at the peak of inflammation (Figure 3.27). This result indicates that inflammation was not ameliorated by partial loss of caspase-8.

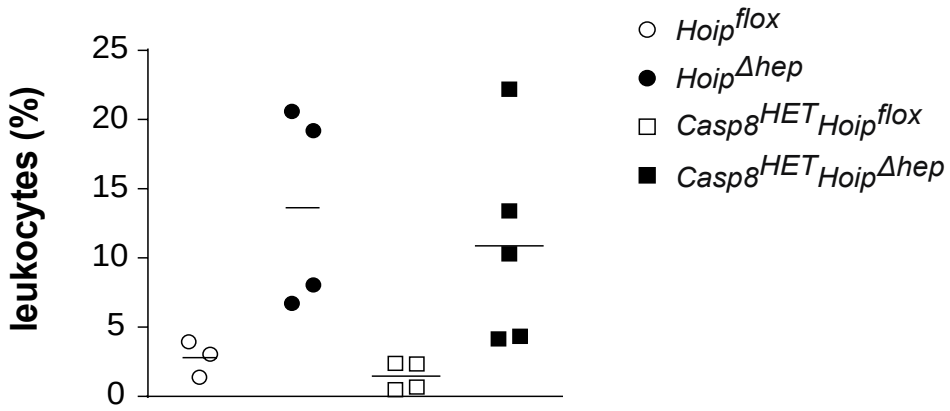

Figure 3.27 Caspase-8 heterozygosity does not ameliorate leukocyte infiltration into *Hoip$^{\Delta hep}$* livers. Percentage of leukocytes present in the livers of *Hoip^{flox}*, *Hoip$^{\Delta hep}$*, *Casp8^{HET} Hoip^{flox}* and *Casp8^{HET} Hoip$^{\Delta hep}$* mice at 4 weeks of age are plotted in the graph. The data is collected and pooled from two independent experiments.

Heterozygosity of caspase-8 did not rescue liver damage evaluated by serum ALT in HOIP-deficient livers, whereas TUNEL^{+} or CC3^{+} cells therein were reduced, which suggests the presence of non-apoptotic cell death. Blockade of caspase-8 activity is a trigger to induce RIPK3/MLKL-dependent necroptosis (Conrad et al., 2016). Thus, heterozygosity of caspase-8 could also sensitise hepatocytes to necroptosis by lowering the amount of caspase-8 in cells. It has been shown that necroptotic cells can be negative for TUNEL (Carneiro et al., 2009), and therefore TUNEL performed in HOIP-deficient livers could have overlooked the presence of necroptotic cells therein.

Pathology triggered by SHARPIN deficiency was completely reverted by RIPK3 deletion and caspase-8 heterozygosity (Rickard et al., 2014), indicating the crucial role of RIPK3 in the *cpdm* phenotype. However, RIPK3 deletion in HOIP-floxed animals cannot be performed by conventional crossings due to the genetic proximity of *Ripk3* and *Hoip* loci (Peltzer et al., 2014). It has been shown that the embryonic lethality of caspase-8 knockout mice can be circumvented by co-deleting necroptosis executer MLKL, although the double knockout mice develop lymphadenopathy at a few months of age (Etemadi et al., 2015). Therefore, *Casp8^{HET} Hoip$^{\Delta hep}$* mice were crossed to MLKL knockout (*Mlkl^{KO}*) mice to evaluate the contribution of necroptosis in the phenotype. Deletion of MLKL in addition to caspase-8 heterozygosity did not reduce ALT values in *Hoip$^{\Delta hep}$* mice (Figure 3.28). This result suggests that one allele of caspase-8 is sufficient to initiate apoptosis in *Mlkl^{KO} Casp8^{HET} Hoip$^{\Delta hep}$* livers, as apoptotic bodies are present in these livers (Figure 3.28).

Strikingly, *Mlkl^{KO} Casp8^{KO} Hoip$^{\Delta hep}$* mice showed serum ALT values comparable to those of *Hoip^{flox}* mice, indicating that the co-deletion of MLKL and caspase-8 completely prevents liver damage induced by HOIP deficiency (Figure 3.28). Accordingly, no cell death were observed in histological analysis of *Mlkl^{KO} Casp8^{KO} Hoip$^{\Delta hep}$* livers.

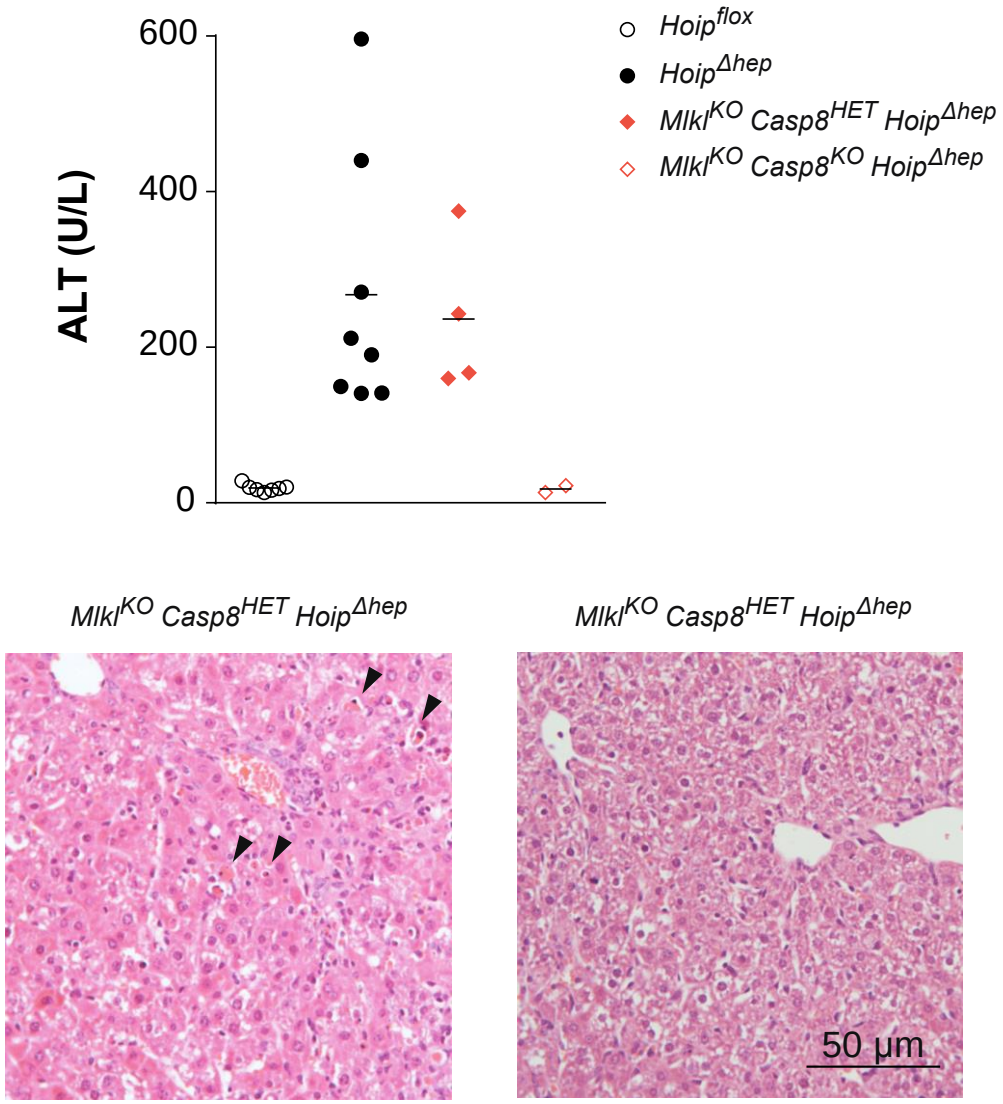

Figure 3.28 MLKL deletion and caspase-8 heterozygosity do not ameliorate liver damage in *Hoip$^{\Delta hep}$* mice, whereas co-ablation of MLKL and caspase-8 rescues it. Serum ALT levels and liver histology of *Mlkl^{KO} Casp8^{HET} Hoip$^{\Delta hep}$* and *Mlkl^{KO} Casp8^{KO} Hoip$^{\Delta hep}$* mice at 4 weeks of age are presented. Black arrowheads in the H&E-stained sections indicate apoptotic bodies. The data is collected and pooled from two independent experiments.

3.2.4 Summary

In this subchapter, the contributions of the TNFR1 signalling, as well as the involvement of apoptotic and necroptotic pathways to the pathogenesis of *Hoip*$^{\Delta hep}$ mice were examined in order to decipher the molecular mechanisms causing liver upon HOIP deficiency in LPCs. In summary, HOIP-deficient hepatocytes were sensitised to TNF-induced cell death and displayed impaired NF-κB activation in response to TNF. Unexpectedly, systemic TNFR1 ablation did not affect the liver damage and cell death. Double TNFR1- and HOIP-deficient hepatocytes underwent apoptosis via caspase-8 and caspase-3 activation to a similar extent to HOIP-deficient cells. However, *Tnfr1*^{KO} *Hoip*$^{\Delta hep}$ exhibited much less severe inflammation as compared to *Hoip*$^{\Delta hep}$ mice.

In addition, the involvement of apoptotic and necroptotic pathways in the observed phenotype was assessed. Halving the gene dosage of caspase-8 did not largely ameliorate liver damage or inflammation. Also, depletion of the necroptosis executer MLKL on top of heterozygosity of caspase-8 also failed to mitigate liver damage. By contrast, complete deletion of both caspase-8 and MLKL abolished liver damage in *Hoip*$^{\Delta hep}$ mice. Taken together, these results illustrated that TNFR1-independent but caspase-8 dependent apoptosis plays a central role in the development of liver damage in *Hoip*$^{\Delta hep}$ mice.

Chapter 4

4 Discussion

Chronic inflammation predisposes the liver to cancer (El-serag, 2011). Disturbance of NF-κB signalling and/or cell death pathway may result in severe pathology in epithelial tissues (Pasparakis, 2012). Dysregulation of TNFR1 signalling and NF-κB signalling components has been associated with liver pathogenesis and tumourigenesis in several mouse models (Luedde et al., 2007; Bettermann et al., 2010; Inokuchi et al., 2010; Nikolaou et al., 2012; Kondylis et al., 2015). However, the role of LUBAC and linear ubiquitination in hepatic cells has been poorly understood. In this thesis, mice specifically lacking HOIP in liver parenchyma were generated and the physiological role of LUBAC in hepatocytes was examined. LUBAC deficiency in liver parenchymal cells leads to hepatocyte apoptosis and inflammation in the liver at an earlier stage and promotes tumour formation. The mechanisms by which LUBAC deficiency results in cell death, hepatitis and eventual oncogenesis is discussed in this chapter.

4.1 Impact of HOIP deletion in liver parenchyma

4.1.1 Cre expression, loss of HOIP and cell death

Alb-Cre expression starts around embryonic day 14.5, and Cre gradually excises loxP-flanked genomic DNA until 6-7 weeks of age, when gene deletion is completed in approximately 90% of the alleles (Postic et al, 1999; Weisend et al, 2009). Embryonic livers at mid-gestation accommodate hepatoblasts and a large amount of hematopoietic progenitor cells. As hepatoblasts differentiate into mature hepatocytes during late gestation, hepatocytes begin to express albumin. In correlation with the increased level of serum albumin protein, Cre proteins are expressed in hepatocytes and excise loxP-flanked DNA.

In line with these reports, *Alb-Cre*-mediated HOIP deletion was efficiently executed in hepatocytes by 7-9 weeks of age in $Hoip^{\Delta hep}$ mice. Due to the low sensitivity of

HOIP antibody in immunohistochemistry it was not possible to assess which percentages of hepatocytes are devoid of HOIP at perinatal stages of the liver. Moreover, it has been unsuccessful to isolate hepatocytes from younger mice due to smaller sizes of the organ and vessels. Based on the fact that deletion mediated by *Alb-Cre* lasts from late gestation to 6 weeks of age, it appears that HOIP is deleted during this period.

A sharp rise in cell death was observed between 1-2 weeks of age, implying the induction of cell death by unknown mechanisms may be exacerbated during this period. Since there is a delay in achieving depletion of a target protein after its gene deletion, depending on the stability of the protein, *Hoip* gene deletion by *Alb-Cre* seems to take place perinatally, which is in line with the literature on *Alb-Cre* (Postic et al, 1999; Weisend et al, 2009). Figure 4.1 represents a modelling of the kinetics of HOIP protein deletion and percentage of dead cells. The number of dead cells should be proportional to the derivative of the number of dead cells, presumably with a certain delay in time. As deletion rate goes up in an accelerating manner, the dead cells increase. On the other hand, when deletion rate slows down, fewer cells undergo cell death. This simulation fits well the kinetics of dead cells per area observed in this study.

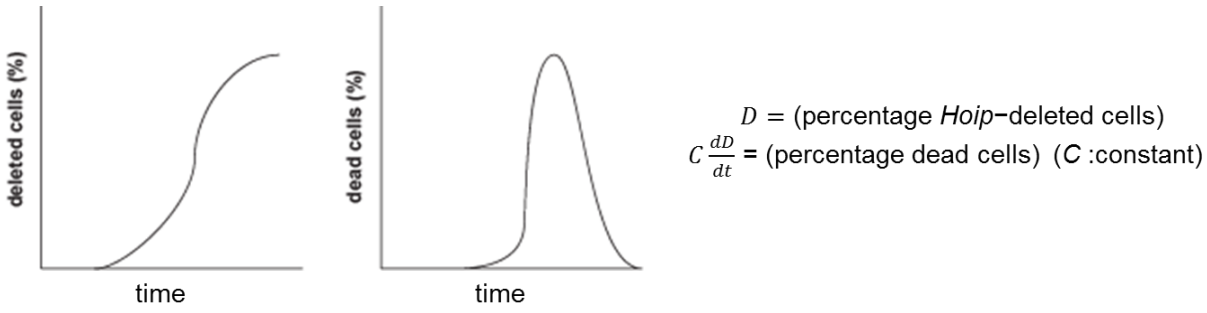

Figure 4.1 Model of kinetics of HOIP deletion and dead cell number in *Hoip*$^{\Delta hep}$ livers

However, the steep surge in ALT values is only observed in 2-4 week-old mice, which follows the peak of dead cells per area in the liver at 2 weeks of age. Measured ALT is the protein that leaks out of damaged hepatocytes. Thus, these factors would need to be considered: (i) biological half-life of ALT in the circulation,

and (ii) liver size and growth during this period. Because ALT could remain in the blood for a certain time after its release, this might cause a delay in the increase in ALT values. Finally, the size of the liver significantly expands during the first month of life in mice as they rapidly gain body weight. The drastic increase in the liver size might account for the delay in the surge of the total number of dead cells as compared to the number of the dead cells per area.

In the case of c-FLIP deletion in the liver, the two Cre drivers targeting LPCs has been shown to give rise to distinct phenotypes. While deletion with *Alb-Cre* causes only liver damage with elevated ALT, modification with *Alfp-Cre* confers perinatal lethality to mice (Piao et al., 2012). Scientists who established *Alfp-Cre* mice noticed that albumin expression was also regulated by an enhancer of alpha-fetoprotein (*Afp*) genes, which is located next to *Alb* gene (Kellendonk et al., 2000). By combining the *Alb* gene regulator with *Afp* gene enhancer, *Alfp-Cre* achieves an efficient induction of Cre from embryonic day 10.5, which is earlier than the initiation of Cre expression by *Alb-cre*. It is not entirely clear when *Alfp-Cre* achieves full penetrance of gene deletion during development, but c-FLIP deletion with *Alfp-Cre* demonstrated an efficient depletion of the protein already at postnatal day 1 (Piao et al., 2012). Although an earlier efficient deletion of HOIP at the perinatal stage is expected with *Alfp-Cre*, $Hoip^{flox/flox}$ *Alfp-Cre* mice were not lethal up to a weaning age. It will be intriguing to investigate whether there is any difference between phenotypes caused by gene deletion with *Alb-Cre* and *Alfp-Cre* at later stages of life.

4.1.2 Cell death precedes inflammation

The emergence of apoptotic bodies in $Hoip^{\Delta hep}$ mice was observed as early as postnatal day 7, which clearly precedes that of inflammation at 4 weeks of age. Initial apoptosis appears to trigger an early induction of cytokines at 2 weeks of age. Histologically, at 2 weeks of age, some apoptotic cells are approached by immune cells (Figure 3.12), which implies that leukocytes react to the cytokines and DAMPs produced by dead cells in HOIP-deficient livers. This process seems exacerbated around 4 weeks of age, when a wide range of immune cells is recruited to the site of inflammation in HOIP-deficient livers. Furthermore, the apparent resolution of inflammation coincided with the sharp decline in the number of dead cells in the liver.

Given that cell death due to loss of LUBAC is the primary driver of inflammation therein, it is highly likely that inflammation is ameliorated because its source, cell death, is reduced.

This observation is in line with accumulating evidence indicating that cell death is a driver of inflammation in various *in-vitro* and *in-vivo* studies. For instance, in LPC-specific truncated CYLD knock-in mice, the first abnormality detected is increased cell death from day 10 onwards, which precedes the induction of *Tnf* mRNA and immune cell activation at day 35 (Nikolaou et al., 2012). Thus, it appears that cell death drives production of inflammatory cytokines, which in turn renders cells prone to undergo cell death further. This is in accordance with the notion that regulated cell death participates in the initiation and amplification of inflammation (Pasparakis and Vandenabeele, 2015).

4.2 Tumourigenic process

4.2.1 Pathological aspects

The initial liver cell death in *Hoip*$^{\Delta hep}$ mice at postnatal day 7 was not accompanied by an inflammatory feature at all. The initial aberration observed, cell death, is reminiscent of a histological feature of patients suffering from drug-induced liver injury (DILI). The most common cause of DILI is an overdose of paracetamol (acetaminophen, *N*-acetyl-para-aminophenol, or APAP) due to its availability and popularity (Tajiri and Shimizu, 2008). However, in contrast to the excessive apoptosis in HOIP-deficient livers, a major characteristic of DILI is hepatocyte necrosis. The mechanism by which APAP induces cell death is not entirely clear. APAP is converted to a reactive metabolite (*N*-acetyl-p-benzoquinone imine, NAP-QI) in hepatocytes. Upon APAP overdose, accumulated NAP-QI depletes the reducing capacity of glutathione. Currently the only effective intervention for DILI is the antioxidant *N*-acetylcysteine (NAC), which promotes the recovery of the level of glutathione in the liver after APAP overdose. NAC counteracts the oxidising action of NAP-QI toward glutathione to facilitate its regeneration. ROS production is associated with carcinogenesis as it causes immune activation and provokes DNA

damage in stromal cells (Ohnishi et al., 2013). In livers devoid of IKK2 or NEMO, a reduced level of superoxide dismutases (SODs), which are enzymes quenching ROS, seems to exacerbate inflammation (Maeda et al, 2005; Vlantis et al, 2015). The expression level of SODs is upregulated by constitutive activation of canonical NF-κB by expressing an active form of IKK2 (Vlantis et al., 2015). Therefore, it will be interesting to pursue whether liver damage and tumourigenesis triggered by HOIP deletion would be ameliorated by treatment with antioxidants or upregulation of SODs.

HOIP-deficient livers seem to lack a robust fibrogenesis, which is often seen in human patients suffering from liver cancer and NEMO or TAK1 deficiency in murine livers (Luedde et al., 2007; Betterman et al., 2010; El-serag, 2011). However, it has been reported that HCV-associated cancer can evolve without cirrhosis (De Mitri et al., 1995). Also there are increasing numbers of liver cancer patients without a prior history of liver cirrhosis, which appears to be linked to NAFLD, particularly in the Western world (Rahman et al., 2013). Insulin resistance is linked to fat accumulation in the liver. Excessive visceral fat deposition promotes the release of pro-inflammatory cytokines. Hyperglycemia caused by insulin resistance leads to increased oxidative stress which also promotes inflammation. Interestingly, in a mouse model, DEN and HFD-induced hepatocarcinogenesis is promoted by inflammatory cytokines IL-6 and TNF (Park et al., 2010).

As the accumulation of lipid droplets was observed in HOIP-deficient livers at 18 months of age, it is reasonable to speculate that *Hoip*$^{\Delta hep}$ mice suffer from NAFLD-related symptoms. The mechanism as to how cell death-driven inflammation driven by cell death leads to accumulation of fatty acids in hepatocytes needs to be addressed. In a NASH mouse model employing CD-HFD, C57BL/6 mice develop $CD8^+$ T cell- and NKT cell-driven steatohepatitis (Wolf et al., 2014). Deletion of the TNF superfamily member LIGHT or its receptor LTβR prevents the development of steatohepatitis and HCC in mice. LIGHT effectively upregulates fatty acid intake in hepatocytes (Wolf et al., 2014), and LIGHT-mediated dyslipidemia is dependent on LTβR (James et al., 2007). In humans, serum LIGHT is increased in NAFLD patients (Otterdal et al., 2015). *Light* mRNA level has a tendency to increase at the peak of inflammation in *Hoip*$^{\Delta hep}$ livers. Moreover, the other LTβR ligand LTβ was highly

upregulated in *Hoip*$^{\Delta hep}$ livers. Therefore, it would be tempting to investigate the role of LTβR and its ligands in *Hoip*$^{\Delta hep}$ livers.

There is no evidence, to date, that loss of LUBAC occurs in human patients suffering from liver diseases. In mouse models of NASH, methionine- and choline-deficient diet (MCD) induces downregulation of LUBAC components and impairment in LUBAC formation (Matsunaga et al., 2015). Yet it remains unsolved whether LUBAC downregulation is responsible for MCD-induced liver damage and steatohepatitis. It will be intriguing to investigate whether hepatotropic virus carriers, ASH, NASH and HCC patients displays any change in the protein levels of LUBAC components. If this is the case, sustaining LUBAC function might be a promising strategy for a novel therapy in such patients.

4.2.2 DNA damage and selection

After hepatitis flares in *Hoip*$^{\Delta hep}$ mice at 4 weeks of age, the inflammation is ameliorated, suggesting that inflammation is transient and not sustained. Is this mere transient inflammation sufficient to account for the eventual tumourigenesis? In the case of a chemically-induced liver cancer model, a single injection of carcinogen DEN in C57BL/6 mice at early age induces liver cancer later in life (Maeda et al., 2005), which means that mutagenesis at an early stage is sufficient to trigger carcinogenesis even without chronic inflammation. According to the 'Big Bang' model of cancer evolution, most of the intra-tumour heterogeneity is derived from early genetic alteration, rather than later clonal expansions (Sottoriva et al., 2015). This model also indicates that some tumour subclones can acquire malignant characteristics at a very early stage of carcinogenesis. If this model applies to *Hoip*$^{\Delta hep}$ livers, their early transient inflammation can be a decisive factor in determining the mutagenic signature of hepatocytes which later give rise to a tumour. An increased DNA damage response was detected in *Hoip*$^{\Delta hep}$ livers at the peak of inflammation (Figure 3.10), which could explain, at least in part, the process of oncogenesis therein. The extent of DNA damage appears to be correlated with that of inflammation since *Tnrf1*^{KO} *Hoip*$^{\Delta hep}$ mice had less γH2AX^{+} cells with reduced inflammation as compared to *Hoip*$^{\Delta hep}$ mice (Figure 3.21). It will be interesting to

know if this decreased inflammation correlates with less severe tumourigenesis at a later stage.

It is still unclear what genes are affected and mutated in *Hoip*$^{\Delta hep}$ mice. It certainly is an interesting question to test whether *Hoip*$^{\Delta hep}$ livers develop well-known oncogenic mutations in their genome, for instance *Tp53* and *Ctnnb1,* at different ages until tumours arise in *Hoip*$^{\Delta hep}$ mice. Nodules from *Tak1*$^{LPC\text{-}KO}$ and *Nemo*$^{LPC\text{-}KO}$ mice exhibited upregulation of proliferation and cell cycle genes (Betterman et al., 2010). The rate of gene alteration in *Tak1*$^{LPC\text{-}KO}$ livers is clearly correlated with the degree of apoptosis and inflammation, as caspase-8 deletion abolishes most of it (Vucur et al., 2013).

Hepatocytes devoid of HOIP are prone to undergo cell death. Despite the efficient deletion of HOIP, the vast majority of HOIP-deficient hepatocytes are still alive. This means that a substantial portion of HOIP-deficient hepatocytes are able to survive the environment. It is also possible that they adapted to the change in LUBAC levels by upregulating some pro-survival factors unexamined here, which in turn could contribute to oncogenesis.

4.2.3 Pro-tumourigenic signalling pathways

IL-6 is one of the most prominent pro-tumourigenic cytokines, notably in liver cancer (He et al., 2010). IL-6 activates transcription factor STAT3, which is a transcription activator of pro-survival genes and frequently mutated in human cancer. In murine liver cancer models, IL-6 promotes chemically-induced liver carcinogenesis and, in preneoplastic lesions, liver cancer progenitor cells grow depending on autocrine IL-6 signalling (Naugler et al., 2007; He et al., 2013). At the peak of early inflammation in *Hoip*$^{\Delta hep}$ mice, no significant increase in the level of *Il6* mRNA was observed (Figure 3.7). However, the future work will investigate the contribution of IL-6 in tumourigenesis in *Hoip*$^{\Delta hep}$ mice by evaluating the level of IL-6 at 18 months of age at which the majority of the animals developed nodules. In addition, STAT3 activation in the pre-cancerous stage will be also examined to determine whether STAT3 activation is involved in the oncogenesis.

Disruption of NF-κB signalling components in LPCs often results in hyperactivation of JNK (Vucur et al, 2013; Nikolaou et al, 2012; Betterman et al., 2010). Deletion of JNK1 diminishes the susceptibility of *Ikk2*$^{\Delta hep}$ mice to chemically-induced carcinogenesis (Sakurai et al., 2006). Furthermore, abrogation of TAK1 and NEMO in LPCs also leads to oncogenesis with JNK hyperactivation (Luedde et al., 2007; Betterman et al., 2010; Inokuchi et al., 2010). JNK activation in *Ikk2*$^{\Delta hep}$ and *Nemo*$^{LPC\text{-}KO}$ livers is reduced by treatment with an antioxidant, suggesting JNK activation is mediated by ROS in these contexts. In *Nemo*$^{LPC\text{-}KO}$ livers, the JNK pathway appears to be activated by TAK1. Aberrant TAK1 activation is also present in LPC-specific truncated CYLD knock-in livers, where CYLD truncation causes accumulation of Lys63-linked ubiquitin chains on TAK1. In fact, ablation of TAK1 in the CYLD-mutant livers results in amelioration of periportal cell death and fibrosis, although LPC-specific CYLD-mutant TAK1-deficient mice suffer from carcinogenesis, similar to *Tak1*$^{LPC\text{-}KO}$ mice (Nikolaou et al., 2012). Thus, the JNK pathway is engaged in the promotion of inflammation, and compensatory proliferation of hepatocytes. Yet, how NF-κB inhibition leads to JNK activation is not entirely clear. In HOIP-deficient hepatocytes, the basal level of JNK activation in primary hepatocytes is unaltered (Figure 3.16). Therefore, analysis of the TAK1-JNK signalling in the inflamed *Hoip*$^{\Delta hep}$ livers will be needed to clarify whether the TAK1-JNK axis promotes cell death, inflammation and regeneration of LUBAC-deficient hepatocytes.

Hyperactivation of the canonical Wnt pathway is one of the common characteristics of human liver cancer by mutation of signalling components, such as β-catenin and Axin (Kan et al., 2013). The role of LUBAC in Wnt signalling is yet unclear. Only a few studies to date investigated its role and claimed that LUBAC has a suppressive role in Wnt signalling. OTULIN interacts with Wnt signalling adaptor DVL2 and augments Wnt signalling output (Rivkin et al., 2013). By contrast, overexpression of HOIP and HOIL-1 suppresses Wnt signalling. OTULIN counteracts LUBAC to promote the signalling via binding to the PUB domain of HOIP (Takiuchi et al., 2014). As the Wnt pathway is crucial for determining liver zonation (Planas-Paz et al., 2016), disruption of Wnt pathway by LUBAC deficiency could impair liver homeostasis and regeneration upon liver damage.

4.3 Role of TNFR1 signalling

TNF-induced cell death is causative for the inflammatory phenotype of *cpdm* mice (Gerlach et al., 2011; Rickard et al., 2014; Kumari et al., 2014). Increased liver cell apoptosis in *cpdm* mice is reduced by genetic deletion of TNFR1 in the whole body (Kumari et al., 2014). Unexpectedly however, apoptosis and TUNEL-positive cell death in HOIP-deficient livers are independent of the presence of TNFR1.

In the case of epidermal keratinocytes in *cpdm* mice, TNFR1 deletion in the epidermis is sufficient to inhibit dermatitis (Kumari et al., 2014). As keratinocytes are a potent source of TNF, cell-autonomous TNF-TNFR1 pathway appears to be causative for keratinocyte death and skin inflammation in *cpdm* mice. In contrast, TNFR1 ablation did not prevent basal cell death in HOIP-deficient hepatocytes although, *in vitro*, they were sensitised to TNF-induced cell death. This result clearly indicates that TNF does not account for hepatocyte death *in vivo* upon HOIP deletion. Moreover, an increased level of TNF does not seem to amplify the death of hepatocytes, since there is no difference in serum ALT values between $Hoip^{\Delta hep}$ mice and $Tnfr1^{KO}$ $Hoip^{\Delta hep}$ mice whereas hepatic TNF level was much less in the latter. It remains enigmatic whether the death of LUBAC-deficient hepatocytes requires some ligands, or whether it occurs spontaneously.

Interestingly, despite the fact that TNFR1 was not involved in hepatocyte death, TNFR1 deletion ameliorated inflammation of HOIP-deficient livers, as characterised by the decrease in leukocyte number and cytokine production. Since $Tnfr1^{KO}$ $Hoip^{\Delta hep}$ mice have a similar degree of cell death, the process after cell death such as the recognition of cell death, reaction to dead cells and/or amplification of inflammation must be hampered by systemic abrogation of TNFR1. These processes are predominantly mediated by non-parenchymal cells. For instance, TNFR1 signalling is involved in activation of APCs in response to inflammatory cytokines (Calzascia et al., 2007). TNF is a potent activator of myeloid cells and TNF inhibits the expression of arginase, which plays an anti-inflammatory role by depriving immune cells of their nutrient, arginine. Therefore, pro-inflammatory functions of immune cells could be hampered by TNFR1 abrogation.

In addition to immune cells, it was considered that TNFR1 signalling in non-parenchymal and non-hematopoietic cells could participate in inflammation in *Nemo*$^{LPC\text{-}KO}$ mice (Ehlken et al., 2015). For example, recruitment of leukocytes from blood is regulated by immune cells and sinusoidal endothelial cells (Shetty et al., 2008). Endothelial cells play a crucial role in retaining immune cells in the tissue by expressing adhesion molecules. Notably ICAM-1 and VCAM-1 are adhesion molecules upregulated by TNF-mediated NF-κB activation (Pober and Sessa, 2007). Some chemokines recruiting lymphocytes, notably CCR5 ligands CCL3-5, are highly expressed in human liver endothelial cells (Shetty et al., 2008). These chemokines are induced by NF-κB signalling and also secreted from hepatocytes and hepatic stellate cells, which can together exacerbate inflammation.

Moreover, TNF is not the only ligand for TNFR1. Another ligand for TNFR1 characterised to date is LTα. LTα activates NF-κB signalling and induce cell death in HOIP-deficient cells, just as TNF (Peltzer et al., 2014). TNFR1 ablation rescues the lethality of HOIP-deficient mouse embryos to a larger degree than TNF knockout. Moreover, TNF knockout in the whole body does not mitigate cell death, inflammation and carcinogenesis in *Nemo*$^{LPC\text{-}KO}$ livers (Ehlken et al., 2015), whereas systemic TNFR1 knockout does (Cubero et al., 2014). Therefore, non-TNF TNFR1 ligand, presumably LTα, may also be involved in the pathogenesis.

4.4 How does LUBAC deficiency kill hepatocytes?

Since TNFR1 abrogation in *Hoip*$^{\Delta hep}$ mice did not alleviate the aberrant cell death in the liver, TNFR1-independent pathways are responsible for the death induction. Homozygous caspase-8 deletion completely prevented the liver damage in *Mlkl*^{KO} *Hoip*$^{\Delta hep}$ (Figure 3.28), whereas MLKL did not rescue it, which suggests caspase-8 dependent apoptosis is the primary cause of liver damage in *Hoip*$^{\Delta hep}$ livers. In this subchapter, I will discuss which pathways might be involved in activation of caspase-8 and subsequent inflammation of LUBAC-deficient livers.

4.4.1 RIPK1

In a search for the molecular mechanism of activation of caspase-8 in *Hoip*$^{\Delta hep}$ livers, the FADD-RIPK1-caspase-8 complex formation was noticed, and this formation was independent of the defect in gene activation. Several studies demonstrated that the RIPK1 kinase activity is required for the formation of the FADD-RIPK1-caspase-8 complex, where cIAP1/2 depletion, TAK1 inhibition and NEMO depletion induce such complex (Tenev et al., 2011; Dondelinger et al., 2013; Dondelinger et al., 2015; Conrad et al., 2016). By contrast, upon TLR3 activation and cIAP depletion, the RIPK1 kinase activity is dispensable to induce cell death, whereas RIPK1 knockdown prevents cell death (Feoktistova et al., 2011). This study indicates that involvement of the kinase activity of RIPK1 in activation of the FADD-RIPK1-caspase-8 complex may be context-dependent. In the case of *Hoip*$^{\Delta hep}$ livers, the FADD-RIPK1-caspase-8 complex formation was not inhibited by the allosteric RIPK1 kinase inhibitor Nec-1s, which suggested that activation of RIPK1 is not required for it, or that RIPK1 activation may have already taken place at the time of the treatment, which rendered the inhibitor unable to inhibit the complex formation. Also, in this thesis, it is not addressed whether RIPK1 inhibition interferes with other processes of liver pathogenesis. To answer this question, RIPK1 inhibition in *Hoip*$^{\Delta hep}$ mice needs to be performed *in vivo*, either by treatment with RIPK1 inhibitor or by crossing those mice with RIPK1 kinase-inactive mice.

RIPK1 is one of the prominent targets of linear ubiquitination in the TNF-RSC, where RIPK1 is ubiquitinated by cIAP1/2 and LUBAC in a Lys63-linked and Met1-linked manner, respectively (Haas et al., 2009; Gerlach et al., 2011; Draber et al., 2015). RIPK1 is also linearly ubiquitinated in the necrosome upon TNF/SM/zVAD stimulation (de Almagro et al., 2015). However, it is unclear whether ubiquitination of RIPK1 occurs at the TNFR1 signalling, in cytosolic compartments before the necrosome formation, or after it. HOIP silencing did not affect TNF/SM/zVAD-induced necrosome formation or cell death (de Almagro et al., 2015), which implies linear ubiquitination is dispensable for necrosome formation and function upon TNF/SM/zVAD stimulation. This research claimed that LUBAC can ubiquitinate RIPK1 in necrosome in SM-treated cells, where cIAP1 is absent but cIAP2 may still be present (de Almagro et al., 2015). In multiple immune signalling pathways, linear

ubiquitin is conjugated to Lys63-linked ubiquitin chains, but not directly on its substrates (Emmerich et al., 2013; Emmerich et al., 2016). Also, cIAP1/2 are often required for the recruitment of LUBAC to receptor signalling complexes, such as those of TNF, CD40 and TCR. In HOIP-deficient livers, RIPK1 is ubiquitinated, particularly the fraction recruited to FADD-caspase-8-c-FLIP complex. It is not known with which ubiquitin linkage types RIPK1 is modified in the complex. Of note, linear ubiquitin was not detected in the complex in both HOIP-proficient and -deficient hepatocytes. Therefore it is possible that linear ubiquitination of RIPK1 is essential for prevention of the FADD-RIPK1-caspase-8 complex, and thereby protection of hepatocytes against apoptosis.

4.4.2 cIAP1/2

Loss of IAP proteins triggered by SM induces the formation of a large protein complex consisting of RIPK1, FADD, caspase-8/10 and c-FLIP, named ripoptosome, formed independently of TNF, TRAIL and CD95L (Tenev et al., 2011; Feoktistova et al., 2011). Importantly, ripoptosome formation is reminiscnent of the complex formed upon HOIP deficiency in hepatocytes. However, basal IAP loss was not detected in HOIP-deficient hepatocytes, unlike NEMO deficiency where it reduces the levels of cIAP1/2 (Kondylis et al., 2015). It is not entirely clear how NEMO ablation impairs the expression levels of cIAP1/2, but it was suggested that loss of NF-κB signalling could be the cause of their downregulation. Although HOIP deficiency in hepatocytes also results in lowered canonical NF-κB signalling, at least in response to exogenous TNF, it does not seem to affect cIAP levels in the basal condition. Whilst NEMO deficiency completely abrogates canonical NF-κB signalling, there seems to be a little residual canonical NF-κB activation in the absence of HOIP, which could suffice to maintain the 'safe' expression levels of cIAP1/2. However, when HOIP-deficient primary hepatocytes were treated with caspase inhibitor zVAD, the levels of cIAP1/2 were reduced as compared to HOIP-proficient cells (Figure 3.24). Thus, there may be a mechanism to regulate cIAP1/2 expression in a caspase activity-dependent manner.

In response to TNF, cIAP1 depletion by treatment with SM is sufficient to induce FADD-RIPK1-caspase-8 complex in the presence of LUBAC in the cytosol (Tenev et al., 2011; Feoktistova et al., 2011). In TNFR1 signalling, and also in CD40 and TCR

signalling, cIAP1/2 are recruited prior to LUBAC to these receptor signalling complexes, and cIAP ablation by treatment with SM prevents LUBAC recruitment. It is not yet clear whether the increased FADD-RIPK1-caspase-8 formation upon IAP loss is dependent on the defect in LUBAC recruitment. To evaluate cIAP1/2's role in inhibition of apoptosis in hepatocytes, immunoprecipitation against FADD could be performed with lysates of cells treated with SM or knockdown of cIAP1/2. It is an interesting question to ask whether or not cIAP1/2 have an additional contribution in suppressing apoptosis, as compared to HOIP.

4.4.3 Necroptosis

In human NASH patients, RIPK3 is overexpressed in hepatocytes (Gautheron et al., 2014). In mouse NASH model employing methionine-choline-deficient diet (MCD) or in *Tak1*$^{LPC\text{-}KO}$ mice, RIPK3 mediates liver damage, hepatocyte growth and liver inflammation in the absence of caspase-8 (Vucur et al., 2013; Gautheron et al., 2014). These processes require the JNK pathway. However, it is not unequivocal whether these functions of RIPK3 are dependent on necroptotic regulation, as RIPK3 has other functions such as regualtion of inflammasome activation (Kang et al., 2013). It will be intriguing to know whether MLKL ablation has the same effect as RIPK3 deficiency in MCD model and *Tak1*$^{LPC\text{-}KO}$ mice.

Recent reports suggest that necroptotic cells are immunogenic. Vaccination of necroptotic tumour cells into the flank of mice is sufficient to induce antitumour immunity and reject tumour cells (Aaes et al., 2016). Necroptotic cells are capable of activating $CD8^+$ T cells via cross-presentation by DCs. Necroptosis induces DC activation and cross-priming of $CD8^+$ T cells more efficiently than apoptotic cells (Yatim et al., 2015). RIPK3 oligomerisation via RHIM domains leads to RIPK1-dependent NF-κB-mediated gene activation and the immunogenicity of necroptotic cell death requires NF-κB signalling (Yatim et al., 2015). Therefore, if there are necroptotic cells in the liver, they could amplify the inflammation.

Caspase-8 deletion in parenchyma leads to mild necrosis in the liver (Vucur et al., 2013). This is in contrast with the severe phenotype of caspase-8 ablation in the skin and intestinal epithelium, where it leads to dermatitis and ileitis, respectively, driven by RIPK3-mediated necroptosis (Kovalenko et al., 2009; Gunther et al., 2011;

Weinlich et al., 2013). Moreover, RIPK1 deletion leads to uncontrolled RIPK3 activation in a kinase-independent fashion (Dannappel et al., 2014; Dillon et al., 2014; Rickard et al., 2014). Thus, deregulation of TNFR1 signalling by LUBAC deficiency could promote necroptosis. Indeed, the skin in *cpdm* mice bears necroptotic cells as evaluated by phospho-MLKL staining and electron microscopy (Shimizu et al., 2016).

Currently, there is no decisive marker for necroptotic death in the field, although some scientists adopted phosphorylation of MLKL as a necroptosis marker (Wang et al., 2014; Shimizu et al., 2016). Necroptotic cells can be TUNEL-negative as some reports highlighted the features of necroptotic death. For instance, cells infected with Shigella die by necroptosis, where cells are negative for TUNEL (Carneiro et al., 2009). Thus, it is possible that TUNEL staining did not fully detect necroptosis in *Hoip*$^{\Delta hep}$ livers.

Yet in HOIP-deficient liver and hepatocytes, phosphorylation of MLKL was not detected in the lysates. This does not exclude the possibility of necroptosis in HOIP-deficient livers. Yet, considering that substantial activation of caspase-8 is seen in HOIP-deficient hepatocytes, caspase-8 is most likely active enough to prevent RIPK1 and RIPK3 from executing necroptosis. MLKL is currently considered to execute necroptosis downstream of RIPK3 (Peltzer et al., 2014; Conrad et al., 2016). Moreover, the locus of *Ripk3* gene is in the proximity of *Hoip* gene, which does not allow us to create RIPK3-deficient HOIP-floxed mice by mating the two strains. Thus, instead of RIPK3 deficiency, MLKL knockout mice was employed in this study. MLKL deletion in *Casp8*^{HET} *Hoip*$^{\Delta hep}$ did not ameliorate liver injury, indicating that MLKL-mediated necroptosis is unlikely to be a major player in the pathogenesis of *Hoip*$^{\Delta hep}$ livers.

4.4.4 LUBAC substrates

Aside from RIPK1, the known substrates of LUBAC in TNFR1 signalling are TNFR1, TRADD and NEMO (Gerlach et al., 2011; Draber et al., 2015). Because caspase-8 activation in HOIP-deficient hepatocytes is independent of TNFR1, ubiquitination of TNFR1 is highly unlikely to be involved in the cell death induction. Secondly, TRADD can be a part of cell death-inducing complex in TNF signalling when gene activation

is impaired or in the absence of RIPK1 (Figure 1.4). TRADD contributes to the 'slow' apoptotic process as compared to FADD-RIPK1-caspase-8, which mediates 'fast' apoptosis in *Nemo*$^{LPC\text{-}KO}$ livers when RIPK1 is absent (Kondylis et al., 2015). In HOIP-deficient hepatocytes, TRADD was not detected in the FADD-associated complex although the band of TRADD could have been overshadowed by an intense signal of the immunoglobulin derived from anti-FADD antibody used in immunoprecipitation, due to their proximity in the molecular size. Although the role of linear ubiquitination on TRADD is entirely unknown at present, in the absence of LUBAC, TRADD might mediate apoptotic signalling.

NEMO is not only a linear ubiquitin binding protein but also the first-described substrate for LUBAC (Tokunaga et al., 2009; Gerlach et al., 2011). NEMO ubiquitination is described to be required for activation of canonical NF-κB pathway (Tokunaga et al., 2009; Jun et al., 2013). It is still unclear whether NEMO ubiquitination, in contrast to ubiquitin binding via its UBAN domain, is required for inhibition of apoptosis.

Ikeda and colleagues reported at a conference that FADD can be linearly ubiquitinated in TNFR1 signalling (Ikeda, European Workshop of Cell Death, 2014), primarily based on *in-vitro* ubiquitination studies. FADD ubiquitination in the FADD-RIPK1-caspase-8 complex was not detected in HOIP-deficient hepatocytes. FADD appears to be the core component of the caspase-8 activating complex in HOIP-deficient hepatocytes. NEMO-deficient hepatocytes undergo apoptosis by activating caspase-8 via FADD, as FADD deletion significantly reduced their apoptosis, where FADD plays a central role in their cell death by forming the FADD-RIPK1-caspase-8 complex (Luedde et al., 2007; Kondylis et al., 2015). Thus, it may be hypothesised that concomitant FADD deletion could abolish caspase-8 activation and, hence, apoptosis of HOIP-deficient hepatocytes.

4.4.5 LUBAC and linear chain associated proteins

LUBAC is constitutively associated with two DUBs, OTULIN and CYLD. These DUBs are associated with HOIP in two distinct pools (Draber et al., 2015; Hrdinka et al., 2016). While the recruitment of OTULIN to TNFR1 or NOD2 signalling complex is controversial, CYLD is recruited to these receptor complexes, depending on HOIP's

presence but independently of HOIP's catalytic activity (Draber et al., 2015). In addition to the role as a suppressor of NF-κB signalling, CYLD promotes necrosome formation by cleaving ubiquitin chains on RIPK1 and thereby necroptosis (O'Donnell et al., 2011; Moquin et al., 2013).

HOIP deficiency might affect CYLD's function, its proper recruitment and/or intracellular localisation. As CYLD truncation in the liver leads to hepatocyte apoptosis (Nikolaou et al., 2012), which is akin to the phenotype of HOIP deficiency, the pro-apoptotic effect of LUBAC deficiency in hepatocytes might be attributable to deregulation of CYLD. It has been shown that SPATA2 mediates binding between HOIP and CYLD, and regulates NF-κB activation and TNF-induced necroptosis (Wagner et al., 2016; Kupka et al., in press). However, at the moment it is completely unknown whether this function of SPATA2 on signalling and cell death is entirely dependent on its binding to CYLD.

A20 recruitment to the TNF-RSC is dependent on the binding to linear ubiquitin and HOIP's catalytic activity (Tokunaga et al., 2013; Draber et al., 2015). A20 serves as an inhibitor of TNF-induced apoptosis (Lee et al., 2000). Particularly mutation of ZF7 of A20, which lacks its binding site to linear ubiquitin, sensitises cells to TNF-induced cell death (Draber et al., 2015; Yamaguchi et al., 2015). Although A20 deletion in LPCs does not trigger spontaneous liver damage, $A20^{LPC\text{-}KO}$ mice are more sensitive to TNF-induced hepatitis, which is dependent on FADD-mediated apoptosis (Catrysse et al., 2016). Also, A20 counteracts NASH by attenuating accumulation of fatty acids in hepatocytes (Ai et al., 2015). Thus, loss of HOIP could disrupt A20 recruitment to signalling complexes which are mediated by linear ubiquitination, and increase susceptibility to cell death and fat deposition.

NEMO recruitment to the TNF-RSC is also LUBAC-dependent (Haas et al., 2009). NEMO deficiency in LPCs leads to much more severe pathology in the liver, as compared to $Hoip^{\Delta hep}$. Therefore it is unlikely that LUBAC deficiency results in complete loss of function of NEMO. Nevertheless, some of the functions of NEMO might be impaired by LUBAC deficiency because NEMO may not be properly recruited to certain complexes. In addition to A20 and NEMO, functions of other linear ubiquitin binding proteins might be disrupted by LUBAC deficiency in hepatocytes. For instance, the recruitment of UBAN-carrying protein ABIN-1 could

be impaired as well. ABIN-1 inhibits FADD-caspase-8 association and protects hepatocytes from TNF-induced cell death depending on the presence of the UBAN domain (Oshima et al., 2009).

Taken together, HOIP abrogation could promote cell death via mislocating LUBAC- and linear ubiquitin-associated factors. It will be tempting to dissect the catalytic activity and the scaffolding function of HOIP in the liver pathogenesis by employing the catalytically inactive mutant of HOIP. Inactive HOIP mutant abrogates linear polyubiquitin production and would affect proper localisation of linear ubiquitin binding proteins in the signalling as previously shown in TNF signalling, while maintaining the recruitment of LUBAC-associated proteins such as SPATA2-CYLD and/or OTULIN intact (Figure 4.2).

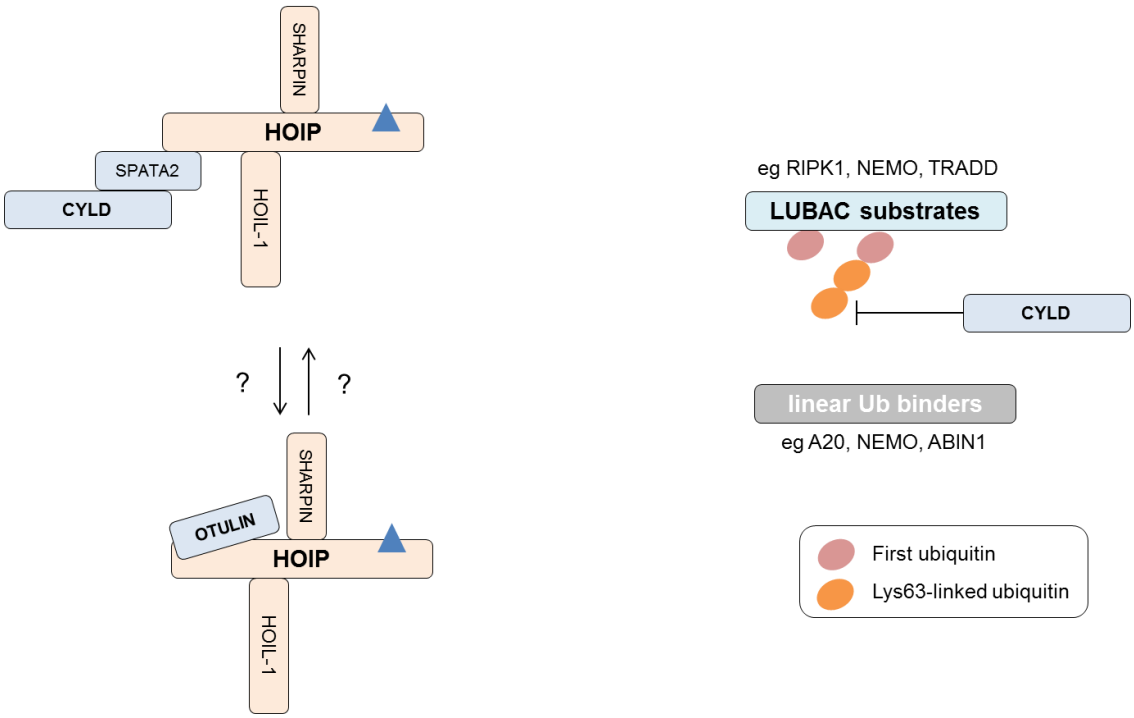

Figure 4.2 Schematic of the potential consequences of HOIP inactivation. Inactivation of HOIP leads to the loss of linear ubiquitin linkage on its substrates. This impairs the recruitment of complex components; for instance, linear ubiquitin receptors are not recruited to LUBAC substrates in the corresponding signalling complexes, which would cause sub-optimal activation of signalling and aberrant regulation of cell death.

4.5 Summary and outlook

In this thesis, the role of LUBAC deficiency on liver homeostasis and the molecular mechanisms thereof has been investigated. LUBAC protects hepatocytes against apoptosis via preventing FADD-RIPK1-caspase-8 cell death-inducing complex. In addition, LUBAC positively regulates canonical NF-κB signalling. These pro-survival functions of LUBAC are abrogated by HOIP depletion, resulting in hepatocyte apoptosis and liver inflammation. Liver inflammation is a crucial incident to create a pro-tumourigenic environment by initiation of the regenerative process and induction of DNA damage (Figure 4.3).

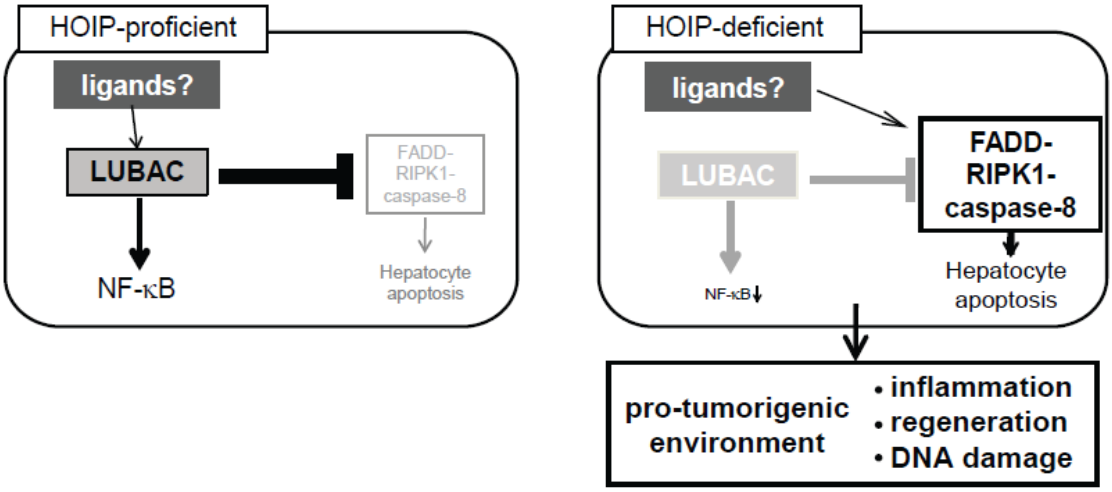

Figure 4.3 Schematic representation of the molecular function of HOIP in hepatocytes

Interestingly, the first aberrant event in HOIP-deficient livers is cell death, which is independent of the TNFR1 presence in hepatocytes. By contrast, the following events, inflammation and DNA damage response require TNFR1 signalling. These results indicate that there is a clear distinction of regulation between cell death and inflammation in the liver.

Previous studies strongly suggested that liver inflammation due to disruption of NF-κB signalling is driven by apoptotic signalling (Vucur et al., 2013; Kondylis et al., 2015). In our mouse model of LUBAC deficiency, it is not entirely clear yet if caspase-8 deletion together with MLKL deletion results in a complete rescue of

inflammation and carcinogenesis, which requires further clarification. The obstacle for examining *Mlkl*^{KO} *Casp8*^{HET} *Hoip*$^{\Delta hep}$ mice is their early development of lymphadenopathy around 2-3 months of age. To circumvent this problem, hematopoietic cells in *Mlkl*^{KO} *Casp8*^{KO} *Hoip*$^{\Delta hep}$ mice could be reconstituted with *Mlkl*^{KO} *Casp8*^{HET} or wild-type bone marrow cells after irradiation. Alternatively, it is possible to employ caspase-8 floxed strain, instead of systemic caspase-8 knockout mice, to avoid its deletion in non-LPCs, particularly in the immune system.

The precise mechanism of caspase-8 activation in HOIP-deficient hepatocytes remains still elusive. How is the FADD-RIPK1-caspase-8 complex formed in HOIP-deficient hepatocytes? Does this require some exogenous stimuli? Or the mere LUBAC deficiency is sufficient to trigger this? The potential involvement of some death receptor signalling can be tested by employing, for instance, TRAIL-R and CD95 knockout animals. TLR signalling can be evaluated by crossing with MyD88 knockout mice except for TLR3 signalling, which can be addressed by TLR3 or TRIF deficiency.

Furthermore, how LUBAC is involved in the prevention of the complex formation is still a conundrum. Is linear ubiquitination of the complex component(s) sufficient for the inhibition, or is the scaffolding function of HOIP, for instance binding to OTULIN and/or SPATA2-CYLD complex, required for it? To answer these questions, a further dissection of the functions of HOIP would be essential. If the loss of linear ubiquitination is solely accountable for the phenotype, there must be one or multiple LUBAC substrates that is linearly ubiquitinated in hepatocytes under steady state and keeps FADD, RIPK1 and caspase-8 in check to prevent them to be assembled and activated.

Acknowledgements

First of all, I would like to express my gratitude to my supervisor Professor Henning Walczak for accepting me and providing me with a very stimulating environment in his laboratory. I would like to thank Japan student service organization (JASSO) for a generous three-year funding for my PhD study.

Furthermore, I would like to thank:

Professor Mala Maini and Dr Pablo Rodriguez-Viciana for being wonderful PhD upgrade assessors and giving me advice on the directions of my project;

Professor Sibylle Mittnacht and Professor Pascal Meier for being the examiners for the viva voce and correcting PhD thesis;

Ms Lorraine Lawrence for excellent histology service and training;

Dr Samira Alliouachene and Dr Benoit Bilanges for instructing hepatocyte isolation techniques;

Dr Alison Winstanley for giving me histopathological insights;

Mr Signore Massimo for mouse transgenic services;

Mr Paul Levy, Ms Toni Clark, Mr Mark White and Mr Peter Ward for taking care of our mouse colonies.

Also, I would like to thank former and current lab members for having me and working together in the lab:

Dr Nieves Peltzer for giving me guidance throughout my PhD, correcting my thesis and many documents and being a cheerful desk neighbour;

Dr Alexandra Sevko for teaching me immunological experiments, broadening my insights on immunology and correcting my thesis;

Dr Elodie Lafont for being a fun bench neighbour, having chit-chats from science to our life, all the original jingles, French lessons and correcting my manuscripts and thesis;

Dr Maurice Darding and Ms Lucia Taraborrelli for being amazing teammates of *in-vivo* LUBAC team and correction of my thesis;

Ms Aida Sarr for all the appreciated genotyping works and laughs;

Ms Helena Draberova for our complex mouse colony management;

Dr Maureen Galmes-Spit for having fun working together on the intestine project and correction of my thesis;

Dr Peter Draber and Mr Torsten Hartwig for being fanatic training buddies and correction of my thesis;

Dr Katarzyna Wojdyla for being a kind desk neighbour and running buddy;

Dr Silvia Surinova, Dr Diego de Miguel Samaniego, Mr Sebastian Kupka and Ms Itziar Areso for correction of my thesis and companionship;

Dr Eva Rieser, Dr Silvia von Karstedt, Dr Antonella Montinaro, Dr Johannes Lemke, Dr Charahzade Kantari-Mimoun, Ms Julia Zinngrebe and Mr Matthias Reichert for being lovely lab mates;

Dr Nessa Adams, Ms Silvia Bianco, Ms Celeste Aouilk-Jaiyeola, Ms Ieva Songailaite and Ms Roxanne Payne for helping me on administrations.

Last but not least, I would like to thank my family and friends:

My grandparents, parents, my cousins and brother for unconditional love and support from abroad;

Wataru Ohira, Rie Yamazaki and Ángel Andreu for great friendship, love and support during and after living together in London.

Thank you very much and *arigato*,

Yutaka Shimizu 清水 裕

Bibliography

Aaes, T.L., Kaczmarek, A., Delvaeye, T., De Craene, B., De Koker, S., Heyndrickx, L., Delrue, I., Taminau, J., Wiernicki, B., De Groote, P., et al. (2016). Vaccination with Necroptotic Cancer Cells Induces Efficient Anti-tumor Immunity. Cell reports 15, 274-287.

Aderem, A., and Underhill, D.M. (1999). Mechanisms of phagocytosis in macrophages. Annual review of immunology 17, 593-623.

Ai, L., Xu, Q., Wu, C., Wang, X., Chen, Z., Su, D., Jiang, X., Xu, A., Lin, Q., and Fan, Z. (2015). A20 Attenuates FFAs-induced Lipid Accumulation in Nonalcoholic Steatohepatitis. International journal of biological sciences 11, 1436-1446.

Alberts B, Johnson A, Lewis J, et al. (2002). Molecular Biology of the Cell. 4th edition.

Akira, S., and Takeda, K. (2004). Toll-like receptor signalling. Nature reviews Immunology 4, 499-511.

Aradhya, S., Courtois, G., Rajkovic, A., Lewis, R.A., Levy, M., Israel, A., and Nelson, D.L. (2001). Atypical forms of incontinentia pigmenti in male individuals result from mutations of a cytosine tract in exon 10 of NEMO (IKK-gamma). American journal of human genetics 68, 765-771.

Balkwill, F., and Mantovani, A. (2001). Inflammation and cancer: back to Virchow? Lancet 357, 539-545.

Berger, S.B., Kasparcova, V., Hoffman, S., Swift, B., Dare, L., Schaeffer, M., Capriotti, C., Cook, M., Finger, J., Hughes-Earle, A., et al. (2014). Cutting Edge: RIP1 kinase activity is dispensable for normal development but is a key regulator of inflammation in SHARPIN-deficient mice. J Immunol 192, 5476-5480.

Bertrand, M.J., Doiron, K., Labbe, K., Korneluk, R.G., Barker, P.A., and Saleh, M. (2009). Cellular inhibitors of apoptosis cIAP1 and cIAP2 are required for innate immunity signaling by the pattern recognition receptors NOD1 and NOD2. Immunity 30, 789-801.

Bertrand, M.J., Milutinovic, S., Dickson, K.M., Ho, W.C., Boudreault, A., Durkin, J., Gillard, J.W., Jaquith, J.B., Morris, S.J., and Barker, P.A. (2008). cIAP1 and cIAP2 facilitate cancer cell survival by functioning as E3 ligases that promote RIP1 ubiquitination. Molecular cell 30, 689-700.

Bettermann, K., Vucur, M., Haybaeck, J., Koppe, C., Janssen, J., Heymann, F., Weber, A., Weiskirchen, R., Liedtke, C., Gassler, N., et al. (2010). TAK1 suppresses a NEMO-dependent but NF-kappaB-independent pathway to liver cancer. Cancer cell 17, 481-496.

Beyaert, R. (2014). An E3 ubiquitin ligase-independent role of LUBAC. Blood 123, 2131-2133.

Bignell, G.R., Warren, W., Seal, S., Takahashi, M., Rapley, E., Barfoot, R., Green, H., Brown, C., Biggs, P.J., Lakhani, S.R., et al. (2000). Identification of the familial cylindromatosis tumour-suppressor gene. Nature genetics 25, 160-165.

Bodmer, J.L., Holler, N., Reynard, S., Vinciguerra, P., Schneider, P., Juo, P., Blenis, J., and Tschopp, J. (2000). TRAIL receptor-2 signals apoptosis through FADD and caspase-8. Nature cell biology 2, 241-243.

Boisson, B., Laplantine, E., Dobbs, K., Cobat, A., Tarantino, N., Hazen, M., Lidov, H.G., Hopkins, G., Du, L., Belkadi, A., et al. (2015). Human HOIP and LUBAC deficiency underlies autoinflammation, immunodeficiency, amylopectinosis, and lymphangiectasia. The Journal of experimental medicine 212, 939-951.

Boisson, B., Laplantine, E., Prando, C., Giliani, S., Israelsson, E., Xu, Z., Abhyankar, A., Israel, L., Trevejo-Nunez, G., Bogunovic, D., et al. (2012). Immunodeficiency, autoinflammation and amylopectinosis in humans with inherited HOIL-1 and LUBAC deficiency. Nature immunology 13, 1178-1186.

Boldin, M.P., Goncharov, T.M., Goltsev, Y.V., and Wallach, D. (1996). Involvement of MACH, a novel MORT1/FADD-interacting protease, in Fas/APO-1- and TNF receptor-induced cell death. Cell 85, 803-815.

Bonizzi, G., and Karin, M. (2004). The two NF-kappaB activation pathways and their role in innate and adaptive immunity. Trends in immunology 25, 280-288.

Bonnet, M.C., Preukschat, D., Welz, P.S., van Loo, G., Ermolaeva, M.A., Bloch, W., Haase, I., and Pasparakis, M. (2011). The adaptor protein FADD protects epidermal keratinocytes from necroptosis in vivo and prevents skin inflammation. Immunity 35, 572-582.

Bosanac, I., Wertz, I.E., Pan, B., Yu, C., Kusam, S., Lam, C., Phu, L., Phung, Q., Maurer, B., Arnott, D., et al. (2010). Ubiquitin binding to A20 ZnF4 is required for modulation of NF-kappaB signaling. Molecular cell 40, 548-557.

Bouchard, M.J., Wang, L.H., and Schneider, R.J. (2001). Calcium signaling by HBx protein in hepatitis B virus DNA replication. Science 294, 2376-2378.

Callahan, J.A., Hammer, G.E., Agelides, A., Duong, B.H., Oshima, S., North, J., Advincula, R., Shifrin, N., Truong, H.A., Paw, J., et al. (2013). Cutting edge: ABIN-1 protects against psoriasis by restricting MyD88 signals in dendritic cells. J Immunol 191, 535-539.

Calzascia, T., Pellegrini, M., Hall, H., Sabbagh, L., Ono, N., Elford, A.R., Mak, T.W., and Ohashi, P.S. (2007). TNF-alpha is critical for antitumor but not antiviral T cell immunity in mice. The Journal of clinical investigation 117, 3833-3845.

Carneiro, L.A., Travassos, L.H., Soares, F., Tattoli, I., Magalhaes, J.G., Bozza, M.T., Plotkowski, M.C., Sansonetti, P.J., Molkentin, J.D., Philpott, D.J., et al. (2009). Shigella induces mitochondrial dysfunction and cell death in nonmyleoid cells. Cell host & microbe 5, 123-136.

Catrysse, L., Farhang Ghahremani, M., Vereecke, L., Youssef, S.A., Mc Guire, C., Sze, M., Weber, A., Heikenwalder, M., de Bruin, A., Beyaert, R., et al. (2016). A20 prevents chronic liver inflammation and cancer by protecting hepatocytes from death. Cell death & disease 7, e2250.

Chan, A.T., and Ladabaum, U. (2016). Where Do We Stand With Aspirin for the Prevention of Colorectal Cancer? The USPSTF Recommendations. Gastroenterology 150, 14-18.

Chen, W., Wu, J., Li, L., Zhang, Z., Ren, J., Liang, Y., Chen, F., Yang, C., Zhou, Z., Su, S.S., et al. (2015). Ppm1b negatively regulates necroptosis through dephosphorylating Rip3. Nature cell biology 17, 434-444.

Chisari, F.V., Klopchin, K., Moriyama, T., Pasquinelli, C., Dunsford, H.A., Sell, S., Pinkert, C.A., Brinster, R.L., and Palmiter, R.D. (1989). Molecular pathogenesis of hepatocellular carcinoma in hepatitis B virus transgenic mice. Cell 59, 1145-1156.

Chu, Y., Vahl, J.C., Kumar, D., Heger, K., Bertossi, A., Wojtowicz, E., Soberon, V., Schenten, D., Mack, B., Reutelshofer, M., et al. (2011). B cells lacking the tumor suppressor TNFAIP3/A20 display impaired differentiation and hyperactivation and cause inflammation and autoimmunity in aged mice. Blood 117, 2227-2236.

Claudio, E., Brown, K., Park, S., Wang, H., and Siebenlist, U. (2002). BAFF-induced NEMO-independent processing of NF-kappa B2 in maturing B cells. Nature immunology 3, 958-965.

Coope, H.J., Atkinson, P.G., Huhse, B., Belich, M., Janzen, J., Holman, M.J., Klaus, G.G., Johnston, L.H., and Ley, S.C. (2002). CD40 regulates the processing of NF-kappaB2 p100 to p52. The EMBO journal 21, 5375-5385.

Corazza, N., Jakob, S., Schaer, C., Frese, S., Keogh, A., Stroka, D., Kassahn, D., Torgler, R., Mueller, C., Schneider, P., et al. (2006). TRAIL receptor-mediated JNK activation and Bim phosphorylation critically regulate Fas-mediated liver damage and lethality. The Journal of clinical investigation 116, 2493-2499.

Damgaard, R.B., Nachbur, U., Yabal, M., Wong, W.W., Fiil, B.K., Kastirr, M., Rieser, E., Rickard, J.A., Bankovacki, A., Peschel, C., et al. (2012). The ubiquitin ligase XIAP recruits LUBAC for NOD2 signaling in inflammation and innate immunity. Molecular cell 46, 746-758.

Dannappel, M., Vlantis, K., Kumari, S., Polykratis, A., Kim, C., Wachsmuth, L., Eftychi, C., Lin, J., Corona, T., Hermance, N., et al. (2014). RIPK1 maintains epithelial homeostasis by inhibiting apoptosis and necroptosis. Nature 513, 90-94.

De, A., Dainichi, T., Rathinam, C.V., and Ghosh, S. (2014). The deubiquitinase activity of A20 is dispensable for NF-kappaB signaling. EMBO reports 15, 775-783.

de Almagro, M.C., Goncharov, T., Newton, K., and Vucic, D. (2015). Cellular IAP proteins and LUBAC differentially regulate necrosome-associated RIP1 ubiquitination. Cell death & disease 6, e1800.

De Mitri, M.S., Poussin, K., Baccarini, P., Pontisso, P., D'Errico, A., Simon, N., Grigioni, W., Alberti, A., Beaugrand, M., Pisi, E., et al. (1995). HCV-associated liver cancer without cirrhosis. Lancet 345, 413-415.

Dillon, C.P., Weinlich, R., Rodriguez, D.A., Cripps, J.G., Quarato, G., Gurung, P., Verbist, K.C., Brewer, T.L., Llambi, F., Gong, Y.N., et al. (2014). RIPK1 blocks early postnatal lethality mediated by caspase-8 and RIPK3. Cell 157, 1189-1202.

Doffinger, R., Smahi, A., Bessia, C., Geissmann, F., Feinberg, J., Durandy, A., Bodemer, C., Kenwrick, S., Dupuis-Girod, S., Blanche, S., et al. (2001). X-linked anhidrotic ectodermal dysplasia with immunodeficiency is caused by impaired NF-kappaB signaling. Nature genetics 27, 277-285.

Dondelinger, Y., Declercq, W., Montessuit, S., Roelandt, R., Goncalves, A., Bruggeman, I., Hulpiau, P., Weber, K., Sehon, C.A., Marquis, R.W., et al. (2014). MLKL compromises plasma membrane integrity by binding to phosphatidylinositol phosphates. Cell reports 7, 971-981.

Dondelinger, Y., Jouan-Lanhouet, S., Divert, T., Theatre, E., Bertin, J., Gough, P.J., Giansanti, P., Heck, A.J., Dejardin, E., Vandenabeele, P., et al. (2015). NF-kappaB-Independent Role of IKKalpha/IKKbeta in Preventing RIPK1 Kinase-Dependent Apoptotic and Necroptotic Cell Death during TNF Signaling. Molecular cell 60, 63-76.

Doria, M., Klein, N., Lucito, R., and Schneider, R.J. (1995). The hepatitis B virus HBx protein is a dual specificity cytoplasmic activator of Ras and nuclear activator of transcription factors. The EMBO journal 14, 4747-4757.

Draber, P., Kupka, S., Reichert, M., Draberova, H., Lafont, E., de Miguel, D., Spilgies, L., Surinova, S., Taraborrelli, L., Hartwig, T., et al. (2015). LUBAC-Recruited CYLD and A20 Regulate Gene Activation and Cell Death by Exerting Opposing Effects on Linear Ubiquitin in Signaling Complexes. Cell reports 13, 2258-2272.

Dubois, S.M., Alexia, C., Wu, Y., Leclair, H.M., Leveau, C., Schol, E., Fest, T., Tarte, K., Chen, Z.J., Gavard, J., et al. (2014). A catalytic-independent role for the LUBAC in NF-kappaB activation upon antigen receptor engagement and in lymphoma cells. Blood 123, 2199-2203.

Dunn, G.P., Old, L.J., and Schreiber, R.D. (2004). The immunobiology of cancer immunosurveillance and immunoediting. Immunity 21, 137-148.

Ea, C.K., Deng, L., Xia, Z.P., Pineda, G., and Chen, Z.J. (2006). Activation of IKK by TNFalpha requires site-specific ubiquitination of RIP1 and polyubiquitin binding by NEMO. Molecular cell 22, 245-257.

Ehlken, H., Krishna-Subramanian, S., Ochoa-Callejero, L., Kondylis, V., Nadi, N.E., Straub, B.K., Schirmacher, P., Walczak, H., Kollias, G., and Pasparakis, M. (2014). Death receptor-independent FADD signalling triggers hepatitis and hepatocellular carcinoma in mice with liver parenchymal cell-specific NEMO knockout. Cell death and differentiation 21, 1721-1732.

Elgueta, R., Benson, M.J., de Vries, V.C., Wasiuk, A., Guo, Y., and Noelle, R.J. (2009). Molecular mechanism and function of CD40/CD40L engagement in the immune system. Immunological reviews 229, 152-172.

Elgueta, R., Benson, M.J., de Vries, V.C., Wasiuk, A., Guo, Y., and Noelle, R.J. (2009). Molecular mechanism and function of CD40/CD40L engagement in the immune system. Immunological reviews 229, 152-172.

Elliott, P.R., Nielsen, S.V., Marco-Casanova, P., Fiil, B.K., Keusekotten, K., Mailand, N., Freund, S.M., Gyrd-Hansen, M., and Komander, D. (2014). Molecular basis and regulation of OTULIN-LUBAC interaction. Molecular cell 54, 335-348.

Ellis, R.E., Yuan, J.Y., and Horvitz, H.R. (1991). Mechanisms and functions of cell death. Annual review of cell biology 7, 663-698.

El-Serag, H.B. (2011). Hepatocellular carcinoma. The New England journal of medicine 365, 1118-1127.

Emmerich, C.H., Bakshi, S., Kelsall, I.R., Ortiz-Guerrero, J., Shpiro, N., and Cohen, P. (2016). Lys63/Met1-hybrid ubiquitin chains are commonly formed during the activation of innate immune signalling. Biochemical and biophysical research communications 474, 452-461.

Emmerich, C.H., Ordureau, A., Strickson, S., Arthur, J.S., Pedrioli, P.G., Komander, D., and Cohen, P. (2013). Activation of the canonical IKK complex by K63/M1-linked hybrid ubiquitin chains. Proceedings of the National Academy of Sciences of the United States of America 110, 15247-15252.

Ermolaeva, M.A., Michallet, M.C., Papadopoulou, N., Utermohlen, O., Kranidioti, K., Kollias, G., Tschopp, J., and Pasparakis, M. (2008). Function of TRADD in tumor necrosis factor receptor 1 signaling and in TRIF-dependent inflammatory responses. Nature immunology 9, 1037-1046.

Etemadi, N., Chopin, M., Anderton, H., Tanzer, M.C., Rickard, J.A., Abeysekera, W., Hall, C., Spall, S.K., Wang, B., Xiong, Y., et al. (2015). TRAF2 regulates TNF and NF-kappaB signalling to suppress apoptosis and skin inflammation independently of Sphingosine kinase 1. eLife 4.

Fiil, B.K., Damgaard, R.B., Wagner, S.A., Keusekotten, K., Fritsch, M., Bekker-Jensen, S., Mailand, N., Choudhary, C., Komander, D., and Gyrd-Hansen, M. (2013). OTULIN restricts Met1-linked ubiquitination to control innate immune signaling. Molecular cell 50, 818-830.

Fischer, U., Janicke, R.U., and Schulze-Osthoff, K. (2003). Many cuts to ruin: a comprehensive update of caspase substrates. Cell death and differentiation 10, 76-100.

Fuchs, S.Y., Chen, A., Xiong, Y., Pan, Z.Q., and Ronai, Z. (1999). HOS, a human homolog of Slimb, forms an SCF complex with Skp1 and Cullin1 and targets the phosphorylation-dependent degradation of IkappaB and beta-catenin. Oncogene 18, 2039-2046.

Ganten, T.M., Koschny, R., Haas, T.L., Sykora, J., Li-Weber, M., Herzer, K., and Walczak, H. (2005). Proteasome inhibition sensitizes hepatocellular carcinoma cells, but not human hepatocytes, to TRAIL. Hepatology 42, 588-597.

Gautheron, J., Vucur, M., Reisinger, F., Cardenas, D.V., Roderburg, C., Koppe, C., Kreggenwinkel, K., Schneider, A.T., Bartneck, M., Neumann, U.P., et al. (2014). A positive feedback loop between RIP3 and JNK controls non-alcoholic steatohepatitis. EMBO molecular medicine 6, 1062-1074.

Gerlach, B., Cordier, S.M., Schmukle, A.C., Emmerich, C.H., Rieser, E., Haas, T.L., Webb, A.I., Rickard, J.A., Anderton, H., Wong, W.W., et al. (2011). Linear ubiquitination prevents inflammation and regulates immune signalling. Nature 471, 591-596.

Ghosh, S., and Baltimore, D. (1990). Activation in vitro of NF-kappa B by phosphorylation of its inhibitor I kappa B. Nature 344, 678-682.

Ghosh, S., May, M.J., and Kopp, E.B. (1998). NF-kappa B and Rel proteins: evolutionarily conserved mediators of immune responses. Annual review of immunology 16, 225-260.

Gijbels, M.J., HogenEsch, H., Bruijnzeel, P.L., Elliott, G.R., and Zurcher, C. (1995). Maintenance of donor phenotype after full-thickness skin transplantation from mice with chronic proliferative dermatitis (cpdm/cpdm) to C57BL/Ka and nude mice and vice versa. The Journal of investigative dermatology 105, 769-773.

Girardin, S.E., Boneca, I.G., Viala, J., Chamaillard, M., Labigne, A., Thomas, G., Philpott, D.J., and Sansonetti, P.J. (2003). Nod2 is a general sensor of peptidoglycan through muramyl dipeptide (MDP) detection. The Journal of biological chemistry 278, 8869-8872.

Glickman, M.H., and Ciechanover, A. (2002). The ubiquitin-proteasome proteolytic pathway: destruction for the sake of construction. Physiological reviews 82, 373-428.

Gunther, C., Martini, E., Wittkopf, N., Amann, K., Weigmann, B., Neumann, H., Waldner, M.J., Hedrick, S.M., Tenzer, S., Neurath, M.F., et al. (2011). Caspase-8 regulates TNF-alpha-induced epithelial necroptosis and terminal ileitis. Nature 477, 335-339.

Haas, T.L., Emmerich, C.H., Gerlach, B., Schmukle, A.C., Cordier, S.M., Rieser, E., Feltham, R., Vince, J., Warnken, U., Wenger, T., et al. (2009). Recruitment of the linear ubiquitin chain assembly

complex stabilizes the TNF-R1 signaling complex and is required for TNF-mediated gene induction. Molecular cell 36, 831-844.

Haybaeck, J., Zeller, N., Wolf, M.J., Weber, A., Wagner, U., Kurrer, M.O., Bremer, J., Iezzi, G., Graf, R., Clavien, P.A., et al. (2009). A lymphotoxin-driven pathway to hepatocellular carcinoma. Cancer cell 16, 295-308.

He, G., Dhar, D., Nakagawa, H., Font-Burgada, J., Ogata, H., Jiang, Y., Shalapour, S., Seki, E., Yost, S.E., Jepsen, K., et al. (2013). Identification of liver cancer progenitors whose malignant progression depends on autocrine IL-6 signaling. Cell 155, 384-396.

He, G., Yu, G.Y., Temkin, V., Ogata, H., Kuntzen, C., Sakurai, T., Sieghart, W., Peck-Radosavljevic, M., Leffert, H.L., and Karin, M. (2010). Hepatocyte IKKbeta/NF-kappaB inhibits tumor promotion and progression by preventing oxidative stress-driven STAT3 activation. Cancer cell 17, 286-297.

Heindryckx, F., Colle, I., and Van Vlierberghe, H. (2009). Experimental mouse models for hepatocellular carcinoma research. International journal of experimental pathology 90, 367-386.

Hershko, A., and Ciechanover, A. (1998). The ubiquitin system. Annual review of biochemistry 67, 425-479.

Hikita, H., Kodama, T., Shimizu, S., Li, W., Shigekawa, M., Tanaka, S., Hosui, A., Miyagi, T., Tatsumi, T., Kanto, T., et al. (2012). Bak deficiency inhibits liver carcinogenesis: a causal link between apoptosis and carcinogenesis. Journal of hepatology 57, 92-100.

Hitotsumatsu, O., Ahmad, R.C., Tavares, R., Wang, M., Philpott, D., Turer, E.E., Lee, B.L., Shiffin, N., Advincula, R., Malynn, B.A., et al. (2008). The ubiquitin-editing enzyme A20 restricts nucleotide-binding oligomerization domain containing 2-triggered signals. Immunity 28, 381-390.

HogenEsch, H., Gijbels, M.J., Offerman, E., van Hooft, J., van Bekkum, D.W., and Zurcher, C. (1993). A spontaneous mutation characterized by chronic proliferative dermatitis in C57BL mice. The American journal of pathology 143, 972-982.

HogenEsch, H., Janke, S., Boggess, D., and Sundberg, J.P. (1999). Absence of Peyer's patches and abnormal lymphoid architecture in chronic proliferative dermatitis (cpdm/cpdm) mice. J Immunol 162, 3890-3896.

Hospenthal, M.K., Mevissen, T.E., and Komander, D. (2015). Deubiquitinase-based analysis of ubiquitin chain architecture using Ubiquitin Chain Restriction (UbiCRest). Nature protocols 10, 349-361.

Hsu, H., Shu, H.B., Pan, M.G., and Goeddel, D.V. (1996). TRADD-TRAF2 and TRADD-FADD interactions define two distinct TNF receptor 1 signal transduction pathways. Cell 84, 299-308.

Hsu, H., Xiong, J., and Goeddel, D.V. (1995). The TNF receptor 1-associated protein TRADD signals cell death and NF-kappa B activation. Cell 81, 495-504.

Hubeau, M., Ngadjeua, F., Puel, A., Israel, L., Feinberg, J., Chrabieh, M., Belani, K., Bodemer, C., Fabre, I., Plebani, A., et al. (2011). New mechanism of X-linked anhidrotic ectodermal dysplasia with immunodeficiency: impairment of ubiquitin binding despite normal folding of NEMO protein. Blood 118, 926-935.

Ikeda, F., Deribe, Y.L., Skanland, S.S., Stieglitz, B., Grabbe, C., Franz-Wachtel, M., van Wijk, S.J., Goswami, P., Nagy, V., Terzic, J., et al. (2011). SHARPIN forms a linear ubiquitin ligase complex regulating NF-kappaB activity and apoptosis. Nature 471, 637-641.

Inohara, N., Koseki, T., Lin, J., del Peso, L., Lucas, P.C., Chen, F.F., Ogura, Y., and Nunez, G. (2000). An induced proximity model for NF-kappa B activation in the Nod1/RICK and RIP signaling pathways. The Journal of biological chemistry 275, 27823-27831.

Inohara, N., Ogura, Y., Fontalba, A., Gutierrez, O., Pons, F., Crespo, J., Fukase, K., Inamura, S., Kusumoto, S., Hashimoto, M., et al. (2003). Host recognition of bacterial muramyl dipeptide mediated through NOD2. Implications for Crohn's disease. The Journal of biological chemistry 278, 5509-5512.

Inokuchi, S., Aoyama, T., Miura, K., Osterreicher, C.H., Kodama, Y., Miyai, K., Akira, S., Brenner, D.A., and Seki, E. (2010). Disruption of TAK1 in hepatocytes causes hepatic injury, inflammation, fibrosis, and carcinogenesis. Proceedings of the National Academy of Sciences of the United States of America 107, 844-849.

Irmler, M., Thome, M., Hahne, M., Schneider, P., Hofmann, K., Steiner, V., Bodmer, J.L., Schroter, M., Burns, K., Mattmann, C., et al. (1997). Inhibition of death receptor signals by cellular FLIP. Nature 388, 190-195.

Janeway, C.A., Jr., and Medzhitov, R. (2002). Innate immune recognition. Annual review of immunology 20, 197-216.

Jost, P.J., Grabow, S., Gray, D., McKenzie, M.D., Nachbur, U., Huang, D.C., Bouillet, P., Thomas, H.E., Borner, C., Silke, J., et al. (2009). XIAP discriminates between type I and type II FAS-induced apoptosis. Nature 460, 1035-1039.

Kaiser, W.J., Upton, J.W., Long, A.B., Livingston-Rosanoff, D., Daley-Bauer, L.P., Hakem, R., Caspary, T., and Mocarski, E.S. (2011). RIP3 mediates the embryonic lethality of caspase-8-deficient mice. Nature 471, 368-372.

Kan, Z., Zheng, H., Liu, X., Li, S., Barber, T.D., Gong, Z., Gao, H., Hao, K., Willard, M.D., Xu, J., et al. (2013). Whole-genome sequencing identifies recurrent mutations in hepatocellular carcinoma. Genome research 23, 1422-1433.

Kanayama, A., Seth, R.B., Sun, L., Ea, C.K., Hong, M., Shaito, A., Chiu, Y.H., Deng, L., and Chen, Z.J. (2004). TAB2 and TAB3 activate the NF-kappaB pathway through binding to polyubiquitin chains. Molecular cell 15, 535-548.

Kane, L.A., Lazarou, M., Fogel, A.I., Li, Y., Yamano, K., Sarraf, S.A., Banerjee, S., and Youle, R.J. (2014). PINK1 phosphorylates ubiquitin to activate Parkin E3 ubiquitin ligase activity. The Journal of cell biology 205, 143-153.

Kang, T.B., Ben-Moshe, T., Varfolomeev, E.E., Pewzner-Jung, Y., Yogev, N., Jurewicz, A., Waisman, A., Brenner, O., Haffner, R., Gustafsson, E., et al. (2004). Caspase-8 serves both apoptotic and nonapoptotic roles. J Immunol 173, 2976-2984.

Kang, T.B., Yang, S.H., Toth, B., Kovalenko, A., and Wallach, D. (2013). Caspase-8 blocks kinase RIPK3-mediated activation of the NLRP3 inflammasome. Immunity 38, 27-40.

Karin, M., and Clevers, H. (2016). Reparative inflammation takes charge of tissue regeneration. Nature 529, 307-315.

Kawai, T., and Akira, S. (2010). The role of pattern-recognition receptors in innate immunity: update on Toll-like receptors. Nature immunology 11, 373-384.

Kellendonk, C., Opherk, C., Anlag, K., Schutz, G., and Tronche, F. (2000). Hepatocyte-specific expression of Cre recombinase. Genesis 26, 151-153.

Keusekotten, K., Elliott, P.R., Glockner, L., Fiil, B.K., Damgaard, R.B., Kulathu, Y., Wauer, T., Hospenthal, M.K., Gyrd-Hansen, M., Krappmann, D., et al. (2013). OTULIN antagonizes LUBAC signaling by specifically hydrolyzing Met1-linked polyubiquitin. Cell 153, 1312-1326.

Kim, C.M., Koike, K., Saito, I., Miyamura, T., and Jay, G. (1991). HBx gene of hepatitis B virus induces liver cancer in transgenic mice. Nature 351, 317-320.

Kim, R., Emi, M., and Tanabe, K. (2007). Cancer immunoediting from immune surveillance to immune escape. Immunology 121, 1-14.

Kimura, Y., and Tanaka, K. (2010). Regulatory mechanisms involved in the control of ubiquitin homeostasis. Journal of biochemistry 147, 793-798.

Kirisako, T., Kamei, K., Murata, S., Kato, M., Fukumoto, H., Kanie, M., Sano, S., Tokunaga, F., Tanaka, K., and Iwai, K. (2006). A ubiquitin ligase complex assembles linear polyubiquitin chains. The EMBO journal 25, 4877-4887.

Kischkel, F.C., Hellbardt, S., Behrmann, I., Germer, M., Pawlita, M., Krammer, P.H., and Peter, M.E. (1995). Cytotoxicity-dependent APO-1 (Fas/CD95)-associated proteins form a death-inducing signaling complex (DISC) with the receptor. The EMBO journal 14, 5579-5588.

Kischkel, F.C., Lawrence, D.A., Chuntharapai, A., Schow, P., Kim, K.J., and Ashkenazi, A. (2000). Apo2L/TRAIL-dependent recruitment of endogenous FADD and caspase-8 to death receptors 4 and 5. Immunity 12, 611-620.

Komander, D., Clague, M.J., and Urbe, S. (2009). Breaking the chains: structure and function of the deubiquitinases. Nature reviews Molecular cell biology 10, 550-563.

Kondylis, V., Polykratis, A., Ehlken, H., Ochoa-Callejero, L., Straub, B.K., Krishna-Subramanian, S., Van, T.M., Curth, H.M., Heise, N., Weih, F., et al. (2015). NEMO Prevents Steatohepatitis and Hepatocellular Carcinoma by Inhibiting RIPK1 Kinase Activity-Mediated Hepatocyte Apoptosis. Cancer cell 28, 582-598.

Kovalenko, A., Kim, J.C., Kang, T.B., Rajput, A., Bogdanov, K., Dittrich-Breiholz, O., Kracht, M., Brenner, O., and Wallach, D. (2009). Caspase-8 deficiency in epidermal keratinocytes triggers an inflammatory skin disease. The Journal of experimental medicine 206, 2161-2177.

Koyano, F., Okatsu, K., Kosako, H., Tamura, Y., Go, E., Kimura, M., Kimura, Y., Tsuchiya, H., Yoshihara, H., Hirokawa, T., et al. (2014). Ubiquitin is phosphorylated by PINK1 to activate parkin. Nature 510, 162-166.

Kucharczak, J., Simmons, M.J., Fan, Y., and Gelinas, C. (2003). To be, or not to be: NF-kappaB is the answer--role of Rel/NF-kappaB in the regulation of apoptosis. Oncogene 22, 8961-8982.

Kulathu, Y., and Komander, D. (2012). Atypical ubiquitylation - the unexplored world of polyubiquitin beyond Lys48 and Lys63 linkages. Nature reviews Molecular cell biology 13, 508-523.

Kumari, S., Redouane, Y., Lopez-Mosqueda, J., Shiraishi, R., Romanowska, M., Lutzmayer, S., Kuiper, J., Martinez, C., Dikic, I., Pasparakis, M., et al. (2014). Sharpin prevents skin inflammation by inhibiting TNFR1-induced keratinocyte apoptosis. eLife 3.

Lechtenberg, B.C., Rajput, A., Sanishvili, R., Dobaczewska, M.K., Ware, C.F., Mace, P.D., and Riedl, S.J. (2016). Structure of a HOIP/E2~ubiquitin complex reveals RBR E3 ligase mechanism and regulation. Nature 529, 546-550.

Lee, E.G., Boone, D.L., Chai, S., Libby, S.L., Chien, M., Lodolce, J.P., and Ma, A. (2000). Failure to regulate TNF-induced NF-kappaB and cell death responses in A20-deficient mice. Science 289, 2350-2354.

Lee, G.H., Ooasa, T., and Osanai, M. (1998). Mechanism of the paradoxical, inhibitory effect of phenobarbital on hepatocarcinogenesis initiated in infant B6C3F1 mice with diethylnitrosamine. Cancer research 58, 1665-1669.

Lee, J.S., Chu, I.S., Mikaelyan, A., Calvisi, D.F., Heo, J., Reddy, J.K., and Thorgeirsson, S.S. (2004). Application of comparative functional genomics to identify best-fit mouse models to study human cancer. Nature genetics 36, 1306-1311.

Li, P., Nijhawan, D., Budihardjo, I., Srinivasula, S.M., Ahmad, M., Alnemri, E.S., and Wang, X. (1997). Cytochrome c and dATP-dependent formation of Apaf-1/caspase-9 complex initiates an apoptotic protease cascade. Cell 91, 479-489.

Liang, C., Zhang, M., and Sun, S.C. (2006). beta-TrCP binding and processing of NF-kappaB2/p100 involve its phosphorylation at serines 866 and 870. Cellular signalling 18, 1309-1317.

Liao, G., Zhang, M., Harhaj, E.W., and Sun, S.C. (2004). Regulation of the NF-kappaB-inducing kinase by tumor necrosis factor receptor-associated factor 3-induced degradation. The Journal of biological chemistry 279, 26243-26250.

Liedtke, C., Bangen, J.M., Freimuth, J., Beraza, N., Lambertz, D., Cubero, F.J., Hatting, M., Karlmark, K.R., Streetz, K.L., Krombach, G.A., et al. (2011). Loss of caspase-8 protects mice against inflammation-related hepatocarcinogenesis but induces non-apoptotic liver injury. Gastroenterology 141, 2176-2187.

Lin, S.C., Chung, J.Y., Lamothe, B., Rajashankar, K., Lu, M., Lo, Y.C., Lam, A.Y., Darnay, B.G., and Wu, H. (2008). Molecular basis for the unique deubiquitinating activity of the NF-kappaB inhibitor A20. Journal of molecular biology 376, 526-540.

Linkermann, A., Brasen, J.H., Darding, M., Jin, M.K., Sanz, A.B., Heller, J.O., De Zen, F., Weinlich, R., Ortiz, A., Walczak, H., et al. (2013). Two independent pathways of regulated necrosis mediate ischemia-reperfusion injury. Proceedings of the National Academy of Sciences of the United States of America 110, 12024-12029.

Lo, J.C., Wang, Y., Tumanov, A.V., Bamji, M., Yao, Z., Reardon, C.A., Getz, G.S., and Fu, Y.X. (2007). Lymphotoxin beta receptor-dependent control of lipid homeostasis. Science 316, 285-288.

Lu, T.T., Onizawa, M., Hammer, G.E., Turer, E.E., Yin, Q., Damko, E., Agelidis, A., Shifrin, N., Advincula, R., Barrera, J., et al. (2013). Dimerization and ubiquitin mediated recruitment of A20, a complex deubiquitinating enzyme. Immunity 38, 896-905.

Luedde, T., Beraza, N., Kotsikoris, V., van Loo, G., Nenci, A., De Vos, R., Roskams, T., Trautwein, C., and Pasparakis, M. (2007). Deletion of NEMO/IKKgamma in liver parenchymal cells causes steatohepatitis and hepatocellular carcinoma. Cancer cell 11, 119-132.

Ma, A., and Malynn, B.A. (2012). A20: linking a complex regulator of ubiquitylation to immunity and human disease. Nature reviews Immunology 12, 774-785.

Ma, D.Y., and Clark, E.A. (2009). The role of CD40 and CD154/CD40L in dendritic cells. Seminars in immunology 21, 265-272.

Mackay, F., and Schneider, P. (2009). Cracking the BAFF code. Nature reviews Immunology 9, 491-502.

Maeda, S., Kamata, H., Luo, J.L., Leffert, H., and Karin, M. (2005). IKKbeta couples hepatocyte death to cytokine-driven compensatory proliferation that promotes chemical hepatocarcinogenesis. Cell 121, 977-990.

Mantovani, A., and Allavena, P. (2015). The interaction of anticancer therapies with tumor-associated macrophages. The Journal of experimental medicine 212, 435-445.

Mantovani, A., Sozzani, S., Locati, M., Allavena, P., and Sica, A. (2002). Macrophage polarization: tumor-associated macrophages as a paradigm for polarized M2 mononuclear phagocytes. Trends in immunology 23, 549-555.

Marquardt, J.U., Andersen, J.B., and Thorgeirsson, S.S. (2015). Functional and genetic deconstruction of the cellular origin in liver cancer. Nature reviews Cancer 15, 653-667.

Massoumi, R., Chmielarska, K., Hennecke, K., Pfeifer, A., and Fassler, R. (2006). Cyld inhibits tumor cell proliferation by blocking Bcl-3-dependent NF-kappaB signaling. Cell 125, 665-677.

Matsunaga, Y., Nakatsu, Y., Fukushima, T., Okubo, H., Iwashita, M., Sakoda, H., Fujishiro, M., Yamamotoya, T., Kushiyama, A., Takahashi, S., et al. (2015). LUBAC Formation Is Impaired in the Livers of Mice with MCD-Dependent Nonalcoholic Steatohepatitis. Mediators of inflammation 2015, 125380.

Mauro, C., Pacifico, F., Lavorgna, A., Mellone, S., Iannetti, A., Acquaviva, R., Formisano, S., Vito, P., and Leonardi, A. (2006). ABIN-1 binds to NEMO/IKKgamma and co-operates with A20 in inhibiting NF-kappaB. The Journal of biological chemistry 281, 18482-18488.

Medzhitov, R., and Janeway, C., Jr. (2000). Innate immunity. The New England journal of medicine 343, 338-344.

Mercurio, F., Zhu, H., Murray, B.W., Shevchenko, A., Bennett, B.L., Li, J., Young, D.B., Barbosa, M., Mann, M., Manning, A., et al. (1997). IKK-1 and IKK-2: cytokine-activated IkappaB kinases essential for NF-kappaB activation. Science 278, 860-866.

Mevissen, T.E., Hospenthal, M.K., Geurink, P.P., Elliott, P.R., Akutsu, M., Arnaudo, N., Ekkebus, R., Kulathu, Y., Wauer, T., El Oualid, F., et al. (2013). OTU deubiquitinases reveal mechanisms of linkage specificity and enable ubiquitin chain restriction analysis. Cell 154, 169-184.

Micheau, O., and Tschopp, J. (2003). Induction of TNF receptor I-mediated apoptosis via two sequential signaling complexes. Cell 114, 181-190.

Miyajima, A., Tanaka, M., and Itoh, T. (2014). Stem/progenitor cells in liver development, homeostasis, regeneration, and reprogramming. Cell stem cell 14, 561-574.

Mocarski, E.S., Guo, H., and Kaiser, W.J. (2015). Necroptosis: The Trojan horse in cell autonomous antiviral host defense. Virology 479-480, 160-166.

Mocarski, E.S., Upton, J.W., and Kaiser, W.J. (2012). Viral infection and the evolution of caspase 8-regulated apoptotic and necrotic death pathways. Nature reviews Immunology 12, 79-88.

Moquin, D.M., McQuade, T., and Chan, F.K. (2013). CYLD deubiquitinates RIP1 in the TNFalpha-induced necrosome to facilitate kinase activation and programmed necrosis. PloS one 8, e76841.

Murakami, S. (2001). Hepatitis B virus X protein: a multifunctional viral regulator. Journal of gastroenterology 36, 651-660.

Muzio, M., Chinnaiyan, A.M., Kischkel, F.C., O'Rourke, K., Shevchenko, A., Ni, J., Scaffidi, C., Bretz, J.D., Zhang, M., Gentz, R., et al. (1996). FLICE, a novel FADD-homologous ICE/CED-3-like protease, is recruited to the CD95 (Fas/APO-1) death--inducing signaling complex. Cell 85, 817-827.

Nanda, S.K., Venigalla, R.K., Ordureau, A., Patterson-Kane, J.C., Powell, D.W., Toth, R., Arthur, J.S., and Cohen, P. (2011). Polyubiquitin binding to ABIN1 is required to prevent autoimmunity. The Journal of experimental medicine 208, 1215-1228.

Naugler, W.E., Sakurai, T., Kim, S., Maeda, S., Kim, K., Elsharkawy, A.M., and Karin, M. (2007). Gender disparity in liver cancer due to sex differences in MyD88-dependent IL-6 production. Science 317, 121-124.

Nenci, A., Becker, C., Wullaert, A., Gareus, R., van Loo, G., Danese, S., Huth, M., Nikolaev, A., Neufert, C., Madison, B., et al. (2007). Epithelial NEMO links innate immunity to chronic intestinal inflammation. Nature 446, 557-561.

Nenci, A., Huth, M., Funteh, A., Schmidt-Supprian, M., Bloch, W., Metzger, D., Chambon, P., Rajewsky, K., Krieg, T., Haase, I., et al. (2006). Skin lesion development in a mouse model of incontinentia pigmenti is triggered by NEMO deficiency in epidermal keratinocytes and requires TNF signaling. Human molecular genetics 15, 531-542.

Nikolaou, K., Tsagaratou, A., Eftychi, C., Kollias, G., Mosialos, G., and Talianidis, I. (2012). Inactivation of the deubiquitinase CYLD in hepatocytes causes apoptosis, inflammation, fibrosis, and cancer. Cancer cell 21, 738-750.

Ninomiya-Tsuji, J., Kishimoto, K., Hiyama, A., Inoue, J., Cao, Z., and Matsumoto, K. (1999). The kinase TAK1 can activate the NIK-I kappaB as well as the MAP kinase cascade in the IL-1 signalling pathway. Nature 398, 252-256.

Oberst, A., Dillon, C.P., Weinlich, R., McCormick, L.L., Fitzgerald, P., Pop, C., Hakem, R., Salvesen, G.S., and Green, D.R. (2011). Catalytic activity of the caspase-8-FLIP(L) complex inhibits RIPK3-dependent necrosis. Nature 471, 363-367.

O'Donnell, M.A., Hase, H., Legarda, D., and Ting, A.T. (2012). NEMO inhibits programmed necrosis in an NFkappaB-independent manner by restraining RIP1. PloS one 7, e41238.

O'Donnell, M.A., Perez-Jimenez, E., Oberst, A., Ng, A., Massoumi, R., Xavier, R., Green, D.R., and Ting, A.T. (2011). Caspase 8 inhibits programmed necrosis by processing CYLD. Nature cell biology 13, 1437-1442.

Oeckinghaus, A., and Ghosh, S. (2009). The NF-kappaB family of transcription factors and its regulation. Cold Spring Harbor perspectives in biology 1, a000034.

Ohnishi, S., Ma, N., Thanan, R., Pinlaor, S., Hammam, O., Murata, M., and Kawanishi, S. (2013). DNA damage in inflammation-related carcinogenesis and cancer stem cells. Oxidative medicine and cellular longevity 2013, 387014.

O'Neill, L.A., Dunne, A., Edjeback, M., Gray, P., Jefferies, C., and Wietek, C. (2003). Mal and MyD88: adapter proteins involved in signal transduction by Toll-like receptors. Journal of endotoxin research 9, 55-59.

Oshima, S., Turer, E.E., Callahan, J.A., Chai, S., Advincula, R., Barrera, J., Shifrin, N., Lee, B., Benedict Yen, T.S., Woo, T., et al. (2009). ABIN-1 is a ubiquitin sensor that restricts cell death and sustains embryonic development. Nature 457, 906-909.

Otterdal, K., Haukeland, J.W., Yndestad, A., Dahl, T.B., Holm, S., Segers, F.M., Gladhaug, I.P., Konopski, Z., Damas, J.K., Halvorsen, B., et al. (2015). Increased Serum Levels of LIGHT/TNFSF14 in Nonalcoholic Fatty Liver Disease: Possible Role in Hepatic Inflammation. Clinical and translational gastroenterology 6, e95.

Pannem, R.R., Dorn, C., Ahlqvist, K., Bosserhoff, A.K., Hellerbrand, C., and Massoumi, R. (2014). CYLD controls c-MYC expression through the JNK-dependent signaling pathway in hepatocellular carcinoma. Carcinogenesis 35, 461-468.

Park, E.J., Lee, J.H., Yu, G.Y., He, G., Ali, S.R., Holzer, R.G., Osterreicher, C.H., Takahashi, H., and Karin, M. (2010). Dietary and genetic obesity promote liver inflammation and tumorigenesis by enhancing IL-6 and TNF expression. Cell 140, 197-208.

Pasparakis, M. (2012). Role of NF-kappaB in epithelial biology. Immunological reviews 246, 346-358.

Pasparakis, M., and Vandenabeele, P. (2015). Necroptosis and its role in inflammation. Nature 517, 311-320.

Peltzer, N., Rieser, E., Taraborrelli, L., Draber, P., Darding, M., Pernaute, B., Shimizu, Y., Sarr, A., Draberova, H., Montinaro, A., et al. (2014). HOIP deficiency causes embryonic lethality by aberrant TNFR1-mediated endothelial cell death. Cell reports 9, 153-165.

Pfeffer, K., Matsuyama, T., Kundig, T.M., Wakeham, A., Kishihara, K., Shahinian, A., Wiegmann, K., Ohashi, P.S., Kronke, M., and Mak, T.W. (1993). Mice deficient for the 55 kd tumor necrosis factor receptor are resistant to endotoxic shock, yet succumb to L. monocytogenes infection. Cell 73, 457-467.

Planas-Paz, L., Orsini, V., Boulter, L., Calabrese, D., Pikiolek, M., Nigsch, F., Xie, Y., Roma, G., Donovan, A., Marti, P., et al. (2016). The RSPO-LGR4/5-ZNRF3/RNF43 module controls liver zonation and size. Nature cell biology 18, 467-479.

Pober, J.S., and Sessa, W.C. (2007). Evolving functions of endothelial cells in inflammation. Nature reviews Immunology 7, 803-815.

Pobezinskaya, Y.L., Kim, Y.S., Choksi, S., Morgan, M.J., Li, T., Liu, C., and Liu, Z. (2008). The function of TRADD in signaling through tumor necrosis factor receptor 1 and TRIF-dependent Toll-like receptors. Nature immunology 9, 1047-1054.

Popov, Y., Patsenker, E., Fickert, P., Trauner, M., and Schuppan, D. (2005). Mdr2 (Abcb4)-/- mice spontaneously develop severe biliary fibrosis via massive dysregulation of pro- and antifibrogenic genes. Journal of hepatology 43, 1045-1054.

Postic, C., Shiota, M., Niswender, K.D., Jetton, T.L., Chen, Y., Moates, J.M., Shelton, K.D., Lindner, J., Cherrington, A.D., and Magnuson, M.A. (1999). Dual roles for glucokinase in glucose homeostasis as determined by liver and pancreatic beta cell-specific gene knock-outs using Cre recombinase. The Journal of biological chemistry 274, 305-315.

Rahighi, S., Ikeda, F., Kawasaki, M., Akutsu, M., Suzuki, N., Kato, R., Kensche, T., Uejima, T., Bloor, S., Komander, D., et al. (2009). Specific recognition of linear ubiquitin chains by NEMO is important for NF-kappaB activation. Cell 136, 1098-1109.

Rahman, R., Hammoud, G.M., Almashhrawi, A.A., Ahmed, K.T., and Ibdah, J.A. (2013). Primary hepatocellular carcinoma and metabolic syndrome: An update. World journal of gastrointestinal oncology 5, 186-194.

Reiley, W.W., Zhang, M., Jin, W., Losiewicz, M., Donohue, K.B., Norbury, C.C., and Sun, S.C. (2006). Regulation of T cell development by the deubiquitinating enzyme CYLD. Nature immunology 7, 411-417.

Rickard, J.A., Anderton, H., Etemadi, N., Nachbur, U., Darding, M., Peltzer, N., Lalaoui, N., Lawlor, K.E., Vanyai, H., Hall, C., et al. (2014). TNFR1-dependent cell death drives inflammation in Sharpin-deficient mice. eLife 3.

Riedl, S.J., and Salvesen, G.S. (2007). The apoptosome: signalling platform of cell death. Nature reviews Molecular cell biology 8, 405-413.

Ritorto, M.S., Ewan, R., Perez-Oliva, A.B., Knebel, A., Buhrlage, S.J., Wightman, M., Kelly, S.M., Wood, N.T., Virdee, S., Gray, N.S., et al. (2014). Screening of DUB activity and specificity by MALDI-TOF mass spectrometry. Nature communications 5, 4763.

Rivkin, E., Almeida, S.M., Ceccarelli, D.F., Juang, Y.C., MacLean, T.A., Srikumar, T., Huang, H., Dunham, W.H., Fukumura, R., Xie, G., et al. (2013). The linear ubiquitin-specific deubiquitinase gumby regulates angiogenesis. Nature 498, 318-324.

Rothwarf, D.M., Zandi, E., Natoli, G., and Karin, M. (1998). IKK-gamma is an essential regulatory subunit of the IkappaB kinase complex. Nature 395, 297-300.

Rothwell, P.M., Wilson, M., Price, J.F., Belch, J.F., Meade, T.W., and Mehta, Z. (2012). Effect of daily aspirin on risk of cancer metastasis: a study of incident cancers during randomised controlled trials. Lancet 379, 1591-1601.

Sakurai, T., Maeda, S., Chang, L., and Karin, M. (2006). Loss of hepatic NF-kappa B activity enhances chemical hepatocarcinogenesis through sustained c-Jun N-terminal kinase 1 activation. Proceedings of the National Academy of Sciences of the United States of America 103, 10544-10551.

Scaffidi, C., Fulda, S., Srinivasan, A., Friesen, C., Li, F., Tomaselli, K.J., Debatin, K.M., Krammer, P.H., and Peter, M.E. (1998). Two CD95 (APO-1/Fas) signaling pathways. The EMBO journal 17, 1675-1687.

Schaeffer, V., Akutsu, M., Olma, M.H., Gomes, L.C., Kawasaki, M., and Dikic, I. (2014). Binding of OTULIN to the PUB domain of HOIP controls NF-kappaB signaling. Molecular cell 54, 349-361.

Schneider, P., Thome, M., Burns, K., Bodmer, J.L., Hofmann, K., Kataoka, T., Holler, N., and Tschopp, J. (1997). TRAIL receptors 1 (DR4) and 2 (DR5) signal FADD-dependent apoptosis and activate NF-kappaB. Immunity 7, 831-836.

Sen, R., and Baltimore, D. (1986). Inducibility of kappa immunoglobulin enhancer-binding protein Nf-kappa B by a posttranslational mechanism. Cell 47, 921-928.

Senftleben, U., Cao, Y., Xiao, G., Greten, F.R., Krahn, G., Bonizzi, G., Chen, Y., Hu, Y., Fong, A., Sun, S.C., et al. (2001). Activation by IKKalpha of a second, evolutionary conserved, NF-kappa B signaling pathway. Science 293, 1495-1499.

Seymour, R.E., Hasham, M.G., Cox, G.A., Shultz, L.D., Hogenesch, H., Roopenian, D.C., and Sundberg, J.P. (2007). Spontaneous mutations in the mouse Sharpin gene result in multiorgan inflammation, immune system dysregulation and dermatitis. Genes and immunity 8, 416-421.

Sharma, P., and Allison, J.P. (2015). Immune checkpoint targeting in cancer therapy: toward combination strategies with curative potential. Cell 161, 205-214.

Shetty, S., Lalor, P.F., and Adams, D.H. (2008). Lymphocyte recruitment to the liver: molecular insights into the pathogenesis of liver injury and hepatitis. Toxicology 254, 136-146.

Shimizu, S., Fujita, H., Sasaki, Y., Tsuruyama, T., Fukuda, K., and Iwai, K. (2016). Differential Involvement of the Npl4 Zinc Finger Domains of SHARPIN and HOIL-1L in Linear Ubiquitin Chain Assembly Complex-Mediated Cell Death Protection. Molecular and cellular biology 36, 1569-1583.

Shimizu, Y., Taraborrelli, L., and Walczak, H. (2015). Linear ubiquitination in immunity. Immunological reviews 266, 190-207.

Skaug, B., Chen, J., Du, F., He, J., Ma, A., and Chen, Z.J. (2011). Direct, noncatalytic mechanism of IKK inhibition by A20. Molecular cell 44, 559-571.

Smit, J.J., Monteferrario, D., Noordermeer, S.M., van Dijk, W.J., van der Reijden, B.A., and Sixma, T.K. (2012). The E3 ligase HOIP specifies linear ubiquitin chain assembly through its RING-IBR-RING domain and the unique LDD extension. The EMBO journal 31, 3833-3844.

Sottoriva, A., Kang, H., Ma, Z., Graham, T.A., Salomon, M.P., Zhao, J., Marjoram, P., Siegmund, K., Press, M.F., Shibata, D., et al. (2015). A Big Bang model of human colorectal tumor growth. Nature genetics 47, 209-216.

Sprick, M.R., Weigand, M.A., Rieser, E., Rauch, C.T., Juo, P., Blenis, J., Krammer, P.H., and Walczak, H. (2000). FADD/MORT1 and caspase-8 are recruited to TRAIL receptors 1 and 2 and are essential for apoptosis mediated by TRAIL receptor 2. Immunity 12, 599-609.

Stieglitz, B., Rana, R.R., Koliopoulos, M.G., Morris-Davies, A.C., Schaeffer, V., Christodoulou, E., Howell, S., Brown, N.R., Dikic, I., and Rittinger, K. (2013). Structural basis for ligase-specific conjugation of linear ubiquitin chains by HOIP. Nature 503, 422-426.

Su, F., and Schneider, R.J. (1996). Hepatitis B virus HBx protein activates transcription factor NF-kappaB by acting on multiple cytoplasmic inhibitors of rel-related proteins. Journal of virology 70, 4558-4566.

Sun, S.C. (2010). CYLD: a tumor suppressor deubiquitinase regulating NF-kappaB activation and diverse biological processes. Cell death and differentiation 17, 25-34.

Sun, S.C. (2011). Non-canonical NF-kappaB signaling pathway. Cell research 21, 71-85.

Tait, S.W., and Green, D.R. (2013). Mitochondrial regulation of cell death. Cold Spring Harbor perspectives in biology 5.

Tajiri, K., and Shimizu, Y. (2008). Practical guidelines for diagnosis and early management of drug-induced liver injury. World journal of gastroenterology 14, 6774-6785.

Takeuchi, O., and Akira, S. (2008). MDA5/RIG-I and virus recognition. Current opinion in immunology 20, 17-22.

Takiuchi, T., Nakagawa, T., Tamiya, H., Fujita, H., Sasaki, Y., Saeki, Y., Takeda, H., Sawasaki, T., Buchberger, A., Kimura, T., et al. (2014). Suppression of LUBAC-mediated linear ubiquitination by a specific interaction between LUBAC and the deubiquitinases CYLD and OTULIN. Genes to cells : devoted to molecular & cellular mechanisms 19, 254-272.

Teng, M.W., Swann, J.B., Koebel, C.M., Schreiber, R.D., and Smyth, M.J. (2008). Immune-mediated dormancy: an equilibrium with cancer. Journal of leukocyte biology 84, 988-993.

Terradillos, O., Billet, O., Renard, C.A., Levy, R., Molina, T., Briand, P., and Buendia, M.A. (1997). The hepatitis B virus X gene potentiates c-myc-induced liver oncogenesis in transgenic mice. Oncogene 14, 395-404.

Thome, M. (2004). CARMA1, BCL-10 and MALT1 in lymphocyte development and activation. Nature reviews Immunology 4, 348-359.

Tokunaga, F., Nakagawa, T., Nakahara, M., Saeki, Y., Taniguchi, M., Sakata, S., Tanaka, K., Nakano, H., and Iwai, K. (2011). SHARPIN is a component of the NF-kappaB-activating linear ubiquitin chain assembly complex. Nature 471, 633-636.

Tokunaga, F., Nishimasu, H., Ishitani, R., Goto, E., Noguchi, T., Mio, K., Kamei, K., Ma, A., Iwai, K., and Nureki, O. (2012). Specific recognition of linear polyubiquitin by A20 zinc finger 7 is involved in NF-kappaB regulation. The EMBO journal 31, 3856-3870.

Tokunaga, F., Sakata, S., Saeki, Y., Satomi, Y., Kirisako, T., Kamei, K., Nakagawa, T., Kato, M., Murata, S., Yamaoka, S., et al. (2009). Involvement of linear polyubiquitylation of NEMO in NF-kappaB activation. Nature cell biology 11, 123-132.

Tsao, D.H., McDonagh, T., Telliez, J.B., Hsu, S., Malakian, K., Xu, G.Y., and Lin, L.L. (2000). Solution structure of N-TRADD and characterization of the interaction of N-TRADD and C-TRAF2, a key step in the TNFR1 signaling pathway. Molecular cell 5, 1051-1057.

Turer, E.E., Tavares, R.M., Mortier, E., Hitotsumatsu, O., Advincula, R., Lee, B., Shifrin, N., Malynn, B.A., and Ma, A. (2008). Homeostatic MyD88-dependent signals cause lethal inflamMation in the absence of A20. The Journal of experimental medicine 205, 451-464.

Ueda, H., Ullrich, S.J., Gangemi, J.D., Kappel, C.A., Ngo, L., Feitelson, M.A., and Jay, G. (1995). Functional inactivation but not structural mutation of p53 causes liver cancer. Nature genetics 9, 41-47.

Upton, J.W., Kaiser, W.J., and Mocarski, E.S. (2012). DAI/ZBP1/DLM-1 complexes with RIP3 to mediate virus-induced programmed necrosis that is targeted by murine cytomegalovirus vIRA. Cell host & microbe 11, 290-297.

Vallabhapurapu, S., Matsuzawa, A., Zhang, W., Tseng, P.H., Keats, J.J., Wang, H., Vignali, D.A., Bergsagel, P.L., and Karin, M. (2008). Nonredundant and complementary functions of TRAF2 and TRAF3 in a ubiquitination cascade that activates NIK-dependent alternative NF-kappaB signaling. Nature immunology 9, 1364-1370.

van der Vliet, H.J., and Nieuwenhuis, E.E. (2007). IPEX as a result of mutations in FOXP3. Clinical & developmental immunology 2007, 89017.

Varfolomeev, E., Goncharov, T., Fedorova, A.V., Dynek, J.N., Zobel, K., Deshayes, K., Fairbrother, W.J., and Vucic, D. (2008). c-IAP1 and c-IAP2 are critical mediators of tumor necrosis factor alpha (TNFalpha)-induced NF-kappaB activation. The Journal of biological chemistry 283, 24295-24299.

Verhelst, K., Carpentier, I., Kreike, M., Meloni, L., Verstrepen, L., Kensche, T., Dikic, I., and Beyaert, R. (2012). A20 inhibits LUBAC-mediated NF-kappaB activation by binding linear polyubiquitin chains via its zinc finger 7. The EMBO journal 31, 3845-3855.

Vince, J.E., Pantaki, D., Feltham, R., Mace, P.D., Cordier, S.M., Schmukle, A.C., Davidson, A.J., Callus, B.A., Wong, W.W., Gentle, I.E., et al. (2009). TRAF2 must bind to cellular inhibitors of apoptosis for tumor necrosis factor (tnf) to efficiently activate nf-{kappa}b and to prevent tnf-induced apoptosis. The Journal of biological chemistry 284, 35906-35915.

Vivier, E., Tomasello, E., Baratin, M., Walzer, T., and Ugolini, S. (2008). Functions of natural killer cells. Nature immunology 9, 503-510.

Vlantis, K., Wullaert, A., Polykratis, A., Kondylis, V., Dannappel, M., Schwarzer, R., Welz, P., Corona, T., Walczak, H., Weih, F., et al. (2016). NEMO Prevents RIP Kinase 1-Mediated Epithelial Cell Death and Chronic Intestinal Inflammation by NF-kappaB-Dependent and -Independent Functions. Immunity 44, 553-567.

Vucur, M., Reisinger, F., Gautheron, J., Janssen, J., Roderburg, C., Cardenas, D.V., Kreggenwinkel, K., Koppe, C., Hammerich, L., Hakem, R., et al. (2013). RIP3 inhibits inflammatory hepatocarcinogenesis but promotes cholestasis by controlling caspase-8- and JNK-dependent compensatory cell proliferation. Cell reports 4, 776-790.

Wagner, S.A., Satpathy, S., Beli, P., and Choudhary, C. (2016). SPATA2 links CYLD to the TNF-alpha receptor signaling complex and modulates the receptor signaling outcomes. The EMBO journal.

Walczak, H. (2013). Death receptor-ligand systems in cancer, cell death, and inflammation. Cold Spring Harbor perspectives in biology 5, a008698.

Walczak, H., Miller, R.E., Ariail, K., Gliniak, B., Griffith, T.S., Kubin, M., Chin, W., Jones, J., Woodward, A., Le, T., et al. (1999). Tumoricidal activity of tumor necrosis factor-related apoptosis-inducing ligand in vivo. Nature medicine 5, 157-163.

Wang, C., Deng, L., Hong, M., Akkaraju, G.R., Inoue, J., and Chen, Z.J. (2001). TAK1 is a ubiquitin-dependent kinase of MKK and IKK. Nature 412, 346-351.

Wang, H., Sun, L., Su, L., Rizo, J., Liu, L., Wang, L.F., Wang, F.S., and Wang, X. (2014). Mixed lineage kinase domain-like protein MLKL causes necrotic membrane disruption upon phosphorylation by RIP3. Molecular cell 54, 133-146.

Wang, L., Du, F., and Wang, X. (2008). TNF-alpha induces two distinct caspase-8 activation pathways. Cell 133, 693-703.

Wang, X.W., Forrester, K., Yeh, H., Feitelson, M.A., Gu, J.R., and Harris, C.C. (1994). Hepatitis B virus X protein inhibits p53 sequence-specific DNA binding, transcriptional activity, and association with transcription factor ERCC3. Proceedings of the National Academy of Sciences of the United States of America 91, 2230-2234.

Weber, A., Boege, Y., Reisinger, F., and Heikenwalder, M. (2011). Chronic liver inflammation and hepatocellular carcinoma: persistence matters. Swiss medical weekly 141, w13197.

Weber, J., Ollinger, R., Friedrich, M., Ehmer, U., Barenboim, M., Steiger, K., Heid, I., Mueller, S., Maresch, R., Engleitner, T., et al. (2015). CRISPR/Cas9 somatic multiplex-mutagenesis for high-throughput functional cancer genomics in mice. Proceedings of the National Academy of Sciences of the United States of America 112, 13982-13987.

Wei, M.C., Lindsten, T., Mootha, V.K., Weiler, S., Gross, A., Ashiya, M., Thompson, C.B., and Korsmeyer, S.J. (2000). tBID, a membrane-targeted death ligand, oligomerizes BAK to release cytochrome c. Genes & development 14, 2060-2071.

Weinlich, R., Oberst, A., Dillon, C.P., Janke, L.J., Milasta, S., Lukens, J.R., Rodriguez, D.A., Gurung, P., Savage, C., Kanneganti, T.D., et al. (2013). Protective roles for caspase-8 and cFLIP in adult homeostasis. Cell reports 5, 340-348.

Weisend, C.M., Kundert, J.A., Suvorova, E.S., Prigge, J.R., and Schmidt, E.E. (2009). Cre activity in fetal albCre mouse hepatocytes: Utility for developmental studies. Genesis 47, 789-792.

Welz, P.S., Wullaert, A., Vlantis, K., Kondylis, V., Fernandez-Majada, V., Ermolaeva, M., Kirsch, P., Sterner-Kock, A., van Loo, G., and Pasparakis, M. (2011). FADD prevents RIP3-mediated epithelial cell necrosis and chronic intestinal inflammation. Nature 477, 330-334.

Wertz, I.E., Newton, K., Seshasayee, D., Kusam, S., Lam, C., Zhang, J., Popovych, N., Helgason, E., Schoeffler, A., Jeet, S., et al. (2015). Phosphorylation and linear ubiquitin direct A20 inhibition of inflammation. Nature 528, 370-375.

Wertz, I.E., O'Rourke, K.M., Zhou, H., Eby, M., Aravind, L., Seshagiri, S., Wu, P., Wiesmann, C., Baker, R., Boone, D.L., et al. (2004). De-ubiquitination and ubiquitin ligase domains of A20 downregulate NF-kappaB signalling. Nature 430, 694-699.

Wolf, M.J., Adili, A., Piotrowitz, K., Abdullah, Z., Boege, Y., Stemmer, K., Ringelhan, M., Simonavicius, N., Egger, M., Wohlleber, D., et al. (2014). Metabolic activation of intrahepatic CD8+ T cells and NKT cells causes nonalcoholic steatohepatitis and liver cancer via cross-talk with hepatocytes. Cancer cell 26, 549-564.

Wolf, M.J., Seleznik, G.M., Zeller, N., and Heikenwalder, M. (2010). The unexpected role of lymphotoxin beta receptor signaling in carcinogenesis: from lymphoid tissue formation to liver and prostate cancer development. Oncogene 29, 5006-5018.

Wu, C.J., and Ashwell, J.D. (2008). NEMO recognition of ubiquitinated Bcl10 is required for T cell receptor-mediated NF-kappaB activation. Proceedings of the National Academy of Sciences of the United States of America 105, 3023-3028.

Xue, W., Chen, S., Yin, H., Tammela, T., Papagiannakopoulos, T., Joshi, N.S., Cai, W., Yang, G., Bronson, R., Crowley, D.G., et al. (2014). CRISPR-mediated direct mutation of cancer genes in the mouse liver. Nature 514, 380-384.

Yamaguchi, N. (2015). The seventh zinc finger motif of A20 is required for the suppression of TNF-alpha-induced apoptosis. FEBS letters 589, 1369-1375.

Yamaoka, S., Courtois, G., Bessia, C., Whiteside, S.T., Weil, R., Agou, F., Kirk, H.E., Kay, R.J., and Israel, A. (1998). Complementation cloning of NEMO, a component of the IkappaB kinase complex essential for NF-kappaB activation. Cell 93, 1231-1240.

Yang, Y., Kelly, P., Shaffer, A.L., 3rd, Schmitz, R., Yoo, H.M., Liu, X., Huang da, W., Webster, D., Young, R.M., Nakagawa, M., et al. (2016). Targeting Non-proteolytic Protein Ubiquitination for the Treatment of Diffuse Large B Cell Lymphoma. Cancer cell 29, 494-507.

Yang, Y., Schmitz, R., Mitala, J., Whiting, A., Xiao, W., Ceribelli, M., Wright, G.W., Zhao, H., Xu, W., Rosenwald, A., et al. (2014). Essential role of the linear ubiquitin chain assembly complex in lymphoma revealed by rare germline polymorphisms. Cancer discovery 4, 480-493.

Yatim, N., Jusforgues-Saklani, H., Orozco, S., Schulz, O., Barreira da Silva, R., Reis e Sousa, C., Green, D.R., Oberst, A., and Albert, M.L. (2015). RIPK1 and NF-kappaB signaling in dying cells determines cross-priming of CD8(+) T cells. Science 350, 328-334.

Yaron, A., Hatzubai, A., Davis, M., Lavon, I., Amit, S., Manning, A.M., Andersen, J.S., Mann, M., Mercurio, F., and Ben-Neriah, Y. (1998). Identification of the receptor component of the IkappaBalpha-ubiquitin ligase. Nature 396, 590-594.

Zarnegar, B.J., Wang, Y., Mahoney, D.J., Dempsey, P.W., Cheung, H.H., He, J., Shiba, T., Yang, X., Yeh, W.C., Mak, T.W., et al. (2008). Noncanonical NF-kappaB activation requires coordinated assembly of a regulatory complex of the adaptors cIAP1, cIAP2, TRAF2 and TRAF3 and the kinase NIK. Nature immunology 9, 1371-1378.

Zhang, H., Zhou, X., McQuade, T., Li, J., Chan, F.K., and Zhang, J. (2011). Functional complementation between FADD and RIP1 in embryos and lymphocytes. Nature 471, 373-376.

Zhang, J., Stirling, B., Temmerman, S.T., Ma, C.A., Fuss, I.J., Derry, J.M., and Jain, A. (2006). Impaired regulation of NF-kappaB and increased susceptibility to colitis-associated tumorigenesis in CYLD-deficient mice. The Journal of clinical investigation 116, 3042-3049.

Zheng, L., Bidere, N., Staudt, D., Cubre, A., Orenstein, J., Chan, F.K., and Lenardo, M. (2006). Competitive control of independent programs of tumor necrosis factor receptor-induced cell death by TRADD and RIP1. Molecular and cellular biology 26, 3505-3513.

Zorn, A.M. (2008). Liver development. In StemBook (Cambridge (MA)).

Appendix

List of publications during the PhD programme

Shimizu, Y., Peltzer, N., Lafont, E., Sevko, A., Sarr, A., Draberova, H., and Walczak, H. The linear ubiquitin chain assembly complex acts as a liver tumor suppressor and inhibits hepatocyte apoptosis and hepatitis. Hepatology, *in press* (manuscript accepted on 18 January 2017).

Shimizu, Y.*, Taraborrelli, L.*, and Walczak, H. (2015). Linear ubiquitination in immunity. Immunological reviews 266, 190-207. (*equal contribution)

Peltzer, N., Rieser, E., Taraborrelli, L., Draber, P., Darding, M., Pernaute, B., **Shimizu, Y.**, Sarr, A., Draberova, H., Montinaro, A., et al. (2014). HOIP deficiency causes embryonic lethality by aberrant TNFR1-mediated endothelial cell death. Cell reports 9, 153-165.